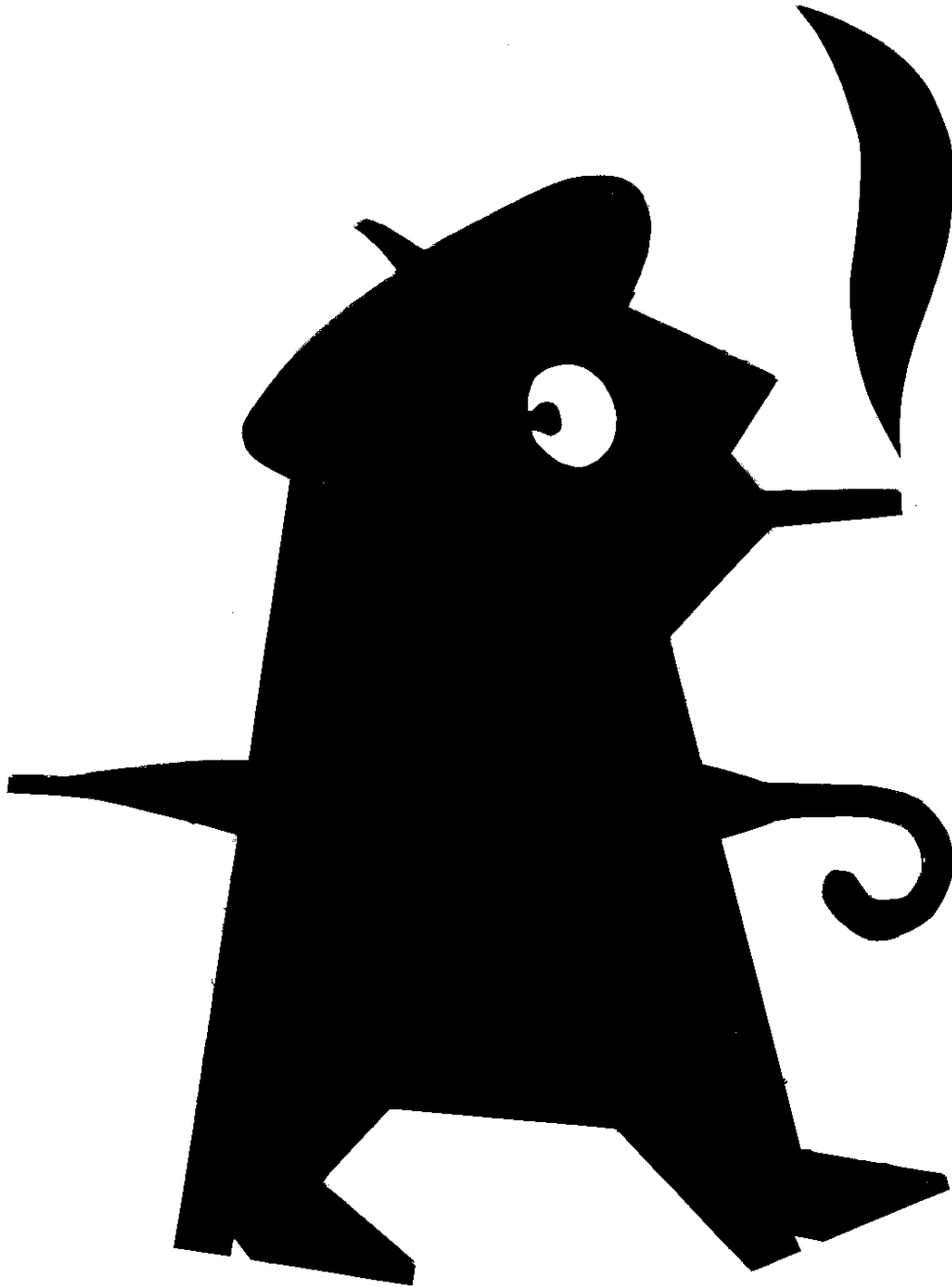# Content-Based Information Retrieval from Forensic Image Databases

Zeno Geradts

Content-Based Information Retrieval from Forensic Image Databases

Zeno Geradts

Colophon

Cover design is in memoriam of the author's father who received this picture from his colleagues. The image resembles the image of the detective Havank, which is also the name of the finger print database in the Netherlands.

Content-Based Information Retrieval from Forensic Databases

Inhoudsgestuurde informatie-extractie vanuit forensische beeldgegevensbestanden
(met een samenvatting in het Nederlands)

PROEFSCHRIFT

Ter verkrijging van de graad van doctor aan de Universiteit Utrecht op gezag van de
Rector Magnificus, Prof. Dr. W.H. Gispen, ingevolge het besluit van het College voor
Promoties in het openbaar te verdedigen op woensdag 19 juni 2002 des ochtends te
10:30 uur

DOOR

Zeno Jean Marius Hubert Geradts

geboren op 26 september 1967 te Oosterhout

Promotor: **Prof. Dr. Ir. M.A. Viergever**
                   Universiteit Utrecht

Co-promotor: **Dr. J. Bijhold**
                   Nederlands Forensisch Instituut

Acknowledgements

This thesis would not appear in its present form without the kind assistance and support of the following individuals and organizations:

Prof. Dr. ir. Max Viergever and Dr. Jurrien Bijhold for their commitment to helping see this project through to its completion, and their equally generous and wise guidance during its development.

Anneke Poortman, ing. Rob Hermsen, ing, Jan Keijzer, Ing. Ies Keereweer and ir. Huub Hardy for their contributions as co-authors of papers that are covered in this thesis.

Dr. Hans Henseler, Ir. Johan ten Houten, Drs. Gerben Wierda, ir. Tom Weeber and Dr. Hage Postema who were my Department Heads during the writing of this book.

Prof. Fionn Murtagh of the Queens University in Belfast who motivated me to do experiments with wavelets.

Dr. Lenny Rudin, with whom I have had good discussions about alternative ideas.

Prof. Dr. Barend Cohen, Dr. Rob Visser and Our Directors Dr. Wim Sprangers and Dr. Albert Koeleman really motivated me to write this thesis.

My colleagues of The Netherlands Forensic Institute with whom I worked together, especially ir. Bert van Leuven and dr. Henk Huizer.

Naoki Saitoh MSc of the National Research Institute of Police in Tokyo, who helped me with a grant in Japan, and with whom I have good contacts on scientific research in Japan.

The MPEG-7 group that has been very helpful and open in their communication.

Dedication

This thesis is dedicated to my parents and grandmothers, without whom none of this would have been even possible.

CONTENTS

List of Figures

List of Tables

1   Introduction

The importance of (image) databases in forensic science has long been recognized. For example, the utility of databases of fingerprints[1] is well known. Over the past four years, DNA databases have received particular attention and have been featured on the front page of newspapers. These databases have proven extremely useful in verifying or falsifying the involvement of a person or an object as a source of evidence material in a crime, and have led to the resolution of old cases. DNA databases are also playing an increasingly prominent role in the forensic literature[2][3]. However, a variety of other databases are also crucial to forensic casework, such as databases of faces, and databases of bullets and cartridge cases of firearms[4]. Research into forensic image databases is a rapidly expanding field of scientific endeavor that has a direct impact on the number of criminal cases solved.

Throughout the 20th century, many databases were available in the form of paper files or photographs (e.g., cartridge cases, fingerprints, shoe marks). Fingerprint databases were computerized in the 1980s, and became the first databases to be widely used in networks. In addition, the Bundes Kriminal Amt attempted to store images of handwriting in a database. These databases were all in binary image format. At the beginning of the 1990s, computer databases of shoe marks, tool marks and striation marks on cartridge cases and bullets[23] became available. Improvements in image acquisition and storage made it economically feasible to compile these databases in gray-value or color format using off-the-shelf computers.

Some forensic databases contain several millions of images, as is the case with fingerprints. If databases are large, the forensic examiner needs a method for selecting a small number of relevant items from a database, because if this cannot be achieved the investigation becomes time consuming and therefore either expensive or impossible. The retrieval of similar images from a database based on the contents of each image requires an automatic comparison algorithm that is fast, accurate, and reliable. To formulate such an algorithm, one must first identify which parts or features of the images are suitable for finding correspondences. The development of the retrieval system then requires a multidisciplinary approach with knowledge of multimedia database organization, pattern recognition, image analysis and user interfaces.

Forensic image databases often contain one or more sub-databases:

- Images that are collected from the scene of crime (e.g., shoe marks) ; with this database it is possible to link cases to each other

- Images of marks that are collected from the suspect (e.g., shoe marks that are made with shoes of a suspect) ; with this database in combination with the database of images that are collected from the scene of crime, it is possible to link suspects with cases

- Reference images (e.g., shoe marks from shoes that are commercially available, that can be used to determine which brand and make of shoe a certain shoe mark is from)

Forensic image databases serve two potential goals: identification or recognition.[5] Recognition aims at distinguishing a particular individual from a limited number of people whose biometric data are known. An example is a system for airport access with face recognition for access control. There are several known faces of terrorists in the database, and if the system gives signals that it recognizes someone as a terrorist (positive), human intervention is needed to verify the conclusion of the system. In these biometric systems false positives are acceptable.

Identification is much more difficult to achieve than recognition, because false positives are unacceptable. Forensic identification is an act of identifying a trace, mark or image with a person or an object. A qualified examiner will testify in court the opinion that a certain trace mark or image is from the person or the object. An example is fingerprint identification.

The compiling of large-scale forensic image databases has made available statistical information regarding the uniqueness of certain features for forensic identification. For example, at the beginning of the 20th century there have been arguments about the number of matching points that are needed for concluding that a fingerprint matches. (depending on the country[6] this could be 8-16 points). Nowadays, however, statistical ranking in fingerprint databases provides more information regarding the uniqueness of fingerprints and the number of points versus the statistical relevancy. Up until very recently, most forensic conclusions were drawn on

experience of the investigator rather than on real statistics. The statistical information now available from databases should result in forensic investigation that is more objective. This is necessary since courts and lawyers are asking questions that are more critical about forensic investigation and conclusions that are based on experience of the investigator instead of real statistics[*].

1.1   Main Contributions

The primary objective of this study is to investigate the applicability of image matching algorithms in forensic image database retrieval.

To accomplish these aims we developed, implemented, and evaluated a wide variety of algorithms for measuring correlations in image databases that are used in forensic science. In the evaluation step, we concentrated on the feasibility and accuracy of matching; computational efficiency was not considered.

The research described in this thesis was carried out at The Netherlands Forensic Institute of the Ministry of Justice over a period of ten years. In view of the fact that the research described was performed up to a decade ago, some of the case studies have witnessed the publication of new approaches, sometimes extending the results obtained by us.

In the final discussion an overview is given of the feasibility and usefulness of the different forensic image databases.

---

[*] On January 9th 2002 U.S. District Court Judge Louis H. Pollak in Philadelphia, ruled that finger print evidence does not meet standards of scientific scrutiny established by the U.S. Supreme Court, and said fingerprint examiners cannot testify at trial that a suspect's fingerprints "match" those found at a crime scene.

1.2   Outline of the thesis

Here, we briefly describe the outline of the thesis and the contents of each of the chapters.

This thesis is based on six peer-reviewed publications and six conference papers:

Chapter 2, **State-of-the-Art** is based on:

- *Geradts Z; Bijhold J; "Content Based Information Retrieval in Forensic Image Databases"; Journal of Forensic Science, 2002, 47(2), pp.40-47 and*
- *Geradts Z; Bijhold J; "New developments in forensic image processing and pattern recognition", Science and Justice, 2001, 41(3), pp.159-166.*

This chapter provides an overview of image matching methods and the extraction of features such as color, shape, and structure. The measurement of database performance is considered and several existing databases are discussed.

Chapter 3, **Databases of Tool marks** is based on:

- *Geradts Z; Keijzer J; Keereweer I; "A New Approach to Automatic Comparison of Striation Marks, Journal of Forensic Sciences, 1994, 39(4), pp. 974-980.*
- *Geradts Z; Zaal D; Hardy H; Lelieveld J; Keereweer I; Bijhold J; "Pilot investigation of automatic comparison of striation marks with coded light", Proceedings SPIE, 2001, 4232, pp. 49-56.*

This chapter describes a database for tool marks we developed. This database (named TRAX) was developed for use on a PC. The database is filled with video-images and administrative data about the tool marks (e.g., width, type of tool mark, etc.). TRAX provides a comparison screen that makes it possible to compare images of tool marks. An new algorithm for the automatic comparison of digitized striation patterns is described and evaluated in this chapter. Results of new experiments with 3D surface scanners are presented and discussed.

Chapter 4, **Databases of Cartridge Cases** is based on:

- *Geradts Z; Bijhold J. Hermsen R, Murtagh F; "Image matching algorithms for breech face marks and firing pins in a database of spent cartridge cases of firearms", Forensic Science International, 2001, 119(1), pp. 97-106.*

- *Geradts Z; Bijhold J; Hermsen R; Murtagh F; "Matching algorithms using wavelet transforms for a database of spent cartridge cases of firearms", Proceedings SPIE, 2001, 4232, pp. 545-552.*

- *Geradts Z; Bijhold J; Hermsen R; "Pattern recognition in a database of cartridge cases", Proceedings SPIE, 1999, 3576, pp. 104-115.*

This chapter discusses several existing systems for collecting spent ammunition data for forensic investigation. These databases store images of cartridge cases and the marks on them. Image matching is used to create a hit list of the cartridges in the database that have marks that are most similar to the marks on the cartridge case under investigation. In this research the different methods of feature selection and pattern recognition have been described that can be used to optimize the results of image matching.

Chapter 5, **Databases of Shoe marks** is based on:

- *Geradts Z; Keijzer J; "The Image database REBEZO for Shoe marks with developments on automatic classification of shoe outsole designs", Forensic Science International, 1996, 82(1), pp. 21-31.*

- *Geradts Z; Keijzer J; Keereweer I; "Automatic comparison of striation marks and automatic classification of shoe marks", Proceedings SPIE, 1995, 2567, pp.151-164.*

This chapter describes methods for recognition of shapes in shoe profiles, with a focus on the database REBEZO that contains video-images of footwear designs. Efforts aimed at the automatic classification of outsole patterns are discussed. The algorithm for automatic classification first segments the separate shapes in a shoe profile, after which Fourier-features are selected for the separate elements and classified with a neural network.

Chapter 6, **Databases of Logos of Drugs Tablets** is based on:

- *Geradts, Z; Bijhold, J; Poortman, A; Hardy, H; "Databases of logos of drugs tablets" submitted for publication.*

- *Geradts Z, Hardy H, Poortman A; Hardy H; Bijhold J; "Evaluation of contents-based image retrieval databases for a database of logos of drugs tablets". Proceedings SPIE, 2001, 4232, pp. 553-562.*

In this chapter we evaluate the different approaches to content based image retrieval of the logos of drug tablets. The retrieval methods are compared using a database of 432 illicitly produced tablets. The results for this database are then compared to the MPEG-7 shape description methods, which comprise the contour-shape, bounding box and region-based shape methods. In addition, we compared the log polar method with the MPEG-7 shape-description methods.

Chapter 7: **Summary and Discussion**

This last chapter discusses the results presented in this thesis in the light of recent developments and the value of the different image databases for forensic investigations. Updates are given where appropriate and other approaches to pattern recognition   in   forensic   databases   are   discussed.

2   State-of-the-Art

Abstract

This chapter provides an overview of existing image databases and the methods for searching the image contents of these databases. Developments in the field of visual information retrieval in general are discussed with respect to their applicability to forensic databases.

2.1   Introduction

Developments in digital photography and video imaging have resulted in a huge increase of the number of still images and video sequences that are stored in digital format. Many organizations now have large image databases in digital format that they would like to access on-line. Therefore, the field of content-based retrieval from image databases has emerged as an important research area in computer vision and image processing.

Visual information retrieval requires a large variety of knowledge. The clues that must be pieced together when retrieving images from a database include not only elements such as color, shape, and texture, but also the relation of the image contents to alphanumeric information, and the higher-level concept of the meaning of objects in the scene[7] (e.g., the conclusions that can be drawn by a human being, like that certain impression marks are made with a screwdriver)

This chapter provides an overview of the different kinds of visual retrieval systems, image features, methods for indexing these features, and methods for measuring the effectiveness of a visual retrieval system.

2.2   Types of visual retrieval systems

Del Bimbo[7] divides visual retrieval systems into three different generations:

First generation visual information retrieval systems

In first generation visual information retrieval systems images are linked in a database, and can be searched by text strings. These text strings can either be related to a feature in the image itself, or to the image (e.g., suspect's name, place and date of crime). These strings are stored and can be searched in a structured way, as in classical SQL-databases.

Text strings are often subject to classification into one of a limited number of allowed strings. This approach is taken because free text is susceptible to spelling errors and allows the use of several strings with the same meaning. Users of databases that employ string classification must be trained in the appropriate classification method in order to (at least partly) prevent users from classifying features non-uniformly.

Text descriptors have several limitations:

- Text descriptors depend on what the user enters into the database. Different users may enter different text descriptions for the same image, and the same user may even enter different text when analyzing the same image on a second occasion.

- Several image features, for example texture and color distribution, are difficult to describe unambiguously using text descriptors.

- Entering text strings in a database requires much effort from the user, and any changes to the classification rules will make the reclassification of images necessary.

An example of a first generation visual information system is a database of shoe marks in which the user visually determines the shapes in the shoe mark (e.g., circles, triangles) and enters these shapes into the database as text strings.

Second-generation visual information systems

Second-generation visual information systems provide different ways of searching the database, enabling searches based on features such as texture, shape, and color. Such feature-based searches can be combined with searches for textual information.

The second-generation systems are based on a similarity search that ranks the images in the database based on a computable measure for their similarity to a chosen image. Similarity searches often involve user interaction, whereby the user provides feedback on the relevance of the search results by selecting a different feature, or modifying the weight of certain features.

Most research in this area now focuses on defining useful features for the comparison of images, efficient database indexing, and the user interface. The literature also gives attention to 3D-databases and video-databases[8].

Third generation visual information systems

Third generation visual information systems are yet to be realized. These systems are envisaged as working in an "intelligent" manner, similar to the functioning of the human visual system. Such systems would learn from previous examples and draw conclusions based on experience. These systems remain yet hypothetical because knowledge of the human visual system is limited.

2.3   System Architecture

Several subsystems can be identified within the architecture of retrieval systems for 2D images:

- Pre-processing of the image to reduce the influence of different acquisition circumstances (e.g., differences in illumination).

- Extraction of low-level features of visual data (e.g., shape and color). Image processing and pattern recognition are used to measure such features.

- Extraction of high-level features and image semantics (e.g., recognition of a shoe brand and type based on the shoe profile). In some cases, semantics

can be extracted automatically from the images based on a combination of low-level features and rules.

- Description in textual form of the image contents and acquisition characteristics (type of camera, image size, image resolution, number of images in a sequence, information available about the individual correspondence with the images, meta data describing the content etc.)

- Visualization, which presents a view of the data for inspection, thereby improving the effectiveness of the search.

- Indexing and pre-selection, this filters out images that are not pertinent to a query and extracts only those database items that are relevant to the query.

- Retrieval: matching procedures and similarity metrics.

- Relevancy feedback: a mechanism by which the user can give feedback by indicating positive or negative relevance of retrieved items.

A flowchart of the process for visual information retrieval is shown in Figure 2-1.

2.4   Visual Content

Previous studies on information retrieval from image databases based on visual contents have used features such as color, texture, shape, structure, and motion, either alone or in combination[9,10].

2.4.1   Color

Color reflects the chromatic attributes of the image as it is captured with a sensor. A range of geometric color models[11] (e.g., HSV, RGB, Luv) for discriminating between colors are available. Color histograms are amongst the most traditional technique for describing the low-level properties of an image.

2.4.2   Texture

Texture has proved to be an important characteristic for the classification and recognition of objects and scenes Haralick and Shapiro[12] defined texture as the uniformity, density, coarseness, roughness, regularity, intensity, and directionality of discrete tonal features and their spatial relationships. Haralick[13] reviewed the two main approaches to characterizing and measuring texture: statistical approaches and

structural approaches. Tuceryan and Jain[14] carried out a survey of textures in which texture models were classified into statistical models, geometrical models, model-based methods, and signal processing methods.

2.4.3 Shape

Traditionally, shapes are expressed through a set of features that are extracted using image-processing tools. Features can characterize the global form of the shape such as the area, local elements of its boundary or corners, characteristic points, etc. Shapes are viewed as points in the shape feature space. Standard mathematical distances are used to calculate the degree of similarity of two shapes.

Preprocessing is often needed to find the relevant shapes in an image. Multiple scale techniques[15,16] are commonly used as filters to elucidate the shapes in an image. In many cases, shapes must be extracted by human interaction, because it is not always known beforehand which are the important shapes in an image.

The property of invariance (e.g., the invariance of a shape representation in a database to geometric transformations such as scaling, rotating, and translation) is important in the comparison of shapes

2.4.4 Structure

The structure of an image is defined as the set of features that provide the "Gestalt" impression of an image. The definition of "Gestalt" is a typical perceptual experience in which the whole is understood as something more than the sum of the parts. Furthermore, this gestalt may be perceived before the parts comprising it. The distribution of visual features can be used to classify and retrieve an image. Image structure can be important for achieving fast pre-selection of a database (e.g., the selection of a part of the database) based on the image contents. A simple example is distinguishing line drawings from pictures by gray values and location in the image.
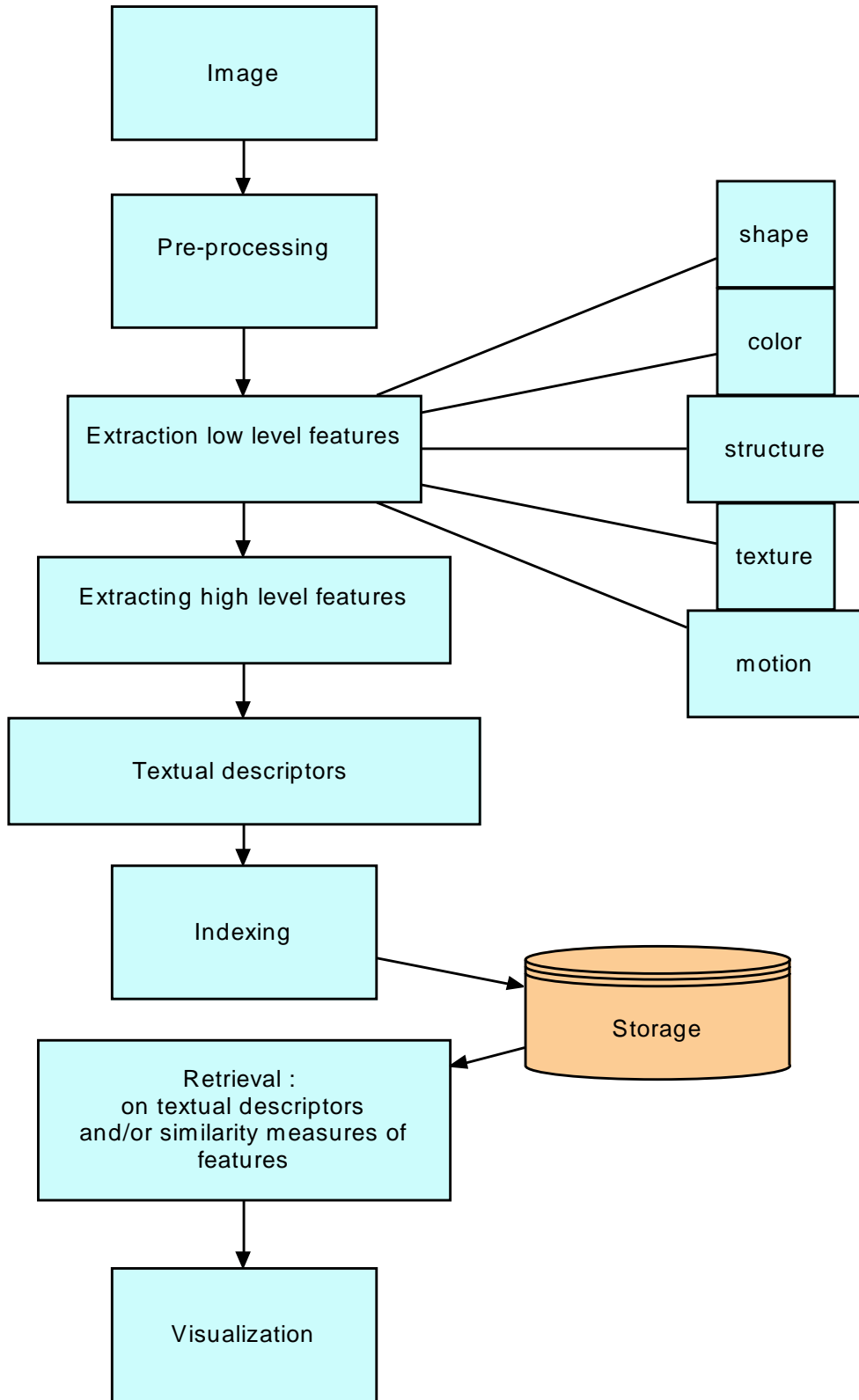
Figure 2-1: Flowchart for a visual information retrieval system

2.4.5 Motion

Motion is an important feature in video databases and is extracted by analyzing consecutive frames in temporal image sequences. There are several models[17] for calculating the motion vectors from a sequence of images.

2.5 Similarity Measures

Similarity measures are used to identify the degree of correspondence between images.

Many similarity measures are based on the L_p distance between two points. For two points (x,y) in R^k; the L_p distance is defined as $L_P(x, y) = \left(\sum_{i=1}^{k} |x_i - y_i|^p \right)^{1/p}$, which is also called the Minkowsky distance. For p=1, we get the city-block distance.

The most appropriate similarity measure depends on the abstraction level of the representation of image objects: raw pixels or features.

Raw Pixels

At the lowest abstraction level, objects are simply aggregations of raw pixels from the image. Comparison between objects or regions is done on a pixel-by-pixel basis, and commonly used similarity measures include the correlation coefficient, Sum of Absolute Valued Differences (SAVD), the Least Square Distance, and mutual information[18]. Comparison at the pixel level is very specific, and therefore is only used when relatively precise matches are required.

Features

Features are the numerical data values extracted from images or objects in the images, such as color, shape and texture.

Several similarity measures are commonly used for feature comparison[19]: the Euclidean distance, the Minkowsky distance, and the chamfer distance[20]. Another approach to measuring similarity is the use of transformational distances.[21] This approach requires the definition of a deformation process that transforms one shape into another, where the amount of deformation is a measure of the similarity. One

such group of models are the elastic models, which use a discrete set of parameters to evaluate the similarity of shapes.

Studies in psychology have pointed out that algorithm-based systems have a number of inadequacies compared to the human visual system. The Earthmover's distance[22] is an example of a new kind of distance measure that, according to the developers, approximates the human visual system well. The developers of the Earthermover's distance claim that it is easy to implement and that efficient indexing methods are possible. Examples in the literature[22] with color and texture comparison are promising.

2.6   Indexing methods

If a database contains many images, the visual information must be indexed to improve the speed of searching the database. This is similar to the case of textual information, for which classic indexing methods such as hashing tables are employed.

Below we give a brief overview of the approaches to indexing[7].

2.6.1   Indexing of String attributes

String attributes of images are expressed in the form of keywords, strings, or scripts. Conventional indexing techniques for textual information can be used to index keywords or alphanumeric strings. Hashing tables and signature files are the most common indexing methods employed. A signature is a code that represents a feature; signatures can be inserted into a hash table. Signature files are particularly useful as filters that excludes uninteresting images before searching.

2.6.2   Indexing of Visual attributes

If visual attributes (shape, color, and texture) are modeled in a multi-dimensional metric feature space, index structures known as point access methods (PAMs), developed for spatial data, can be used.[23] If the database is small (i.e., up to a few thousand images), the entire database can fit into main memory; otherwise, the index must be read from the hard disk, which results in a decline of performance. The performance of PAMs depends on the distance measure and the number of features used to represent the properties. When the number of features exceeds ten, the

performance of most PAMs diminishes with increasing number of features [7]. For this reason, high-dimensional features are usually mapped to a lower-dimensional space. Index structures can be either static or dynamic.

Static structures do not allow the addition or removal of items, whereas dynamic structures allow changes in the database without the need to rebuild the complete index. In visual information retrieval, weights are used to indicate the relative relevance of visual features. These weights are often adjusted at run time. Index structures should therefore incorporate similarity computation so that clusters of similar images can be created dynamically.

There are also other methods for indexing, e.g. K-d-trees[24], R-trees[25], and SS-trees[26], which are dynamic data structures for feature indexing[7.] SS-trees were specifically developed to permit similarity indexing in imaging databases. A new development is the use of active indexes.[27] These indexes are based on the idea that the images in a database can request image-processing operations, display themselves in an appropriate way, or search for related images. The active indexes are constructed in the form of dynamically changing nets. The implementations of indexing with dynamic data structures is not within the scope of this thesis.

2.7   Performance

If we evaluate the retrieval performance of an image database, it is necessary to have a test set and a ground truth, which means that it is known which images match with the image that is queried in the database. For quality assurance, it is important to have a representative test database, which can be used to measure the performance of the database. This means that the test set will be compared with the complete database. The optimal situation for retrieval is that the relevant images are retrieved, and that there are no missed relevant images.

In traditional retrieval[28], a measure of performance by an evaluator is given in Table 1 (provided the ground truth is known).

Table 1: Judgment by evaluator

	Relevant	Not Relevant
Retrieved	**A (correctly retrieved)**	**B (falsely retrieved)**
Not retrieved	**C (missed)**	**D (correctly rejected)**

Recall and precision measures are used to evaluate the performance of a retrieval method.

Recall $= \dfrac{relevant\_correctly\_retrieved}{all\_relevant} = \dfrac{A}{A+C}$ (In the field of medicine "recall" is also known as "sensitivity"[29])

The recall is frequently visualized in a graph of recall vs. percentage of the database.

Precision $= \dfrac{relevant\_correctly\_retrieved}{all\_retrieved} = \dfrac{A}{A+B}$ (also known as positive predictive value).

For optimal performance of database retrieval, the recall and precision should be as close as possible to one.

When a user makes a query, it is important tha the highest ranked matches represent true positives and also that all true positives are highly ranked in the matching procedure. Otherwise, the user must browse the complete database to ensure that no items were missed.

Apart from recall and precision measures, computational complexity is also important in evaluating the performance of a retrieval method.

The construction of a representative test set is crucial to all recognition applications. Several test sets have been compiled for testing the performance of recognition methods (e.g., the National Institute of Standards and Technologies has developed representative test databases[30] for faces and fingerprints)

2.8 Biometric databases

Biometric systems are an important area of research in visual information retrieval systems. In this section, examples of biometric systems are discussed in relation to the methods described earlier.

For biometric systems, a group of measures are used to identify or recognize a person. For a measure to be suitable for a biometric system, it must satisfy several requirements:[31]

- Universality: the biometric measure must be a characteristic possessed by all people.
- Uniqueness: no two individuals should have the same biometric measure
- Permanence: the biometric measure should not change with time.

Examples of biometric measures are fingerprints, palm prints, DNA, iris, face, handwriting, gait, and speech. In the next section, some implementations of databases of fingerprints, faces, and handwriting are described, which meet most of the requirements mentioned above. A video registration of gait appeared not to meet these requirements.

2.8.1 Fingerprints

In human fingerprints, there are three basic fingerprint patterns: Loops, Arches, and Whorls. Within these patterns are characteristic details that are referred to as minutiae points .

The most commonly used system for classifying fingerprints manually is the Henry Classification scheme[32] . This classification system dates back to the early 1900s, when fingerprints were classified manually, however it is not used in present day commercial Automatic Fingerprint Identification Systems (AFIS).

Three approaches[33] have been used in commercial automatic fingerprint systems:

- Syntactic: the ridge patterns and minutiae are approximated as a string of primitives. When a new pattern arrives the string of primitives is formed and passed to a parser whose output yields the class of the input pattern. It is also possible to extract features based on minutiae and then present the features using a graph data structure. Exploiting the topology of features provides structural matching.

- Neural network: the feature vector is constructed and classified by a neural network. Several types of feature vectors and neural networks have been used.

- Statistical : the feature vector is constructed and classified by a statistical approach.

Two approaches have been developed for the process of measuring the similarity of classified fingerprints: point matching and structural matching. In point matching, two sets of minutiae code are aligned using their locations. In addition, the sum of the similarities between the overlapping minutiae is calculated. The similarity between two minutiae is measured using the attributes of the minutiae. In structural matching, a graph is constructed for each fingerprint that codes the relative locations of minutiae. As a similarity measure, these graphs are compared for two fingerprints.

A problem confronting fingerprint matching is the lack of reliable algorithms for extracting minutiae. Existing algorithms result in spurious minutiae because of an inability to cope with anomalies introduced by factors such as scars, over-inking, and sweat. For this reason human intervention is generally needed after application of these algorithms in order to check that the fingerprint classification is correct.
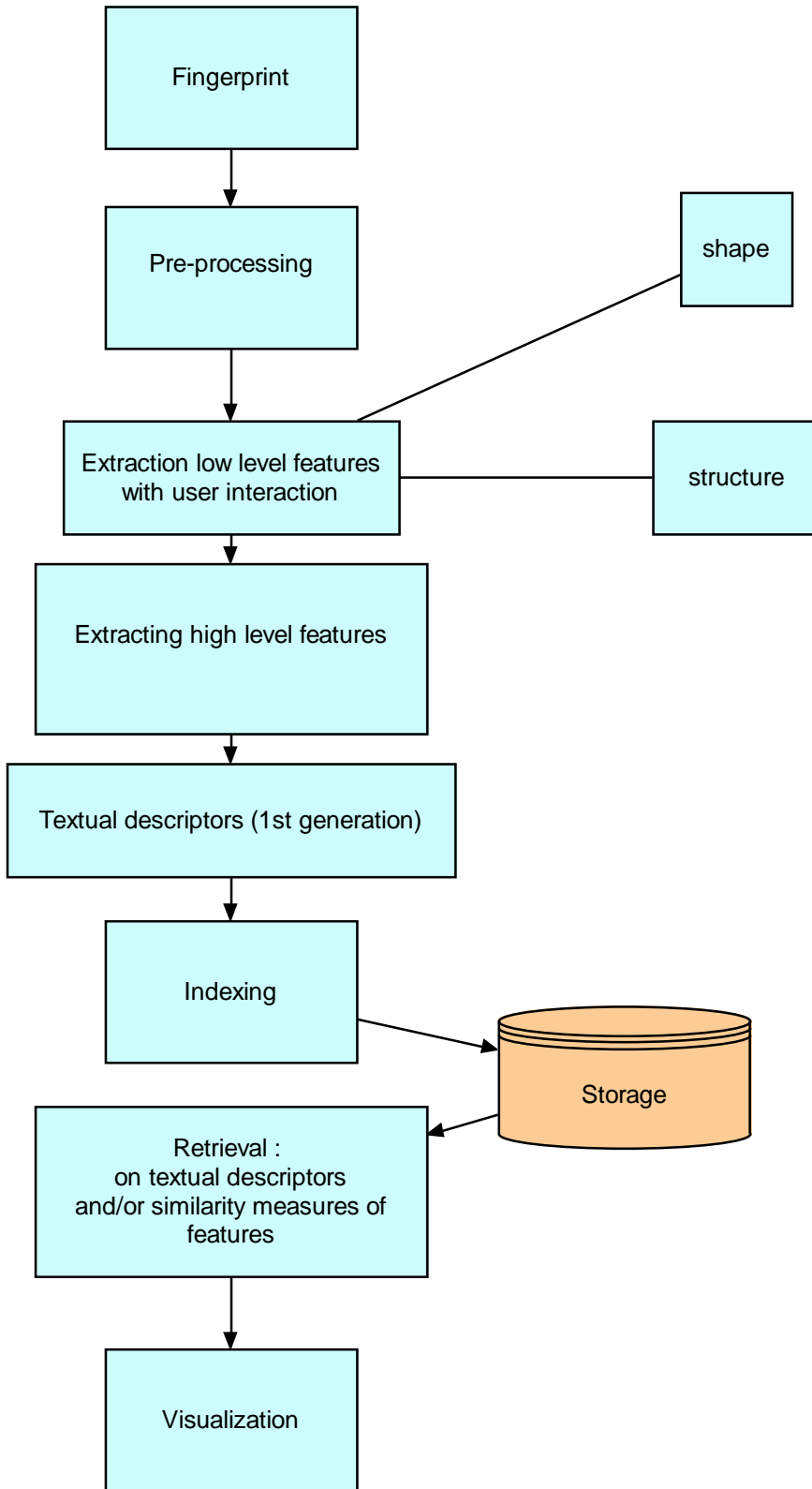
Figure 2-2: Flowchart for fingerprint system
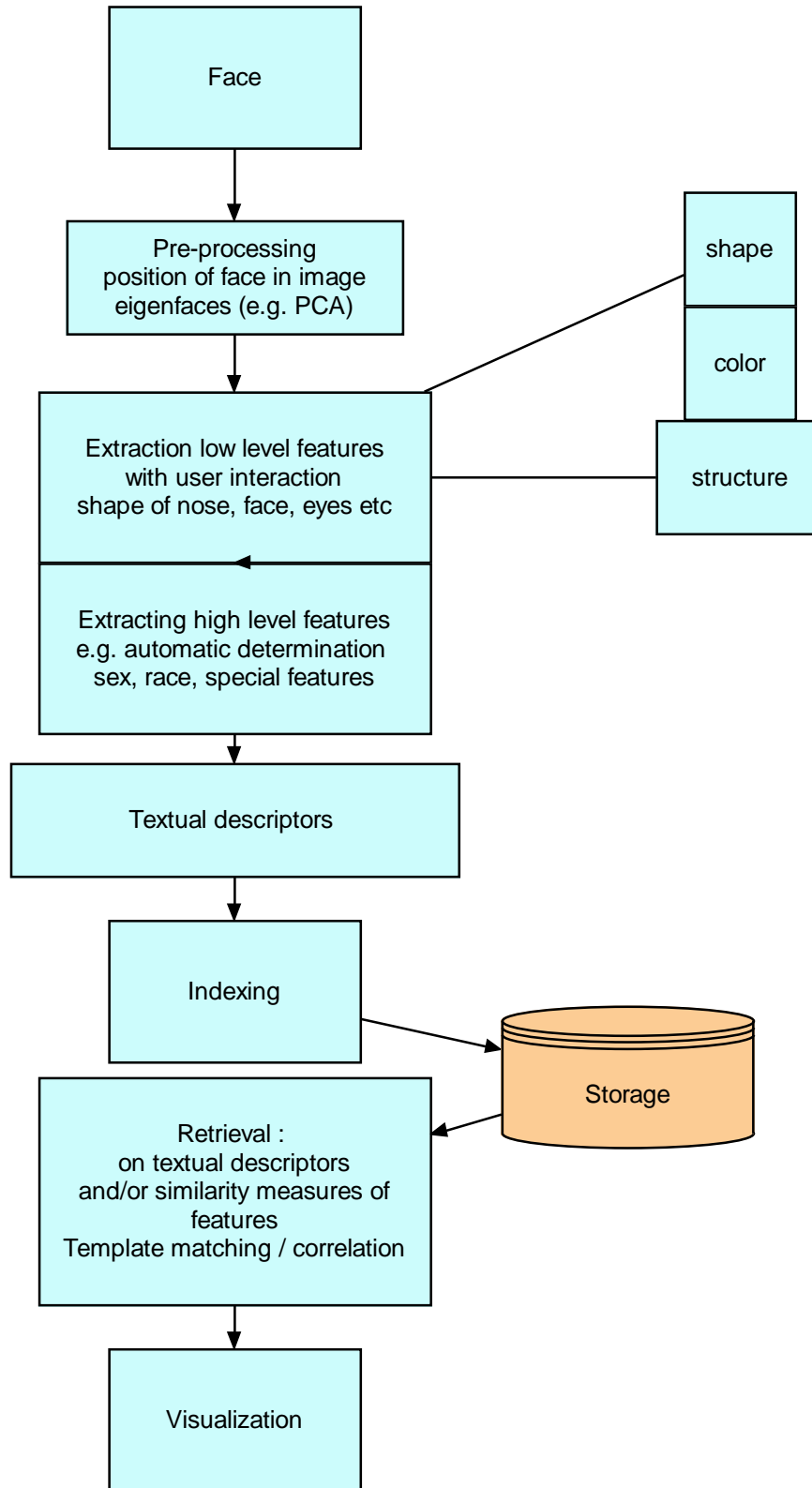
Figure 2-3: Flowchart for face recognition

2.8.2 Faces

Images of faces are easy to obtain with a camera, and are important for the surveillance industry. Recognizing faces in camera images is particularly difficult because the faces are not acquired in a standardized approach. The face can be in any position and the lighting and magnification can vary. Furthermore, hairstyle, facial hair, makeup, jewels, and glasses all influence the appearance of a face. Longer-term effects on faces are aging, weight change, and facial changes such as scars or a face-lift.

Images of faces are generally taken under standardized conditions for police investigations.[34] Before a face can be analyzed, it must be located in the image[35]. For face recognition systems to perform effectively, it is important to isolate and extract the main features from the input data in the most efficient way.

Template matching for face recognition involves the use of pixel intensity information, either from the original gray-level dataset or from a pre-processed version of the image. The templates can be the entire face or regions corresponding to general feature locations such as the mouth and eyes. Cross correlation of test images with all training images is used to identify the best matches.

One of the main problems that must be overcome in face recognition systems is removing redundant sampling to reduce the dimensionality[36]. Sophisticated pre-processing techniques are required to attain the best results.

Some face recognition systems represent the primary facial features (e.g., eyes, nose, and mouth) in a space based on their relative positions and sizes. However, important facial data may be lost using this approach[37], especially if variations in shape and texture are considered an important aspect of the facial features.Statistical approaches are also used in the analysis of faces. For example, Principal Components Analysis (PCA[38]) is a simple statistical dimensionality reducing technique that is frequently employed for face recognition. PCA's extract the most statistically significant information for a set of images as a set of eigenvectors (often referred to as 'eigenfaces'; an example is shown in Figure 2-4). Once the faces have

been normalized for their eye position they can be treated as a one-dimensional array of pixel values.

In Figure 2-3 a schematic overview of the methods used for face recognition is shown.

For forensic identification, it is desirable to have reference images of the suspect in the same position as in the questioned image.. Approaches for positioning a suspect are described by van den Heuvel[39] and Maat[40]. Positioning takes much time, and this is the reason that in commercial systems are designed to work without restrictions on positioning.

In practice, it appears that it is not possible to identify persons with regular CCTV-systems. The expectations of face recognition software is sometimes too high, as can be seen in a trial in Palm Beach for searching terrorists[41]. It appeared that the system falsely identified several people as suspects and at times been was even unable to distinguish between men and women.
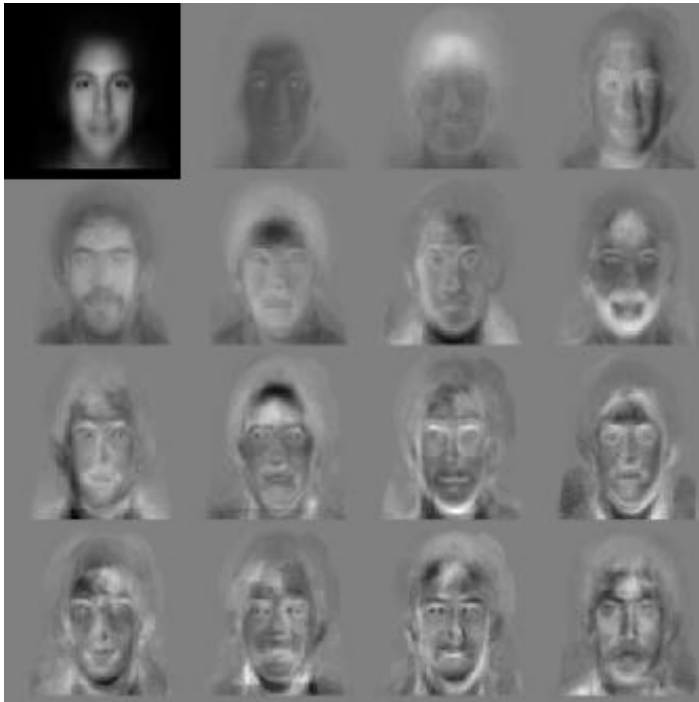
Figure 2-4 : Example of Eigenfaces from MIT Image Software
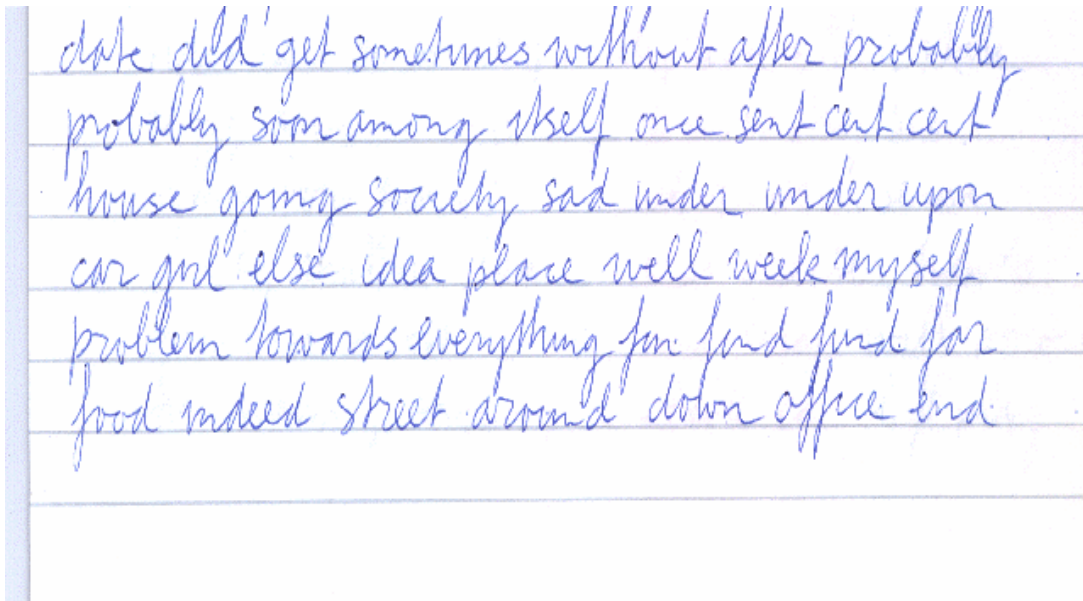
Figure 2-5: Example of Handwriting

2.8.3 Handwriting

Various handwriting comparison systems[42] exist on the market. One system that has been in service for over 20 years is the Fish system, which was developed by the Bundes Kriminal Amt in Germany. Another well-known system is Script, developed by TNO in The Netherlands.

In both systems, handwriting is digitized using a flatbed scanner and the strokes of certain letters are analyzed with user interaction. The features of the handwriting are represented as content semantics.

The Fish system[43] was in prototype at the Bundes Kriminal Amt in Wiesbaden in 1981, where it was mainly used to analyze terrorist writings. In the 1990s, this system was delivered to The Netherlands Forensic Institute for regular casework and to the Secret Service for analyzing letters to the President.

The Fish system was developed on a VAX/VMS and uses five processes for automatic and interactive graphic feature extraction of handwriting:

- *Text Independent Features*

The white/black pixel chain statistics and the auto-correlation function, are measures for the texture.

- *Interactively measured features*

These are computer-aided measurements of general features of the writing carried out by the user. The user selects a figure or character of the handwriting. The measured characteristics are the height, width and the vertical length of strokes and the angle of strokes

- *Isolations*

Individual graphic elements can be marked and isolated. These elements are later compared to reference samples. Isolations are especially important if only a few characters of the handwriting are available.

- *Meta data*

The handwriting expert might recognize special characteristics of the writing (structure) that are not recognized by the computer (e.g., writing method, handwriting characteristics, or unusual writing of characters, numbers, use of margins and other signs). Shape deformation is used for matching.

- *Line Tracings*

The pencil movement is traced automatically after the user has marked some points on the letter.

In 1991, the Fish system comprised 55,000 handwriting samples from 25,000 individuals. Thus, much effort has been devoted to compiling this database of handwriting.

The Script system[44] has been in use since 1996 by the Metropolitan Police in The Hague, and several pilots have been made in other parts of The Netherlands. The system works on a regular PC and uses interactively measured features that are comparable to Fish. The procedure is much more sophisticated and automated compared to Fish. The Script system uses also Meta data that are similar to those of Fish.

A problem with Fish and Script is that the effort needed to fill and search them is huge. Nowadays handwriting is found less often at the scene of crime due to factors such as increased use of computers and the discontinuation in The Netherlands of guaranteed cheques; hence, the number of critical cases involving handwriting has decreased. From the limited results in practice, it can be concluded that the use of these systems is economically not feasible in regular casework. In Figure 2-6, a flowchart for handwriting databases is shown.
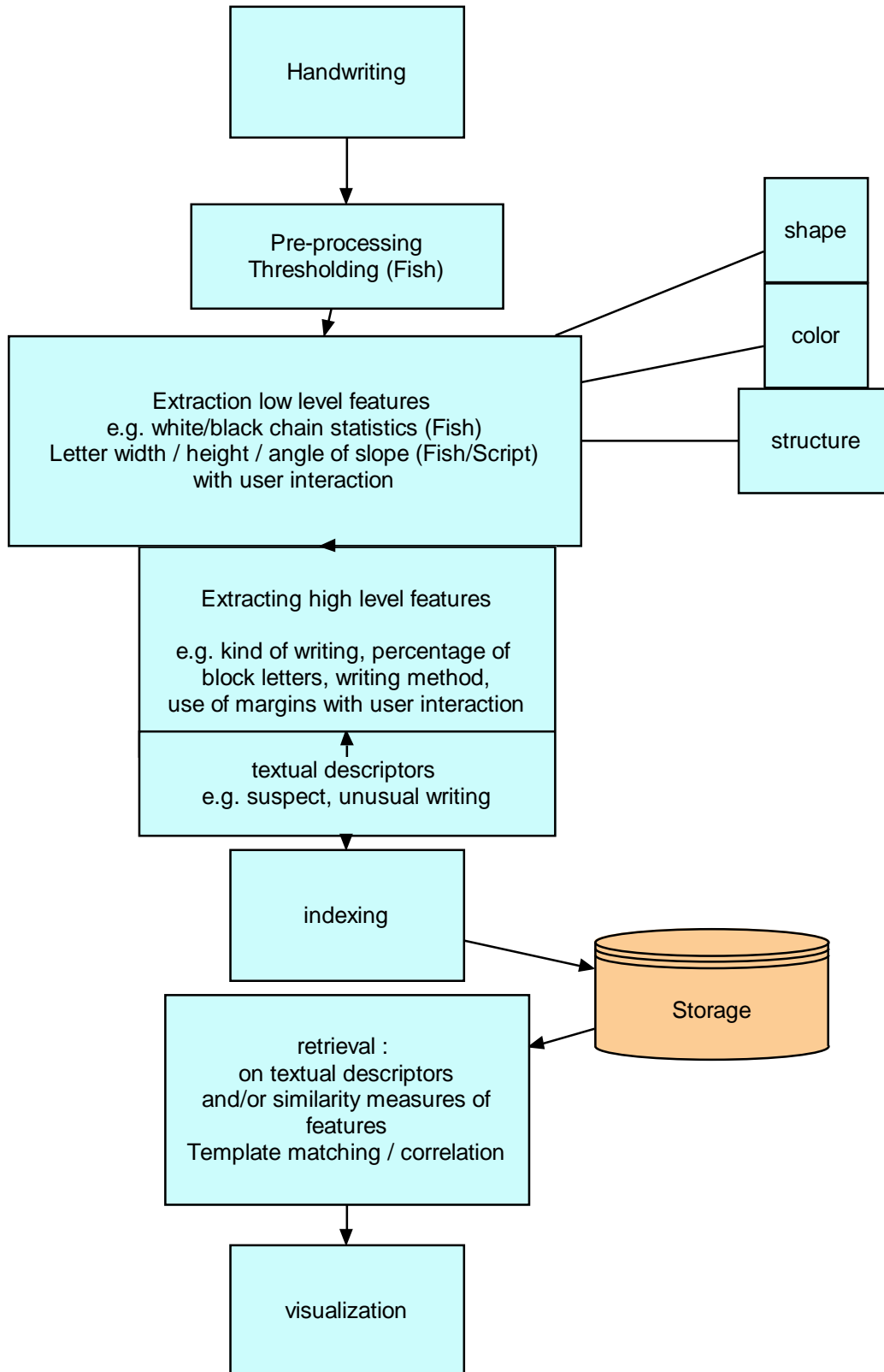
Figure 2-6: Flowchart for Handwriting systems

2.8.4 Gait

Gait is a new biometric[45] aimed to recognize subjects by the way they walk. Gait has several advantages over other biometrics, most notably that it is non-invasive and perceivable at a distance when other biometrics are obscured.

Nowadays, many crimes, including bank robberies, are captured using CCTV surveillance systems sited at stores, banks and other public places. These recordings are often passed to our institute for the purpose of identification. If a criminal has covered his face, recognition is much more difficult. Then the next question whether or not the gait of the perpetrator is comparable with the gait of the suspect. For this purpose, it was necessary to find parameters in the gait that are characteristic of a subject.

Since there is little known about the characteristics of gait from the literature and even less about the use of gait in forensic identification, we have started a research project on gait analysis. Human gait contains numerous parameters. These parameters can be categorized into spatial-temporal and kinematic parameters of CCTV-images, gait analysis is even more difficult, since in practice often a few images available and the subjects wear clothes.

Because it was impossible to investigate all gait parameters in our study[46], a selection has been made on the criterion that the gait parameters could also be obtained in non-experimental settings. In our experiments, markers were used as shown in Figure 2-7. The subjects wore only their underwear and shoes.

From this pilot project, it appeared that with this measurement the gait was not unique. Precision and recall were too small to allow recognition. For forensic analysis of CCTV-images, gait analysis is even more difficult, since in practice, only a few images are available and the subjects wear clothes.

∝ :hip angle   φ :thigh angle   Ψ :trunk angle
β :knee angle   δ :foot angle
γ :ankle angle

Sagittal view   Frontal view   Transversal view
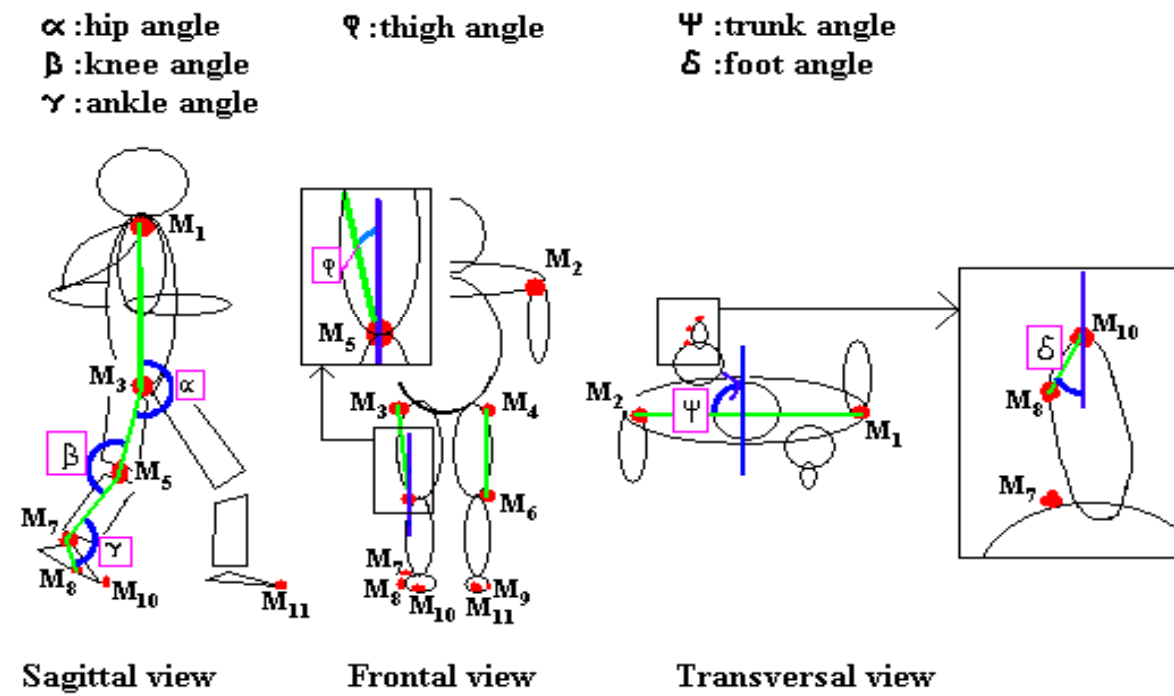
Figure 2-7: Positions of the markers and the calculated angles for gait analysis

3   Databases of Tool marks

Abstract

A tool mark imaging system database (named TRAX) has been developed. The database is filled with video-images and alphanumeric data about the tool marks (width, kind of tool mark, etc.). The angle of the tool with the surface, the material of the surface, and the way the tool is moved on the surface, influence the shape of the striation mark. A new algorithm, referred to as the adaptive zoom-algorithm for extracting a representative signature of this striation mark has been developed. The similarity measure is based on the Standard Deviation of the Grey-value Differences.

Furthermore, the comparison of these signatures should also deal with wear of the tool and variations between test marks and the mark found at the scene of crime. For that reason the adaptive zoom-algorithm is also used for the comparison of signatures. The development is based on the way a tool mark examiner conducts the comparison.

The algorithm works well for side light images of deep and complete striation marks and is implemented in TRAX. A test showed that by using 3D images of striation marks, the results of correlation improved.

3.1   Introduction and Motivation

Tool marks are often found at the scene of crime. They can appear in a wide variety of shapes depending on the tool and on the surfaces where the tool mark is formed. In many burglary cases, pliers, screwdrivers, or crowbars are used for entering a building. These tools will cause marks that appear in different shapes: striation marks and impression marks. In several police regions.

.
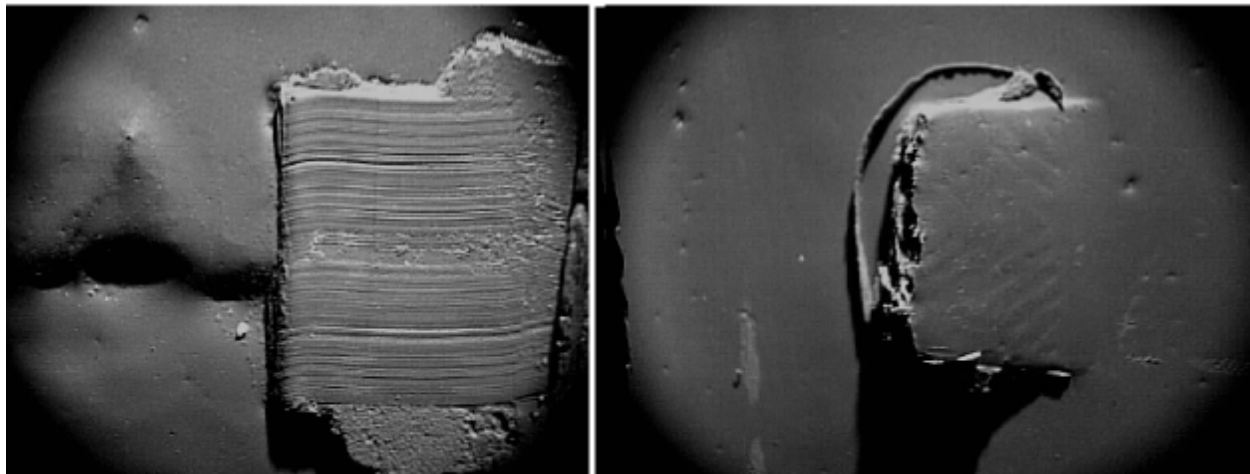
Figure 3-1: Silicon casts of tool marks in the database. Left: striation mark; right: impression mark of a screwdriver

in The Netherlands, the images of the tool marks that are found at the scene of crime are stored in a database. When a suspect has been found with tools, test marks are made with these tools and compared with the database. In Figure 3-1 an example is shown of a striation and an impression mark in a police database.

This chapter describes the forensic investigation of toolmarks and the use of our tool mark and investigation system. A new algorithm is presented for the extraction and matching of signatures. The results of experiments on two-dimensional and three-dimensional data are presented.

3.1.1 Forensic Investigation

In our research described in this chapter, we focus on striation marks, since they are most time-consuming for an examiner making comparisons. Since the tool can have many different angles to the surface, and for each angle a different striation mark is formed, the examiner has to make several test striation marks with different angles of the tool in wax or another test material that is softer than the tool

In the case of a screwdriver, the examiner will make at least three test striation marks in wax under different angles for each side of the screwdriver (Figure 3-3). All of these test marks have to be compared with the striation marks. To acquire a standard

condition of the surface where the striation mark is visualized, casts are made of the striation marks with the gray silicon material Silmark[47]. For tool mark investigation, it is necessary to use a comparison macroscope in which a side-by-side comparison is possible of the cast of the test mark with the cast of the scene of crime.

Striation marks are caused by irregularities in the upper part of the blade of the screwdriver when scraping off material of a surface that is softer than the tool itself. If the upper part of the blade of the screwdriver is damaged or has grinding marks, these can be identifying characteristics. Depending on these damages and grinding marks, and the quality of the tool mark itself, a qualified examiner can conclude that the blade of the screwdriver has caused the striation mark under investigation.

A complexity with tool mark examination is that the tool mark found at the scene of crime might be partial. In this case, the striation mark should be matched to the test striation mark by shifting the tool mark. Furthermore, the screwdriver could be damaged in the meantime because it has been used, and this will cause the striation marks to differ. In addition, the striation mark can be (partially) "zoomed" because of stretch or shrinkage of the material (e.g. elastic deformation) in which the tool mark has been formed. Finally, the angle as shown in Figure 3-4 might also give a gradient in the tool mark.

Striation marks are very time consuming for the examiner to compare with the database manually. The striation marks found at the scene of crime should be compared side by side with the test marks. Since we have at least six striation marks (for a crowbar more than for a screwdriver), a case with one striation mark found at the crime scene will result in at least twelve comparisons (the striation mark can also be upside-down). If a database contains fifty striation marks from the scene of crime,

the examiner makes at least six hundred comparisons. This will take at least five hours (30 seconds per comparison) for the examiner without resting.

In order to reduce the time of examination, it is necessary to implement a comparison algorithm for striation marks. In our research, we have studied two methods for data acquisition: 2D-acquisition by side light and 3D-acquisition by coded light approach.

Figure 3-2: Leica Comparison Macroscope UFM4

3.1.2 Tool mark Imaging System

In this chapter, we describe the Tool Mark Imaging System, TRAX, that we have developed in co-operation with the Dutch Police. The system is developed for image acquisition, entering textual descriptors, image retrieval, and image comparison.
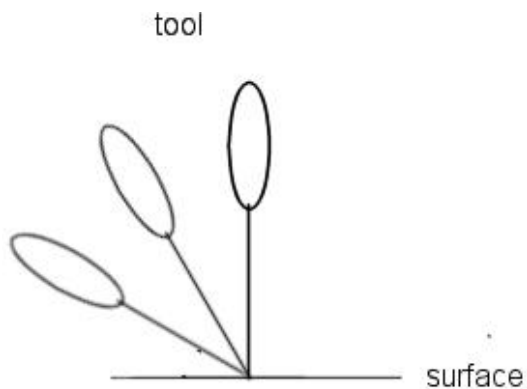
Figure 3-3: Test striation marks have to be made in at least three different angles to the surface.
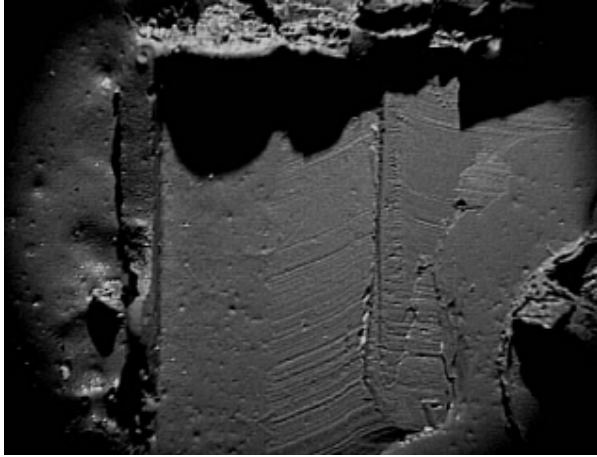
Figure 3-4: Example of a striation mark of a screwdriver that makes an angle to the surface. The striation mark is partial.

The tool mark images in the TRAX database are created by a standard procedure. A casting is made with a gray silicon casting material, and subsequently these images are stored in the database. The toolmarks should also be physically stored, for forensic identification.

The database is used for pre-selection by comparing a test mark made with the tool, with the toolmarks in the database in a side-by-side comparison screen. This screens shows on the left side the life image of a test mark and on the right side an image of a tool mark from the database.

From the pre-selection process, relevant tool marks are selected and subsequently the physical tool mark is compared with a test mark of the tool on a comparison microscope. For forensic identification, the tool itself is needed to determine the causes of the striation marks.For the tool mark system the following textual descriptors are used:

- Width of tool mark

- Type of tool (e.g., screwdriver; crow bar)

Case number of police system with administrative data of case itself (date, modus operandus, suspect, place etc.)

Figure 3-5: Screen for adding a tool mark in the TRAX system
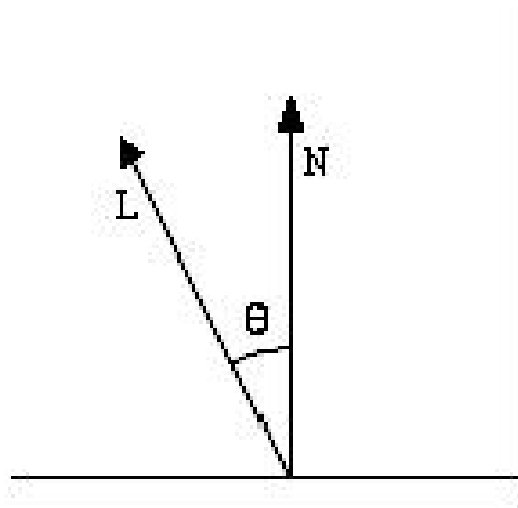
Figure 3-6: Lambert's law; the angle θ between the light vector L and the normal N determines the intensity of the light reflected from the surface.

3.2   Side Light

Investigation of tool marks investigation is normally carried out by means of side light, since this makes it possible to visualize the fine marks, depending on light source and angle. In this chapter, an explanation is given of side light with gray casting material.

Dull surfaces, such as that of gray casting material, reflect light with the same intensity in all directions[48]. Diffuse reflection is sometimes also called Lambertian reflection because Lambert's Law is used to calculate the intensity of the reflected light. Lambert's law states that the intensity of the reflected light is proportional to the cosine of the angle θ between the light vector L and the surface normal N (Figure 3-6). Lambert's law can be formulated as

$$I = I_p k_d \cos q \qquad\qquad\qquad\qquad\qquad \textbf{(1)}$$

Where I_p is the Intensity of the light source at a particular wavelength, and k_d, the diffuse-reflection coefficient, is a material property varying between zero and one. The angle θ must be between 0° and π/2 radians. The surface will otherwise be directed from the light source and shadowed. The direction to the observer is irrelevant since the light is reflected equally in all directions from the surface.

We can see that the intensity of the reflected light depends strongly on the lighting condition. Consequently, under different light circumstances or as a cause of light variations due to surface inequality, the striation mark might appear differently. If sidelight is used, the angle and intensity of the light source should be the same for each image. Accordingly, we have chosen for fluorescent light with an angle of 45 degrees with the tool mark surface. In order to avoid variations due to different surface, we have chosen the gray casting material Silmark as tool mark surface.

3.3   3D-acquisition: Coded light approach

Three-dimensional acquisition is an attractive alternative to sidelight, since sidelight does not always visualize the fine striations in a tool mark. Furthermore, the side light image is also influenced by relief in the casting itself. The method that we used for 3D imaging is the coded light approach. With this method, it is possible to acquire a 3D-image in a few seconds. This method is faster than the implementations of surface scanning laser triangulation methods that we have tested in the past.
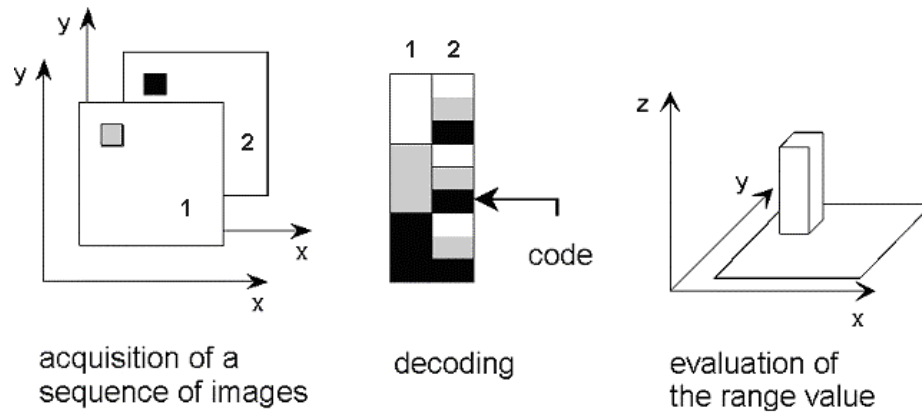
Figure 3-7: Range data acquisition using coded light (example with one spike)
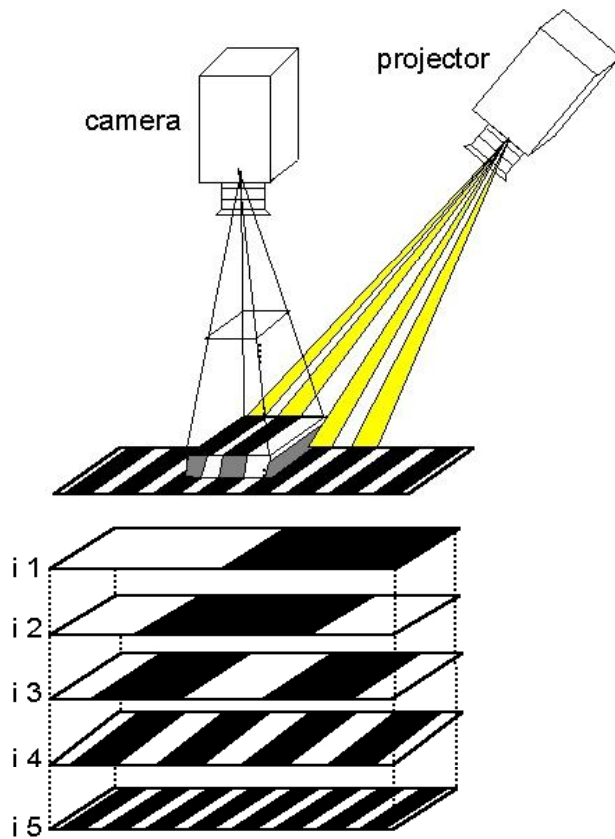
Figure 3-8: Coded Light Approach (Example of five patterns that are projected on the surface).

Figure 3-9: **OMECA coded light equipment**

The Coded Light Approach (CLA) is an absolute measurement method, requiring only a small number of images to obtain a full depth-image. This can be achieved with a sequence of projections using a grid of switchable lines (light or dark). All the lines are numbered from left to right. The numbers are encoded with the so called 'Gray-Code'. Despite its name, the gray-code is a binary code. In this code, adjacent lines differ by exactly one bit leading to good fault tolerance. By using a special line projector, line patterns are projected. A bright line represents a binary 'zero', and a dark line a 'one'. All object points illuminated by the same switchable line see the same sequence of bright and dark illuminations. In Figure 3-7 an example of five patterns with different frequencies in patterns are shown. The depth information is measured by a phase-shift at the edges of the object.

The sequence of intensity values corresponds to the code reflected by the object and acquired in a pixel of the camera. The code leads to a light section and determines the angle of projection of the lighting stripe. The position of the activated pixel with respect to the CCD yields the viewing angle (Figure 3-7). The determination of the

corresponding object height occurs without considering the adjacent pixels. From the knowledge of the angle of projection, the viewing angle and the geometric parameters of the set-up, all three coordinates of the object point can be calculated. In Figure 3-8 all of the calculated object points of a measurement are represented in a three-dimensional diagram.

High reliability identification of light planes with minimal assumptions on the nature of the scene is achieved by sequentially projecting several patterns. A robust and widely applied coded light system based on spatio-temporal modulation has been described by Kato[49]. Gray codes are used to label light planes, and each illumination pattern represents one of the bit planes of the Gray code labels.

In this study, we used the coded light system OMECA[50]. In this system, lines are projected on the surface by means of a micro mirror device. The system consists of a CCD-camera, a frame grabber, a micro mirror device, and a computer that controls the stripes that are projected, and calculates the depth of the surface. The advantage of a micro mirror projector compared to an LCD-projector is that we have a higher light

intensity and that the pattern itself has more contrast. In Figure 3-9, the apparatus is shown as used in our laboratory. With this apparatus, it is possible to measure a striation pattern with a precision of several microns[51].

3.4 Construction of a signature

Since the complete image of a tool mark gives much irrelevant information that prevents image matching, it is necessary to reduce the information to a signature to obtain a striation mark.

As can be seen in Figure 3-10, there exist fluctuations in a striation mark. For this reason, it is often not sufficient to sample one line out of the striation mark as a signature. We have developed an averaging algorithm, that utilizes the information of several lines in the striation mark to obtain a better signature. The explanation of this algorithm, referred to as adaptive zoom algorithm, is based on gray values. For the three-dimensional approach, gray values can be replaced by depth values z.

The user first has to select a relevant area of the image, where the striation marks are clearly visible. In Figure 3-10 an example is shown of a selection by a user.
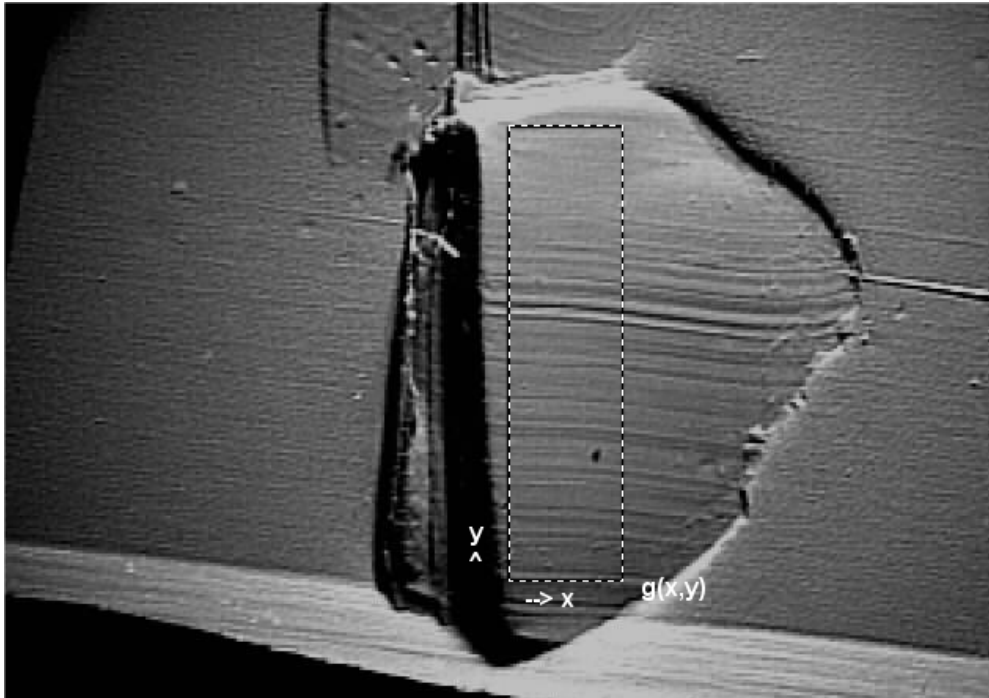
Figure 3-10: The user selects a part of the Striation mark g(x,y)
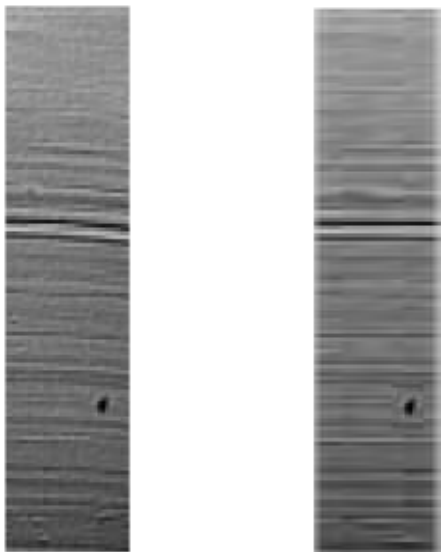
Figure 3-11 : left side : sample striation pattern of figure 3-10; right side : the result (horizontally and straight striation lines) after adaptive zoom calculation and application of the deformation matrix.

Averaging algorithm

Given an image g(x,y) were g(x,y) is the gray value of the image at position x,y, we can average the gray values for N vertical lines, so as to obtain signature S:

$$S(y) = \frac{\sum_{x=0}^{x=N} g(x, y)}{N}$$ **Equation 2**

The disadvantage of this approach is that all striation lines should be horizontal. In most cases, the striation lines are not horizontal in the plain (see Figure 3-10 and Figure 3-12 where the striation lines are horizontal only of the angle b is equal to 90°). To compensate for this, we have implemented a method that will follow the striation lines themselves, which is referred to as the adaptive zoom algorithm. This method is inherently adaptive, since it also compensates for striation marks that have a local variation due to elasticity of the surface and other movements of the tool during the striation.

Adaptive zoom

The adaptive zoom algorithm is developed for calculating a deformation matrix of the user selection that results in horizontal striation lines which are straight as is shown in the right side of Figure 3-11.

Table 2: Example of comparing two lines with the adaptive zoom algorithm. A shift of +1/2 will result in the lowest difference for this case for a gray value of 200 in line 1. This will be chosen as the value for the signature.

Shift Line 2 vs. Line 1	Gray Value Line 1	Gray Value Line 2 with shift	Difference in gray value
-1	200	75	-125
-0.5	200	125 (75+175)/2	-50
0	200	175	-25
+0.5	200	200 (175+225)/2	0
1	200	225	50
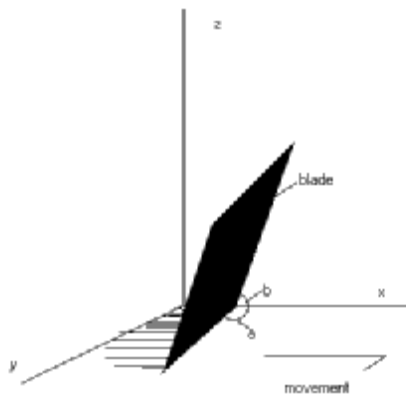
Figure 3-12: Schematic view of blade making a striation mark with the angles a (plane x-y versus blade) and b (plane x-z versus blade).

The adaptive zoom method is based on comparing the first vertical line g(1,y) with the line g(x(i),y), where i is the number of lines selected by the user. The pixels of each line are compared until an optimal deformation of g(1,y) versus the line g(x(i),y) is found where the grey values on a position x should match as much as possible.

From the deformation of a line, an offset is computed that is used to shift the next line prior to the match with g(1,y) in y direction. The adaptive zoom algorithm is repeated for all lines. The result is a deformation matrix for the complete area. The shift between two subsequent lines is at most one pixel.

As an example of the working of the algorithm, in Table 2 an example of one pixel-by-pixel comparison is shown. In the algorithm, also a shift of half a pixel is possible. This is calculated by averaging the subsequent pixels in the y-direction. The maximum change in shift per pixel is also one pixel, as otherwise the offset that is calculated could become unstable by small distortions in the striation mark. A flow chart of the algorithm is shown in Figure 3-13.

Finally, the average signature is displayed, and the user can validate the result by visual inspection. In Figure 3-14 an example is shown of the outcome of the proposed algorithm for a 3D-profile that is displayed in gray values (the signature is broadened

fifty times). The user can check whether the resulting signature is characteristic for the striation mark.

If the striation mark does not have much variation, another possibility is to select one line and present this to the user as a signature. The user should check if there is a striation match between the signature and the striation mark itself.

A problem that remains for the 3D coded light approach if a slope of the striation mark. In Figure 3-15 an example is shown of an image with such a slope of the striation profile. Since this slope may be assumed linear (it is caused by the fact that the cast is not completely flat on the surface or by lighting), the user can select the edges of the tool mark in both directions. We compensate for the tilt by employing the assumed linearity, and subtracting the relative differences of the four points of edges of the casting with a linear algorithm.

3.5   Similarity measure

In order to retrieve relevant striation mark images from the database, it is necessary to compute a similarity measure between the striation marks that are compared.

The similarity measure has to be stable under the following conditions:
1. Slight differences in lighting or depth
2. A shift in the tool mark in the y-direction
3. A local distortion in the y-direction due to elasticity in the material
4. An angle of the tool with the surface, which results in a smaller and more dense tool mark
5. Differences due to extra damage of the screwdriver

In order to handle slight differences in lighting, the standard deviation of the difference of two signatures s_1 and s_2 is used as a similarity measure m. This compensates for a bias in intensity.

$$m(s_1, s_2) = stdev(s_1 - s_2) \hspace{4cm} \textbf{(3)}$$
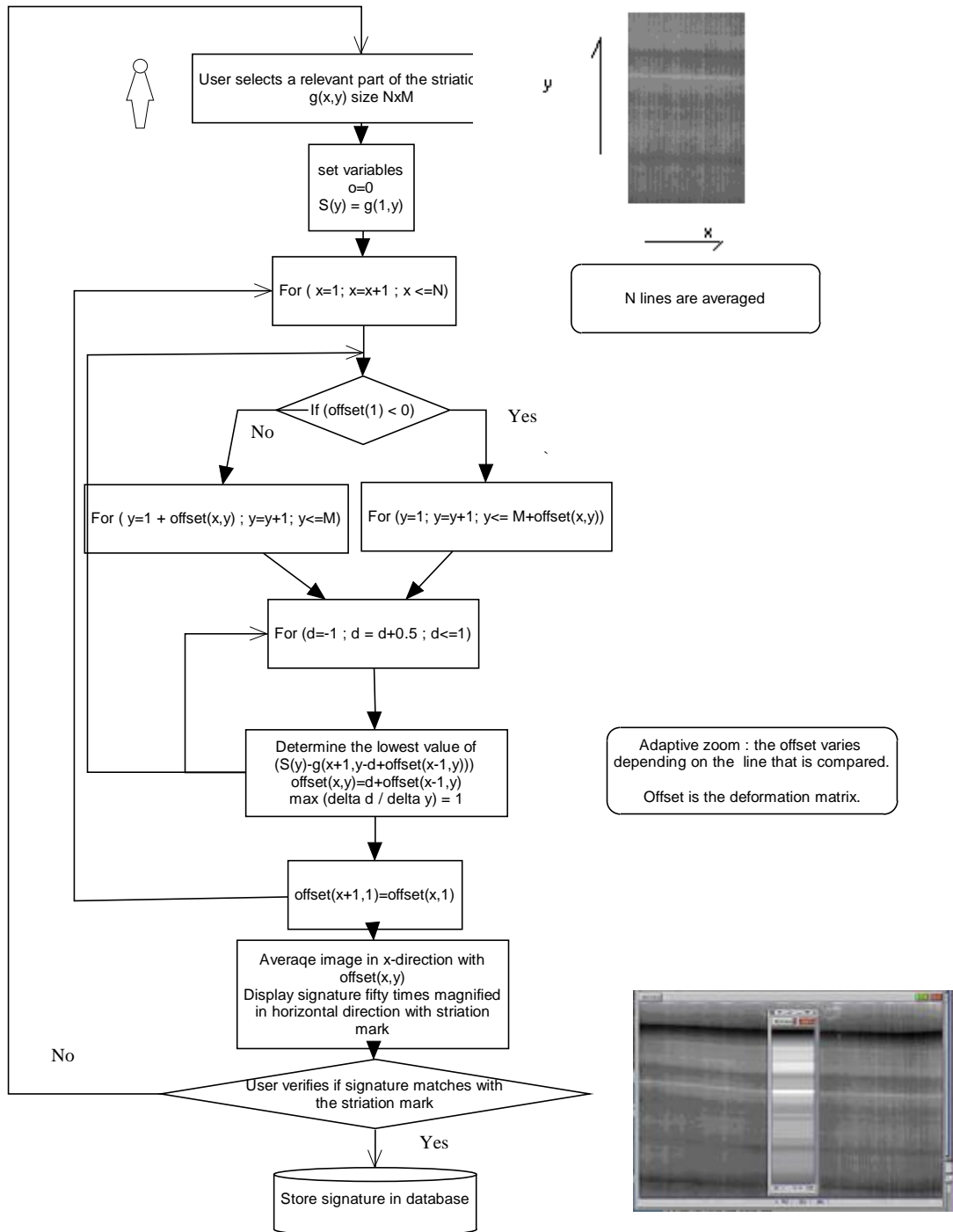
Figure 3-13: Flowchart of algorithm used for determining signature
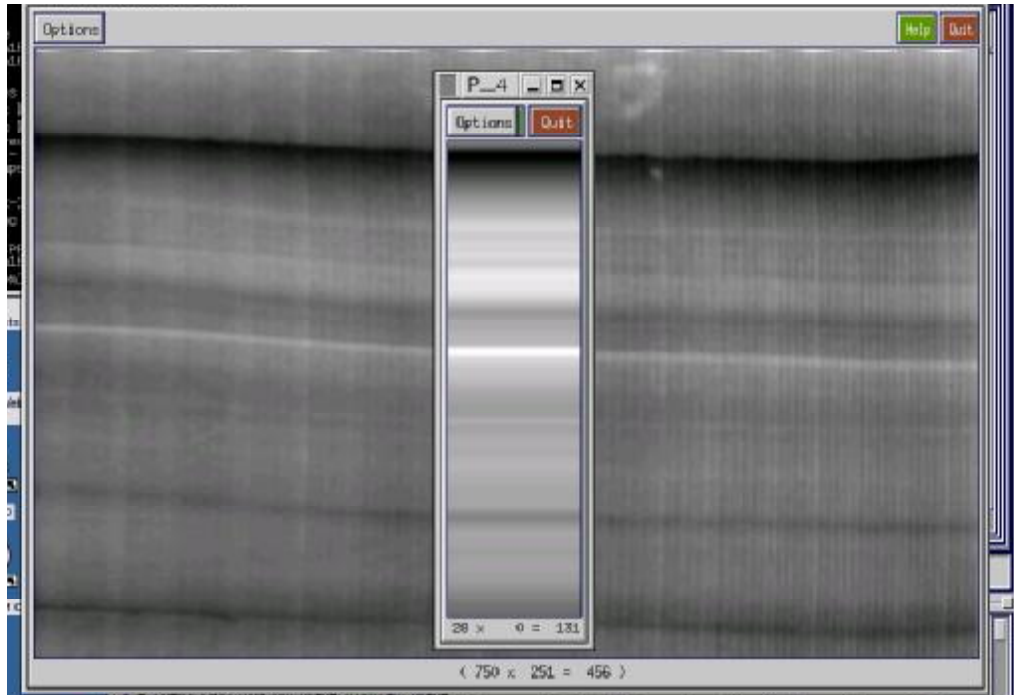
Figure 3-14: The result of sampling an area of a striation mark in a striation mark digitized with the OMECA 3D.
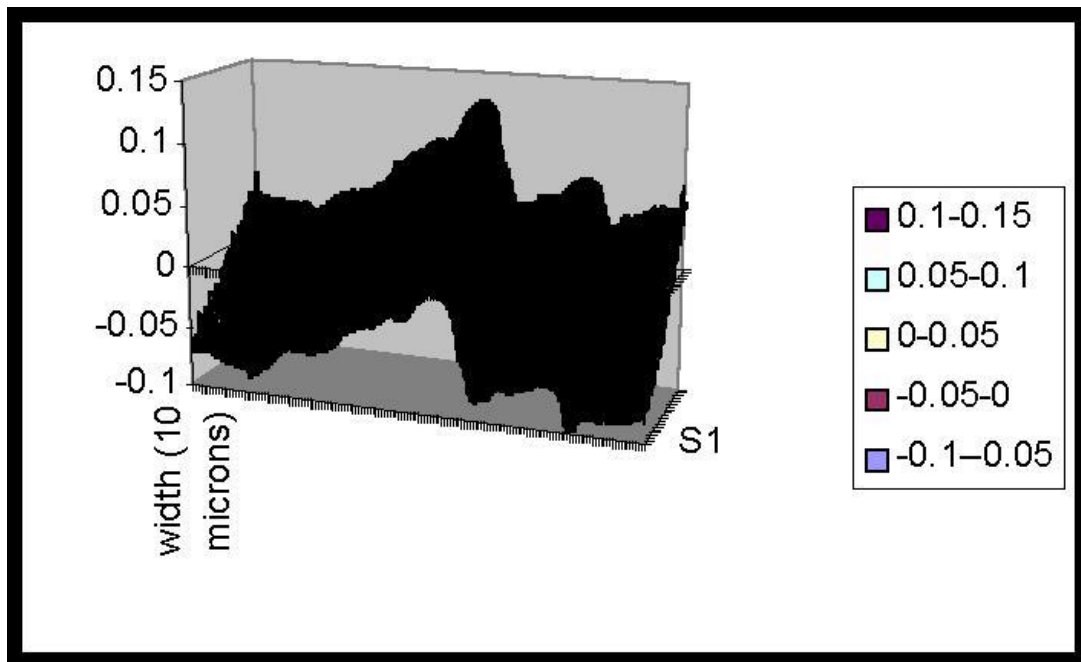
Figure 3-15: 3D-image of a tool mark with a slope in the striation profile

The shift in the tool mark in the y-direction is addressed by shifting the signatures relatively to each other. The maximum shift between the signatures is P. The local distortion in y-direction due to elasticity and the angle of the tool with the surface is accounted by implementing the adaptive zoom as the similarity measure minS of two signatures s_1 and s_2:

The procedure shown in Figure 3-16 gives us a similarity measure for two signatures under a wide variety of conditions. This allows us to compare any two images in the database or a new image with all images in the database. The result will be a list of matches of tool marks with the lowest similarity measure Smin at the top of the list. In Figure 3-17 a flowchart of the system is shown.

3.6 Experiments

TESTSET

A small test has been prepared in which six screwdrivers are used. Of these six screwdrivers, test marks were made with an angle of 45 degrees on wax. These striation marks were molded with gray silicon casting material. Then these marks were digitized with the coded light approach and with side light. It appeared that there are some artifacts and variations in the image due to: aliasing, camera resolution and variations in the tool mark itself.

Since the current setup of our OMECA-coded light apparatus is limited to 6 mm, a part of the striation mark has been scanned. For each striation mark, we have chosen to scan 6 mm of the 10 mm striation marks. The gray scale images are also acquired with this apparatus.

RESULTS

The results of the similarity measures (Figure 3-16) are shown in Table 3 and Table 4. From this experiment, it appeared that all tool marks that were compared to each other, were retrieved well. If we compare the results of the side light images with the 3D-images, the algorithm will distinguish the striation marks with, on average, a 30 percent higher similarity measure in the 3D coded light approach.
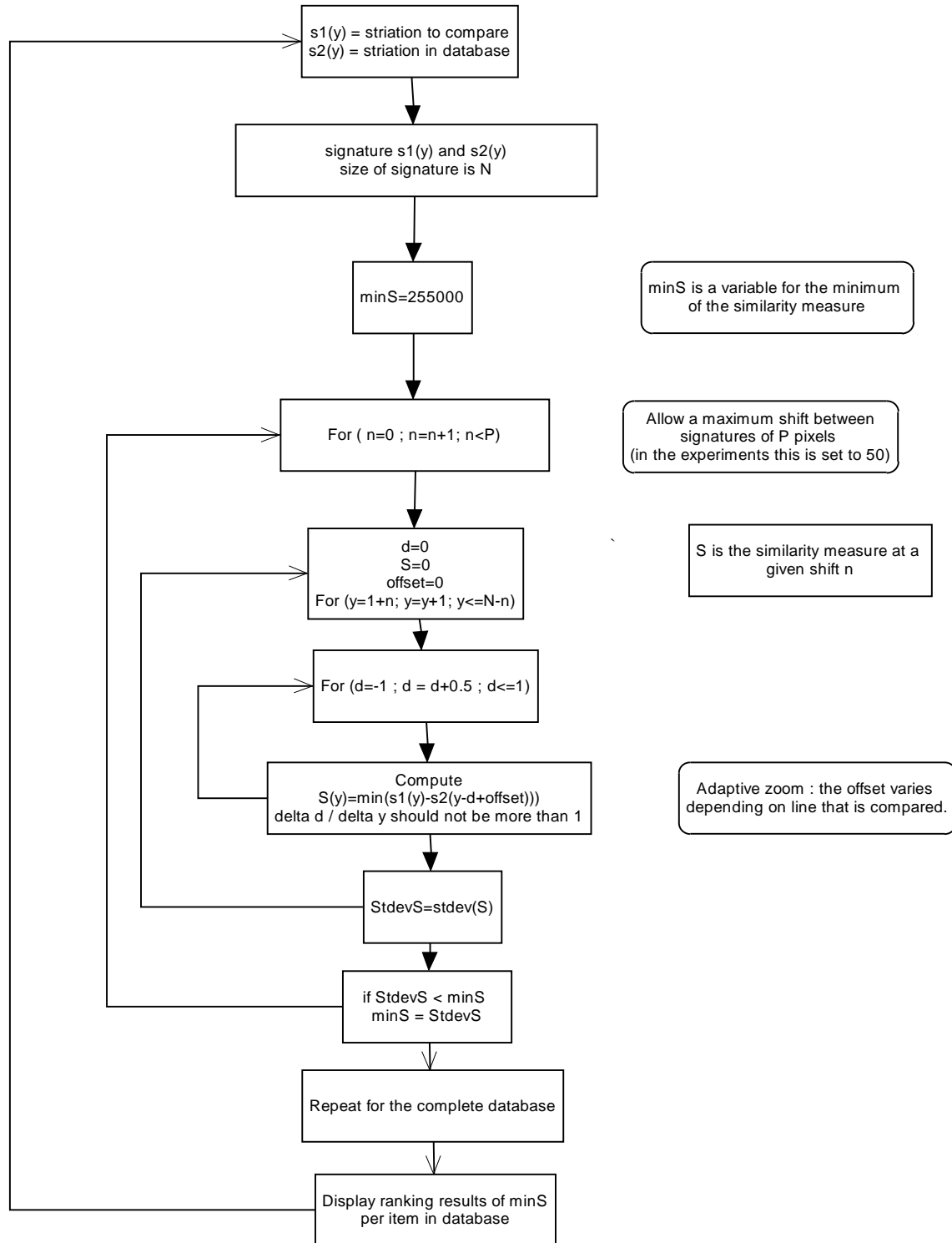
Figure 3-16: Flowchart of computation method of similarity measure with signatures by adaptive zoom

```
┌─────────────────────┐
│      Toolmark       │
│  Structured Light   │
│    or Side Light    │
└─────────────────────┘
           │
           ▼
┌─────────────────────┐         ┌──────────────────────────────┐
│                     │         │            Shape             │
│ Extraction low level│────────▶│ Extracting the signature of the │
│     features.       │         │        striation mark        │
│                     │         └──────────────────────────────┘
└─────────────────────┘
           │
           ▼
┌─────────────────────┐
│                     │
│ Textual descriptors │
│                     │
└─────────────────────┘
           │
           ▼
      ╭───────────╮
      │  Storage  │
      ╰───────────╯
           │
           ▼
┌─────────────────────┐
│     retrieval :     │
│ on textual descriptors │
│ and similarity measures │
│  based on algorithm │
└─────────────────────┘
           │
           ▼
┌─────────────────────┐
│                     │
│    visualization    │
│                     │
└─────────────────────┘
```
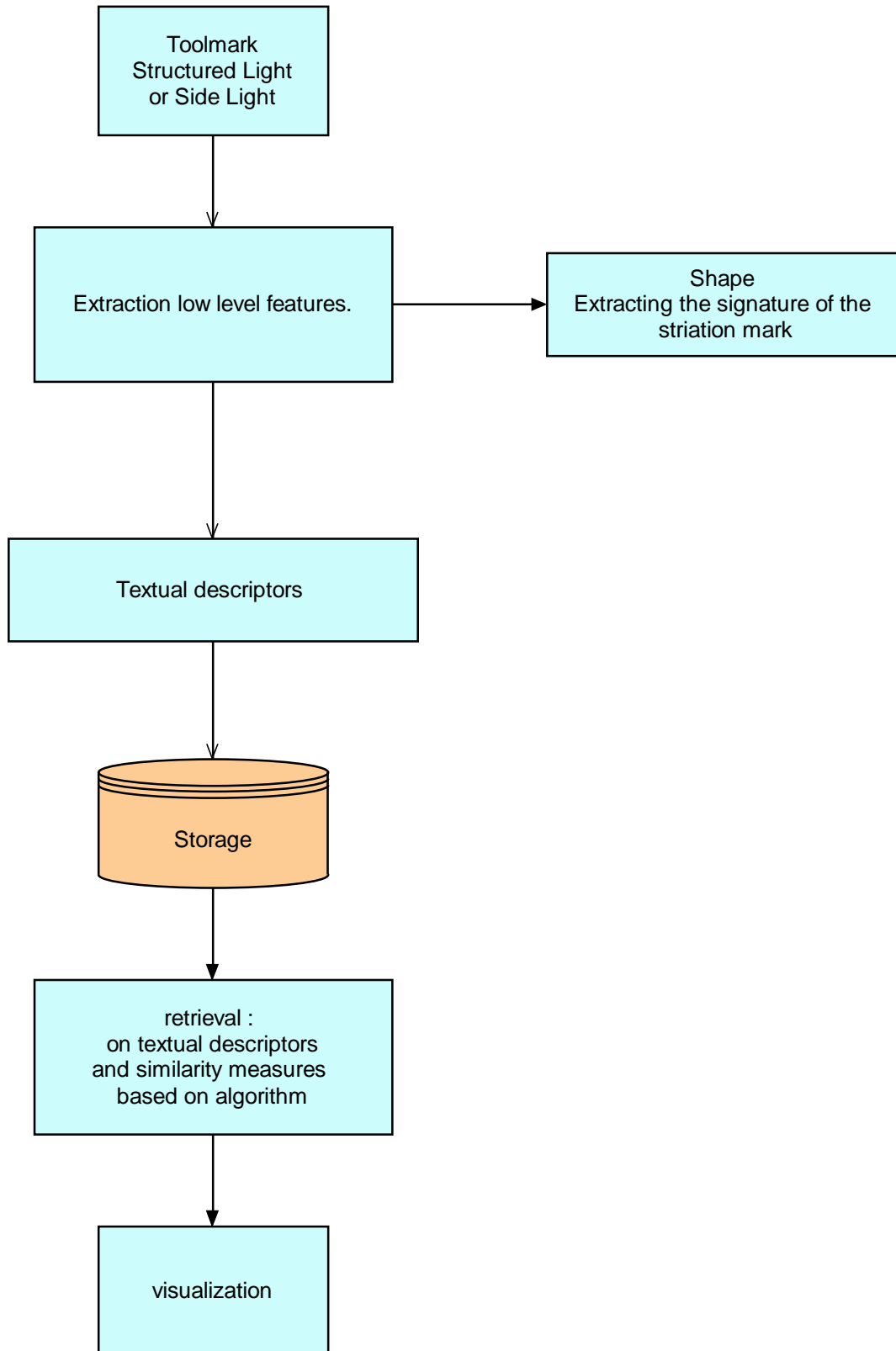
Figure 3-17: Flowchart for tool mark visual information retrieval system

Table 3: Similarity measures for side light comparisons of the six screwdrivers

	1	2	3	4	5	6
1	17.3	43.5	74.2	61.3	51.3	54.5
2	68.6	27.7	46.3	55.3	78.3	62.4
3	40.4	58.7	15.4	79.1	40.3	73.5
4	48.0	45.7	39.8	20.2	36.8	86.9
5	54.3	80.7	59.6	45.2	23.2	86.4
6	67.4	71.5	83.8	42.0	62.3	20.6

Table 4: Similarity measures for 3D comparisons of the six screwdrivers

	1	2	3	4	5	6
1	16.0	47.7	81.2	114.4	44.4	107.0
2	55.8	25.6	71.8	113.7	82.1	110.8
3	81.3	47.4	20.8	66.8	47.3	104.5
4	101.8	103.4	56.4	17.5	70.2	70.2
5	91.2	90.4	100.0	89.3	13.4	97.5
6	92.8	88.3	113.7	83.0	97.3	11.8

3.7   Conclusions and discussion

In this study, a system has been developed for storing images of tool marks and their textual descriptors. For automatic matching of striation mark a new algorithm, the adaptive zoom-algorithm, has been developed for creating the signature of the striation mark and/or matching as well. With the adaptive zoom algorithm it is possible to select a signature of an area of a striation mark, even if there are small distortions in the tool mark or if the striation mark is not exactly horizontal. With a small test set of six screwdrivers, test striations have been made. The matching

algorithm retrieved the relevant striation marks that were made with the same screwdrivers. The results with this algorithm have been compared for side light and coded light approach. It appeared that the similarity measures for the coded light approach were slightly better.

For the matching of tool marks several methods have been described in literature[52] [53] [54] [55] that did not consider local variations in striation marks. Commercial systems exist on the market for automatic tool mark comparison [56] and IBIS[57] for bullets. The system for bullets will extract a signature of the striation mark and compare these. For bullets it is recommended to use pre-selection of bullets with the same composition, since otherwise differences in the striation marks might result depending on differences in hardness of the material. One advantage with bullets compared to tool marks with screwdrivers is that the striation marks are more reproducible, since most often the bullet can only leave the firearm in one direction.

In the past, we have examined if the output generated by a human examiner could be used in a neural network. However, this method did not work for cases[58] that were not in the database. The trained network only worked correctly for the data set it was trained with.

Based on the research described in this chapter, it appears that the use of three-dimensional information of a striation mark is useful compared to the two-dimensional side light image because the depth information makes the method less sensitive to the influence of lighting of the surface.

In future research, the adaptive zoom method should be tested on larger databases of striation marks. Comparing striation marks with the current set-up of the OMECA equipment is not recommended because the area of scanning is limited to 6 mm. The equipment should be modified before continuing with large-scale experiments.

If larger databases are available, statistics on the characteristics of a striation mark are possible, and this will improve the knowledge on variations in these marks for forensic identification.

A different approach that might reduce the time of examination is digitizing the shape of the blade of the screwdriver, and then comparing the striation marks with the 3D visualization of the blade. In this case, we would not have to make test marks

anymore, since the shape of the striation mark can be calculated from the shape of the blade, and less time is needed for making the comparison with the database (if a proper way of digitizing the blade is used). In Figure 3-15 is shown that the shape of the blade of the screwdriver might also be used for distinguishing the tool mark easily. In this approach, a fast pre-selection is possible based on a smoothed curve with a compact signature of the shape.

The practical use of these databases is still limited. In The Netherlands, there exist several databases of tool marks; however, automatic comparison has not been implemented. Several efforts have been made towards automatic retrieval of striation marks. The results of these algorithms are promising provided sufficient time is available for examination.

4   Databases of Cartridge Cases

Abstract

Databases of cartridge cases have been used in forensic laboratories extensively. In these databases image-matching methods have been implemented that are proprietary. For quality assurance, it is necessary to understand the background of the matching algorithms, and to improve the results by implementing other algorithms.

In this study, three methods for matching of breech face marks have been compared: standard deviation of the difference, log polar, and KLT. These methods have been tested with the following pre-processing methods: histogram equalization and filtering with one of the first four scales of the à trous wavelet transform.

For testing we mixed 49 known matching cartridge cases with 4900 images of breech face marks in a database. The standard deviation of the difference of histogram-equalized images of the breech faces resulted in first matching ranks in the database if they are acquired under strict standards for lighting and positioning. A brute force approach by shifting and rotating the cartridge case was not feasible, since too much computing power was required.

Log Polar matching of the third scale from the à trous wavelet transform worked well. With this method, all images were retrieved in the first position of the ranking. KLT in combination with the third scale of a trous worked for 11 breech face marks, as the relevant images were retrieved in the first position. The KLT-method is computationally efficient, and could be used as pre-selection, since all relevant

images were retrieved in the first five percent of the database. On this pre-selection the log polar method could next be used to this selection to retrieve the matching shapes.

For further evaluation of these algorithms, it is necessary to test them in the databases of cartridge cases with a wider variety of casework.

4.1   Introduction

This chapter describes a comparative study of automated matching algorithms of breech face marks on cartridge cases. This study is a part of an evaluation of the different systems on the market for handling databases of cartridge cases and bullets.

In this chapter, first an overview is given of forensic investigation of firearms and cartridge cases, including a survey of commercial systems. Then, a selection of matching algorithms is discussed, in which the most promising are evaluated in experiments with a complete database.

The reason to compare the different methods of image matching is that the methods are proprietary. For quality assurance in a forensic laboratory, it is important to understand why a certain image is not found in the matching list and to have more background on the image-matching engine. Another reason for this research is to improve the results of image matching.

Side light (Breechface)   Ring Light (Firing pin)
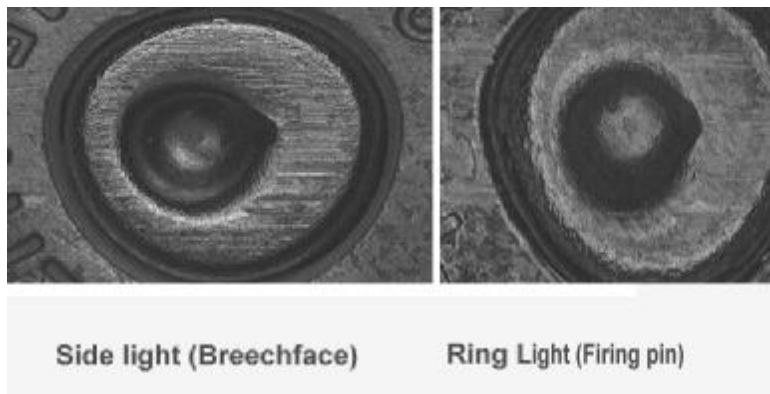
Figure 4-1 : Image of breech face in the primer area with sidelight (left frame) image of firing pin with ring light (right frame)

4.1.1 Forensic Examination

When a firearm is loaded and fired the mechanisms that are exposed to the cartridge case cause impressions and striations that can be characteristic for the firearm being used. The striation marks on bullets are caused by the irregularities in the firearm barrel.

Often the cartridge case is the most important forensic specimen in the identification of weapons, as bullets are commonly deformed by the impact. The examiner can also determine, using class characteristics, what kind of firearm (often make and model) has been used.

The cartridge case ejected shows marks at the primer (Figure 4-1) that are caused by the firing pin and the breech face as the cartridge is repelled back in the breach by the force of rifling. The feeding, extraction and ejection mechanisms of the firearm will also leave characteristic marks.

For forensic comparison, a number of test fires are made with the firearm. In forensic laboratories the marks on cartridge cases and bullets are compared with the test fired ones. By comparing the marks, it is possible for the qualified examiner to conclude that a certain bullet or cartridge case has been fired with a certain firearm.

4.1.2 Ballistic Imaging Systems

DRUGFIRE [59] and IBIS[60,61,62,63] are databases for acquiring, storing and analyzing images of bullets and cartridge cases. These two systems have been evaluated at our laboratory.

Both systems capture video images of bullet striations and of the markings left on cartridge cases. These images are used to produce a digital signature that is stored in a database. The system then compares a signature to that of another fired bullet - or cartridge case - or to an entire database of fired bullets and cartridge cases. The user enters the cartridge case in the database for comparison, and can limit the search to using specific characteristics (e.g., caliber, date limit). Then, the system produces a hit list that shows a ranking of all cartridge cases based on the similarity, as measured by the system, between the cartridge under investigation and the cartridges in the database. The system functions properly if all relevant matches are in the top of the hit list.

The methods of image matching applied in these systems are not known. However patents[60,61,62] applied by IBIS mentions that state-of-the-art image matching methods are used. The system of IBIS is now used most often, and since the images are acquired in a reproducible way by a special kind of lighting, the ring light, it is expected that this system will give the best matching results.

Other systems for analyzing cartridge cases are the systems Fireball[64], CIBLE and TAIS. These systems also use image-matching techniques, however they were not available for investigation at our laboratory.

Three-dimensional measurement of the striation marks by laser triangulation[65] or by fusing the images with different angles of coincidence are described in the literature[66]. Since the firearm examiner is used to compare side light images rather than three-dimensional images, development and acceptance of 3D-image matching methods progresses slowly. Accordingly, this study is focused on the matching of side light and ring light images.

4.2 Image matching

In order to carry out the comparison of matching methods, we tested various techniques, which are available from the literature[67]. Recently, the interest in content-based searching of image databases has increased considerably; image matching is a crucial step in content-based retrieval. Several commercial and research systems as QBIC, Virage and Photobook[68,69] search similar images in the databases based on the contents of the images. They generally take features from the images, and index these features as descriptors that are easily searchable. The results of searching are generally influenced by the following factors:

- Noise in the image due to the acquisition process

- Rotation and shift

- Difference in light source

   Further differences that are typical for databases of cartridge cases:

- Difference in cartridge case metal (material, type, brand)

- Wear of firearm

- Wear of cartridge case

- Marks between two shots can be different for statistical reasons in the shooting process; this means that sometimes parts of striation and impression marks are visible that are not visible with the next shot

In present-day forensic investigations, the firearm examiner determines which marks on cartridge cases are similar. The approach examined in this chapter involves automatic comparison, by using the shape of the firing pin and the texture of the impression marks. Since the light conditions and the images of the marks do change depending on the marks, methods have been developed that compare the features of gray-scale images. In practice, it turned out to be important to have an appropriate preprocessing image step to compensate for the variation of light. In the optimal situation, the algorithm should only compare the marks caused by the firearm, and not any other features of the cartridge case, as damage and symbols.

In this research, approaches are described that are either pixel based or feature based. The reason to use feature-based methods is to improve the calculating speed and to keep the selection restricted to marks.

4.3   Test database

For our evaluation of image matching algorithms, we studied two kinds of images (Figure 4-1)

- Images of breech faces which are illuminated with side light

- Images of firing pins which are illuminated with ring light

We used a database of 4900 images, which were acquired by different firearm examiners from different institutes around the world using the Drugfire system under different circumstances (light sources and a number of views of the cartridge case). Table 5 shows the different calibers and the kind of images (side or ring light images). We tested the algorithms on all images (without prior knowledge).

For testing, we added 49 images from a test set to the database. The test set consists of side light images of 49 different cartridge cases that have a known match. They are consistent in light conditions. These cartridge cases are fired from 19 different firearms of caliber's 9 mm Parabellum (15), .45 automatic (3) and .32 (1).

Depending on the case, there were 2-5 matching cartridge cases (Table 6). Some of these cartridge cases are from different test shots. The marks of the cartridge cases and the shapes of the firing pin were visually similar between the matches. Five cartridge cases had a rotation of more than 10 degrees to each other. The 49 cartridge cases were also available as ring light images of the firing pin. There were marks in all ring light images of the firing pin that could be distinguished from each other visually.

The images are acquired by using a protocol. The firearms examiner determines in the 12-o'clock point of the cartridge case by examining the marks and positions the cartridge case at the 3-o'clock position. Often the striation lines in the breech face of the firearm are parallel. The image is rotated in such a way that the striation marks are most visible by using side light.

Table 5 : Number of images of cartridge cases in the database

Caliber	Number
9 mm Parabellum	2402
.32 automatic	893
.25 automatic	393
.380 automatic	326
.45 automatic	236
9 mm short	230
.40 S&W	118
.22 long rifle	109
Others	193
Total	4900

Table 6 : Number of matching cartridge cases in the test set vs. caliber

Number of matching cartridge cases	9 mm Parabellum	.45au	.32au	Total
2	9	1	1	22
3	4	2	0	18
4	1	0	0	4
5	1	0	0	5
Total	15	3	1	49

The evaluation of methods consists of mixing the 49 images with the complete database, and evaluating how often the images will be placed on the top positions of the hit list. However in cases were calculation time is a problem, the 49 images are compared to each other. For validation of the algorithm itself, the cartridge case is also compared to itself. The experiments are based on practical cases, and this can also influence the correlation results.

4.4   Methods and results

The methods that are used have been evaluated in a time frame of four years of research. In first instance we started with the most precise method that is pixel-based comparison. Observing the need for improvement for calculation time, faster methods were used. In this chapter the methods are explained and results are presented.

4.4.1 Pre-processing

For pre-processing of the cartridge cases two different methods have been tested:
   § histogram equalization and masking
   § wavelets

Pre-processing is used to compensate for differences in lighting and for enhancing the marks that have to be matched.
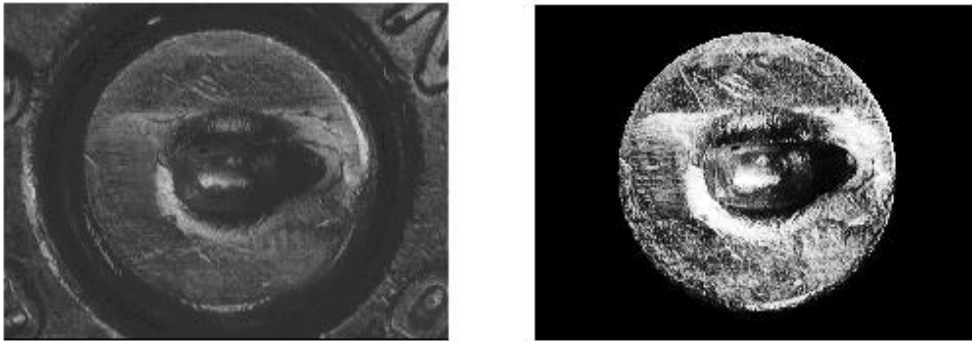
Figure 4-2: Preprocessing operation (left: original image; right processed image)

4.4.1.1 Histogram Equalization and masking

 On the images in the database and the test set, histogram equalization[70] is used in an effort to compensate for differences in lighting conditions and visualize the marks.

Since we would like to compare just the inner circle of the image (where most impression marks are), we select the circle manually and all pixels outside of this circle will get a zero gray value (Figure 4-2) This pre-processing has been carried out to all images that are in our databases.

4.4.1.2 Wavelets

There are a huge number of articles[71] on pattern recognition based on wavelet transforms. A wavelet transform is a localized function of mean zero. Wavelet functions are often wave-like but clipped to a finite domain.

Wavelet transforms are computationally efficient and they allow exact reconstruction of the original data. The reason for choosing a wavelet transform is that wavelets are suitable of filtering properties at different scales (from coarse to fine) in the image. The challenge is to choose a wavelet scale and type that are optimal for the breech face marks (fine striation and impression marks).

We have chosen a wavelet transform that works on discrete data known as à trous (with holes) algorithm[72]. In this wavelet, the image is sampled by means of a

smoothing function, the B3 spline. The different scales of à trous that are calculated can be added to each other and the result will be the original image.

Scale 1 of the à trous algorithm will give the finest details and the noise in the image. The higher scales will give the coarse variation of lighting in the image. In Figure 4-3 an example is given of four scales of a cartridge case computed with the à trous algorithm. Most information on the marks is visible in the third scale, however in the experiments all scales have been tested.

4.4.2 Matching Results

In this section, we discuss the results of the different image matching methods (standard deviation of the difference, log polar and KLT) that we have considered for this database. We have compared the test set of 49 images with the complete database of 4900 side light images based on these methods . We have tested the method based on five situations :

- the histogram equalized images

- the four scales of the à trous wavelet scales

4.4.2.1 *Standard Deviation of the difference*

For a computationally simple kind of matching procedure, we take the variance of the difference in gray values between two images (which was also used in previous research[73]).

The hit list is created by sorting the variance from small values for the best matching to high values for images that do not match well.

The user of the database has to position the cartridge cases according to standard procedure; a relatively rare error is that the position is 180 degrees rotated. This can happen when the examiner finds the wrong position of the cartridge case in the firearm based on the marks.

Since we did not know if the protocol was strictly applied for all images in our database, we decided to test the influence of small rotations on the matching results. It appeared that a rotation of a cartridge case up to five degrees did not affect its ranking.

The first test was done with histogram equalized images. We subtracted the images from the test set from each image in the database and compared the standard deviations of the resulting differences. It appeared that 21 out of the 49 images were in the top positions, fifteen were in the top 5 percent of the database. This means that the examiner should compare 250 cartridge cases in the database of 4900 images before knowing there is no match. This does not work well in practice, since it is a time consuming task. Five more cartridge cases were in the top 50 percent of the database. These five cartridge cases had a rotation of more than 10 degrees to each other, and this caused the difference. For this reason this approach is not effective, unless the cartridge cases are positioned within five degrees accuracy to each other. The results for the a trous wavelet transformed images, did not improve the results of the matching algorithm.

From examination of the images, it appeared that some of these primer areas of the cartridge cases were slightly rotated and translated to each other. We tried to compensate this influence by a "brute force" method of rotating and translating the images, and calculating the minimum of the standard deviation of the difference in gray values. With those compensations, all images were found in the top positions.

This approach worked both in the polar coordinates as well as in the raw images. The computation is done by rotating 360 degrees in steps of one degree and shifting 40 pixels in x and y-direction (which is the estimated maximum of shift) in steps of one pixel. The computation took more than one month on a Pentium-II PC 333 Mhz for 49 images; for this reason this "brute force" method has not been used with the complete database.

4.4.2.2 Log Polar Transform

A classical technique for registering two images with translation misalignment involves calculating the 2D cross-image matching function[74]. The maximum of this function yields the translation necessary to bring the images into alignment. This function has the disadvantage of being sensitive to rotation and scale change. Even small rotations of a few degrees can reduce the peak of the cross image matching function to the noise level.
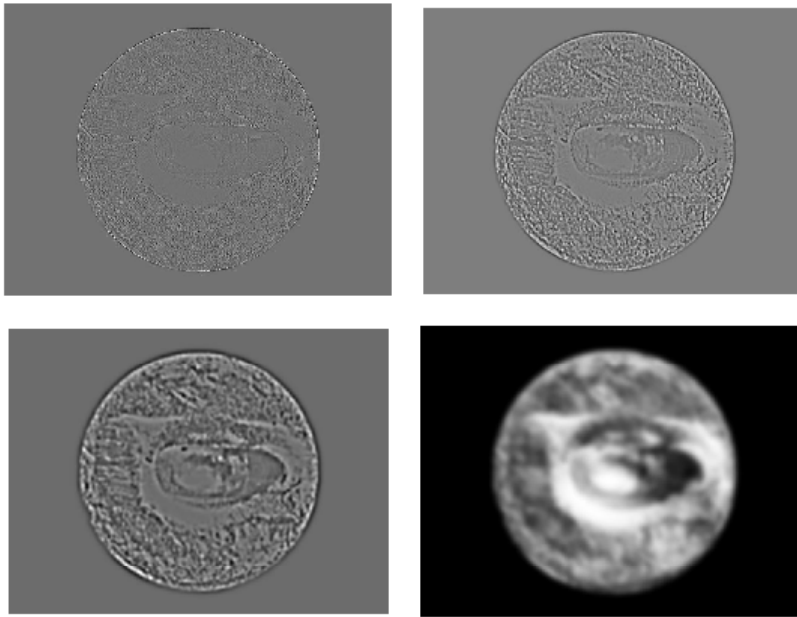
Figure 4-3: **Four scales of a wavelet transformed primer area of a cartridge case computed with the à trous wavelet transform**

By using invariant image descriptors in place of the original images, it is possible to avoid this problem. One such descriptor is the log-polar transform of the Fourier magnitude, which removes the effect of rotation, and uniform scaling into shifts in orthogonal directions[75].

We tested the log polar transform on histogram equalized images of the primer area. It appeared that five out of the 49 cartridge cases were ranked in the first position. All images were however in the first 6 percent (top 300) of the complete database. For this reason the method can be used as a faster selection method. The log polar transform took 7 days to calculate for the complete database of 4900 images.

Better results were found when applying the third scale of the à trous transform on the images of the primer area. By pre-processing the images this scale, all matching images were in the top positions.

4.4.2.3 KLT Method

There are extensive studies of image matching for tracking[76] (following an object in a scene). Since tracking has many similarities with searching in a database of images[77], we have tested a tracking algorithm. Tracking algorithms are optimized for their speed. Determining whether a feature is of interest can be used for ranking it in a hit list. Tracking also has the problem of registration, since the camera might move, with image intensities that change in a complex way.

One of the methods that appears to work for a wide range of tracking problems, and that works fast, is the Kanade Lucas Tomasi (KLT) method[78]. Prominent features, e.g., strong edges) are located by examining the minimum eigenvalue of each 2x 2-gradient matrix. The features are tracked using a Newton-Raphson method of minimizing the difference between the two images.

Based on the KLT method, the details in the images that are prominent are selected as points. From each image, these points are calculated by comparing two images of one shifted cartridge case. For the experiments, we have shifted the cartridge case five pixels, and have calculated the 100 most prominent points, which are stored in the database. The number of points that are matched between two cartridge cases, is a measure of similarity between two images.

For our test set of 49 images compared to the database of 4900 images, it appeared that the histogram equalized images did not work well, since no images were retrieved in the first positions, and some images were retrieved on the last positions of the matching list.

The third à trous wavelet scale gave the best results. Of the 49 images, 11 were retrieved in the first position out of the 4900 images. Furthermore, all images were retrieved in the first five percent of the database.

4.4.2.4 Overview of results

In Table 7 a comparison between the matching methods used in this chapter, is shown.

Table 7 : Number of relevant matches in top positions for the test set and percentage of database that has to be searched before all relevant images are retrieved.

	Standard Deviation of Difference	"Brute Force" registration within test set	Log Polar	KLT
Histogram equalized image	21 / 50 %	49 / 0 %	5 / 6 %	0 / 45 %
Scale 1	5 / 78 %	-	3 / 15 %	2 / 34 %
Scale 2	7 / 79 %	-	21 / 4 %	3 / 15 %
Scale 3	21 / 53 %	49 / 0 %	49 / 0 %	11 / 5 %
Scale 4	4 / 82 %	-	2 / 45 %	3 / 45 %

4.5   Conclusions and Discussion

We tested three different image matching algorithms (standard deviation of the difference, log polar and KLT) for breech face marks on cartridge cases and two different pre-processing algorithms, were 49 cartridge cases from 19 different firearms with known matches were mixed with a database of 4900 cartridge cases.

In cases where the positioning, and the light conditions among the marks in the cartridge cases were reproducible, a simple computation of the standard deviation of the subtracted gray levels put the matching images on top of the hit list.

For images that were rotated and shifted, we have built a "brute force" way of image translation and rotation, and the minimum of the standard deviation of the difference is computed. For images that did not have the same light conditions and were rotated relatively to each other, all matches were found with the third scale of the à trous-wavelet computation. Since the method was very time consuming in computation, we have limited this experiment to the 49 cartridge cases, and compared them to each other.

For the log polar transform and KLT pre processing by the third scale of the à trous wavelet transform worked best. For log polar all relevant images were retrieved in the top position of the ranking. For KLT, eleven images were in the first position, and all 49 were in the first five percent of the database.

From our experiments, we conclude that if images are entered in the database using a standard protocol, a simple computation of the standard deviation of the difference of the image is feasible. If there are differences in positioning, the log polar transform of the third à trous wavelet scale works better. As a measure for pre-selection of images, the KLT method is an option. In Figure 4-4 the flowchart of the approach is shown.

The cartridge cases in our experiments, had clear breech face marks. In practice this is not always the situation, so for that reason other marks (firing pin, extractor marks) could also be used in the database. For further improvement, the user might select the areas that are relevant on the cartridge case for their marks. Sometimes the firearm examiner has information that marks on the cartridge cases are not caused by the firearm itself. Examples of this damage are text imprints in the firing pin.

For further evaluation of matching algorithms, it is necessary to test them in the databases of cartridge cases with a wide variety of casework.

The use of optical processors[79, 80] or parallel processors implemented in hardware is an option to improve the speed of image matching of the brute force method. Implementations of faster matching algorithms should be considered for future research.

The cartridge case systems are widely used compared to tool marks databases. These systems have correlation engines, and modification to a 3D system will result in better correlation ranks. In The Netherlands, we use the system *Drugfire*, also used by many agencies in the United States. The company that produces this system is phasing out the software, since there appeared to be patent infringement problems with the other company, IBIS. In the United States, the IBIS system for cartridge cases will be the standard. This system has a more reproducible way of imaging the cartridge cases, and better results are possible with this system. In practice, the system results in "cold" hits. The systems for cartridge cases also help for statistical evaluation of forensic evidence. The identifying characteristics should be compared, and if the database is sufficiently filled, it is possible to make these kinds of comparisons.
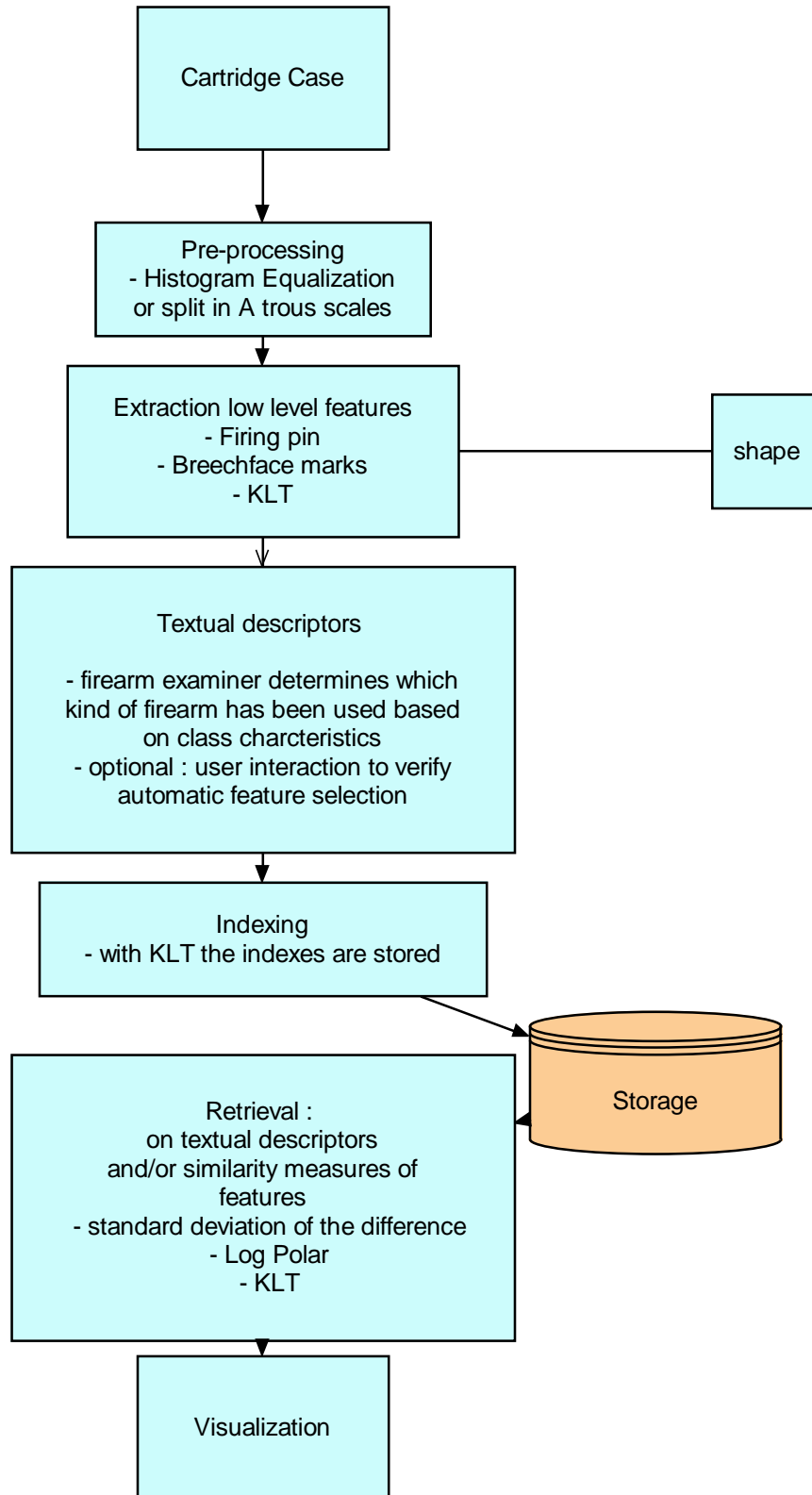
Figure 4-4 : Flow chart of cartridge case visual information system

5 Database of Shoe marks

Abstract

A system for image acquisition and comparison and a database of footwear shoe profiles (named REBEZO) have been developed. The database consists of three files : shoes of suspects, shoe marks from scenes of crime and shoes from shops. An algorithm has been developed for the automatic classification of shapes in the shoe profiles. The algorithm first segments a shoe profile in distinguishable shapes. For these shapes Fourier features and invariant moments are calculated. The Fourier features are selected and classified with a neural network that is composed of a single-hidden layer feed forward network trained with back propagation. The neural network works for simple shapes (triangles, circles), but falls short with more complex shapes. Invariant moments can be used to differentiate a line from a rectangle. More research is required before automatic classification of shoe marks may become of practical use.

5.1 Introduction and Motivation

Shoe marks are often found at the scene of crime[81], and may constitute extremely important evidence. Some criminals think of hiding fingerprints and DNA material, but shoe marks are more difficult to erase.

Shoe marks can be formed either three-dimensionally, as e.g. by an impression in clay, or two-dimensionally by dust, fluid (water, blood) or electrostatic prints.

Figure 5-1 : Latent shoe mark on carpet that is treated with Leuco Crystal Violet

Three-dimensional shoe marks

Three-dimensional shoe marks are often found outside buildings. Examples of these shoe marks are impressions in sand, clay, and snow. These shoe marks are recovered from the crime scene by casting them with dental stone and are photographed before a cast is made. Three-dimensional shoe marks give depth information of the shoe profile.

Two dimensional shoe marks

Two-dimensional shoe marks are found on surfaces as linoleum, stone, carpet, and wood. Often these shoe marks are latent, which means that they are not visible under standard conditions. To make the latent prints visible, there is a wide variety of methods :

- with side light
- by using a chemical (e.g., leuco crystal violet if blood stains have been found, an example is shown in Figure 5-1)
- by lifting them with gelatin foil (for dust prints)
- by using an electrostatic device
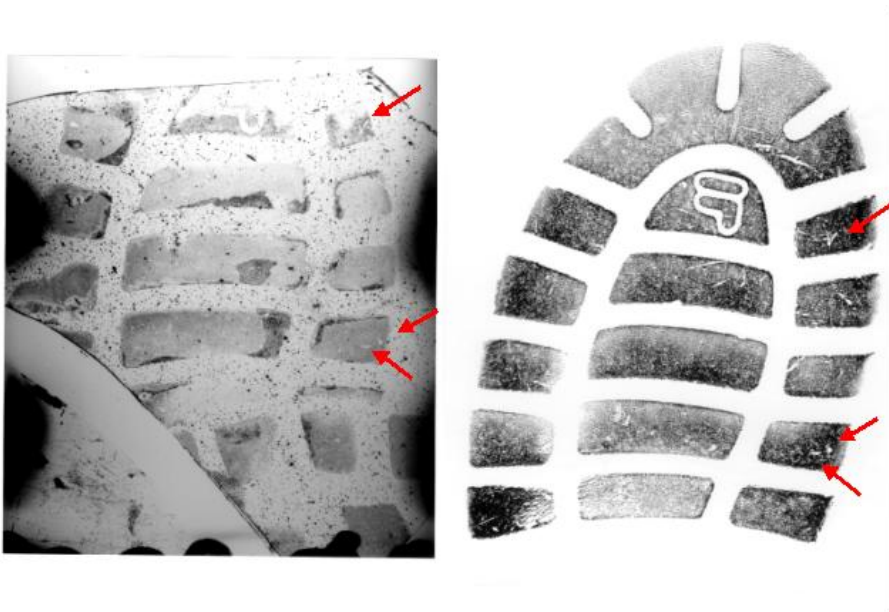
Figure 5-2 : Example of shoe mark with characteristics (arrows point at them). At the left side a shoe mark of the scene of crime is shown; at the right a test shoe mark with a shoe of a suspect.

In this chapter, we describe forensic investigation of shoe marks, the use of a database of shoe marks and a study on automated classification of shapes in shoe marks.

5.1.1 Forensic Investigation

For forensic investigation, the usable shoe marks are taken from the crime scene. If there is a suspect with shoes that have a similar outsole profile as the shoe mark, the shoe should be compared with the shoe mark and a forensic identification (depending on the characteristics) is possible as is shown in Figure 5-2. If the shoe mark is two-dimensional, test prints have to be made of the shoe of the suspect. If they are three-dimensional, the shoe can be compared to the cast directly. First the separate shapes (triangles, rectangles etc.) of the shoe profile have to be compared and measured. If the location and the sizes of the profiles are approximately equal, the forensic scientist can determine that shoes with similar shoe profiles have been used.

If there is wear of the shoe itself, and if cuts and other irregularities that are caused by sharp objects in the shoe sole are visible, it is possible to identify the shoe with the shoe mark. It depends on the shape of the characteristics whether or not an identification can be made (an example is shown in Figure 5-2.) Since this

examination is subjective, as with the firearm and tool mark examination, it depends on experience and methodology used by the examiner which conclusion is drawn from the comparison.

5.1.2 Database of shoes and shoe marks

In The Netherlands, there are many crimes each year in which shoe marks are recovered. The collections of shoes from suspects and shoe marks at the police districts are very large. Accordingly, it takes much time to compare them. An aim for developing a database for shoe marks is that this will result in time reduction for the comparison. Moreover, identification is dependent on the number of characteristics in the shoe profiles. In 1993, 14000 shoe marks were recovered from the crime scene, 2000 were compared with shoes of suspects, and approximately 500 identifications were made.

It is useful to enter images of shoe profiles in a database, since the amount of shoe marks found at the crime scene is growing rapidly. The police will have a better pre-selection compared to manual systems. Furthermore, the communication of images with other police regions and investigating officers is possible, which results in more crimes that can be solved on forensic evidence.

In 1992, the project REBEZO was started at our laboratory in co-operation with the police. At first, the idea was to have a reference collection of shoes that are sold in The Netherlands. The police requested for more information in this database, and for this reason the next three files are combined :

- A collection of profiles of shoes which can be bought in shops, the reference collection (3D)
- A collection of profiles of shoes from suspects (2D and 3D)
- A collection of shoe marks found at the crime scene (2D or 3D)

The crime-scene examiners can search in the databases. They determine with the aid of the database the possible make and model of the shoe that caused the shoe mark. They can also find a suspect with a similar shoe mark in the system. The system REBEZO is meant to be used for pre-selection of shoes and shoe-prints. A

qualified examiner conducts the examination of the shoe and the shoe mark and will draw a conclusion based on characteristics.

The main successes of databases of shoe prints is in criminal intelligence, since shoe marks from different crimes can be linked.

Adding shoe marks and shoes of suspects to the system
The user acquires an image of the shoe and/or the shoe mark with an image-capturing device that is connected to a computer. For reproducible results, it is necessary to use standard procedures. In the procedures, the direction of the shoe mark and the magnification that is used are described. In Figure 5-3 a screen for adding the shoe mark is shown.

For retrieving the images based on shapes of shoe profiles a classification scheme is required. The classification scheme that is used in REBEZO, has been developed in The Netherlands with the Dutch police, based on research in other countries[81] [82] [83] [84] [85].

The codes shown in Figure 5-4 are used for classification. A more detailed description of the codes is available. The computer program shows an example image when clicking on the different codes (Figure 5-5). In a trial of the database with five trained crime-scene officers, it appeared that they classified more consistently with example images of the classification codes compared to textual classification codes. In the classification used by the Dutch police the shoe is, unlike in foreign classification, not divided in different parts, in order to reduce the time needed for classification.

With our classification, an example of codes being entered by an examiner is shown in Figure 5-3. The shoe mark consists of :
     13. profile
     24. vertical lines
     41. squares
     42. rectangles
     54. irregular surfaces with more than four angles

Figure 5-3 : Screen for adding the shoe mark to the system

The codes attributed to a shoe mark are subjective. For the example of Figure 5-3, some users might not see regular lines in the shoe profile, whereas others classify the profile as not regular. To solve this problem, a limited number of trained people should classify the shoe profile in a standardized way.

Comparison screen

The user can compare two shoe marks with each other on a comparison screen. Figure 5-6 shows a screen with on the left the live image of a shoe mark and on the right a test print of a shoe from the database. In REBEZO, the three databases of shoes of suspects, shoes commercially available and shoe marks from the scene of crime can also be compared to each other.

Furthermore, it is possible to rotate, mirror, and invert the images. These options are useful for comparing negatives (prints) with positives (the shoe itself), and profiles of right shoes with those of left shoes.
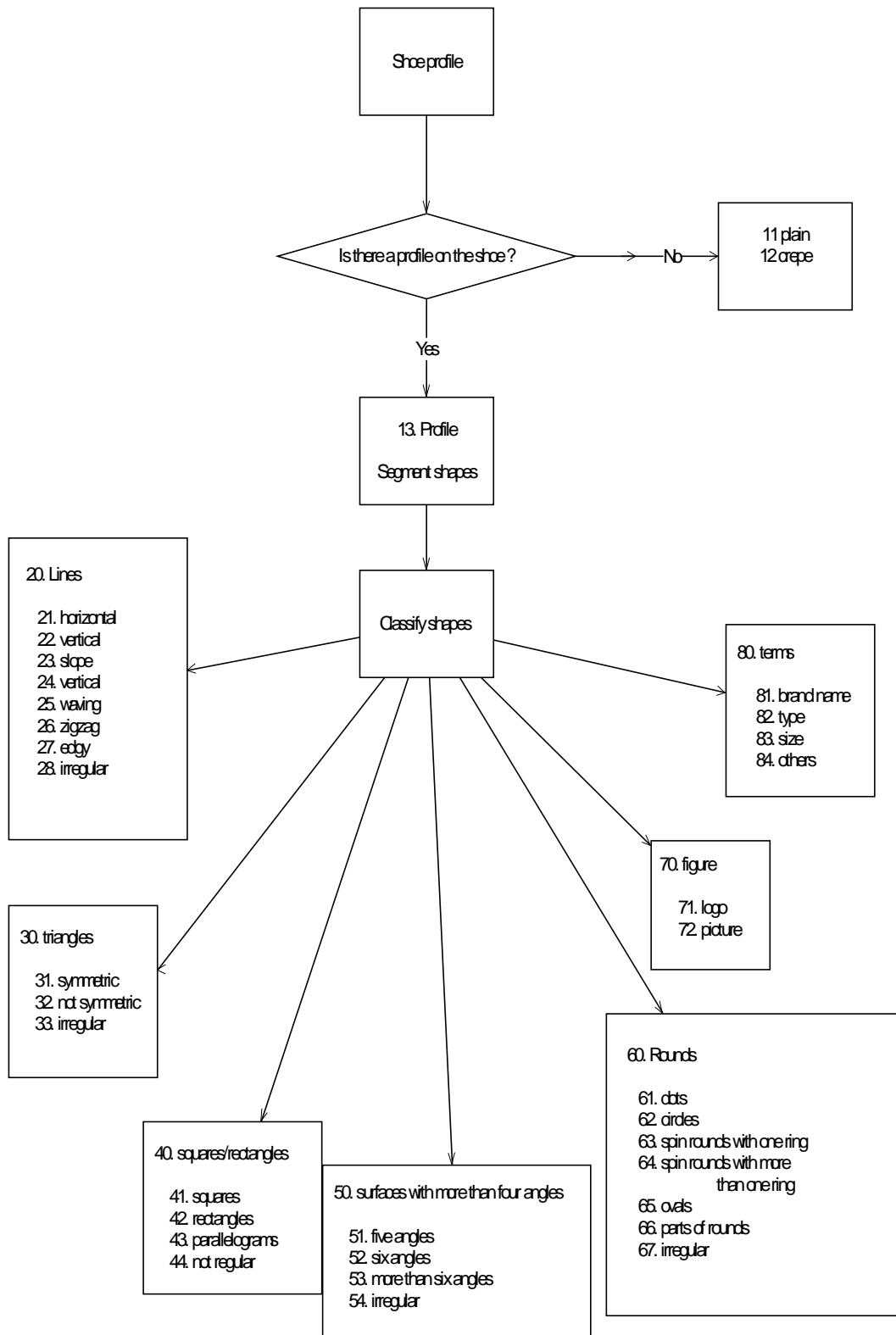
Figure 5-4 : Classification codes
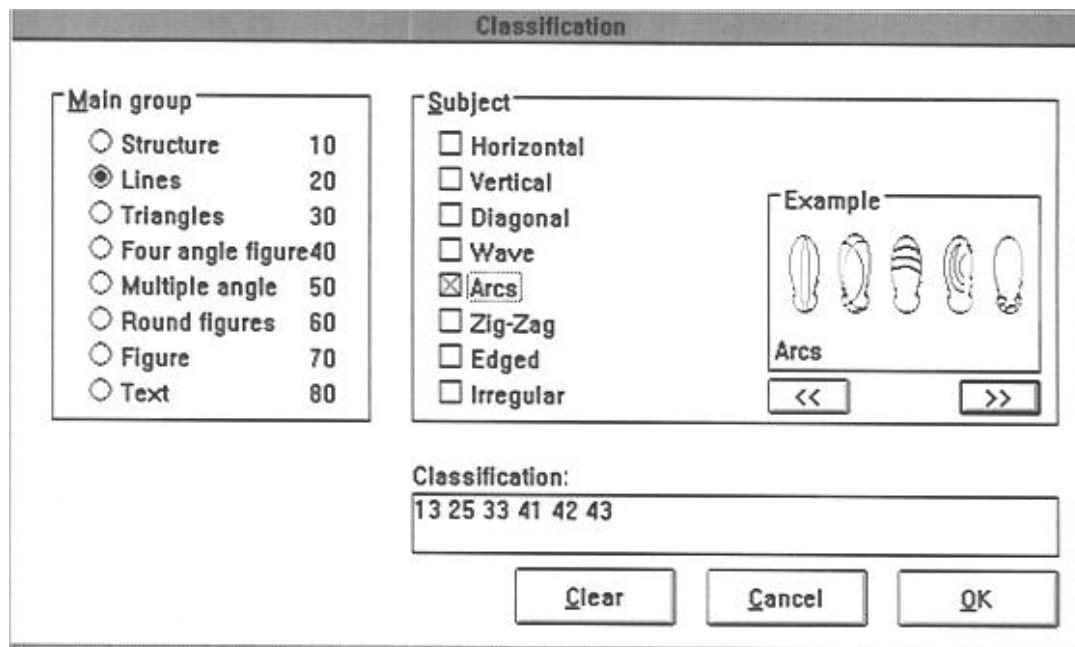
Figure 5-5 : Example of classification pattern screen

Reference collection

For acquiring the shoes that are commercially available, a reference collection is built by making three-dimensional impressions in Biofoam[86] boxes (Figure 5-7). The material is fragile foam that deforms under minimal pressure to conform to the shape of the object deforming it. This material is often used to make anatomical impressions of the feet. The impressions are photographed and stored on Photo-CD.

5.2   Segmenting, Labeling and Contour Tracing of shapes in a shoe mark

It has already been mentioned that shoe marks may be classified differently by different experts. For this reason, a research project has been started on the automatic classification of shapes in a shoe mark. The aim of the project is to supply the classification codes. For this project the image-processing package Khoros[87] has been used.
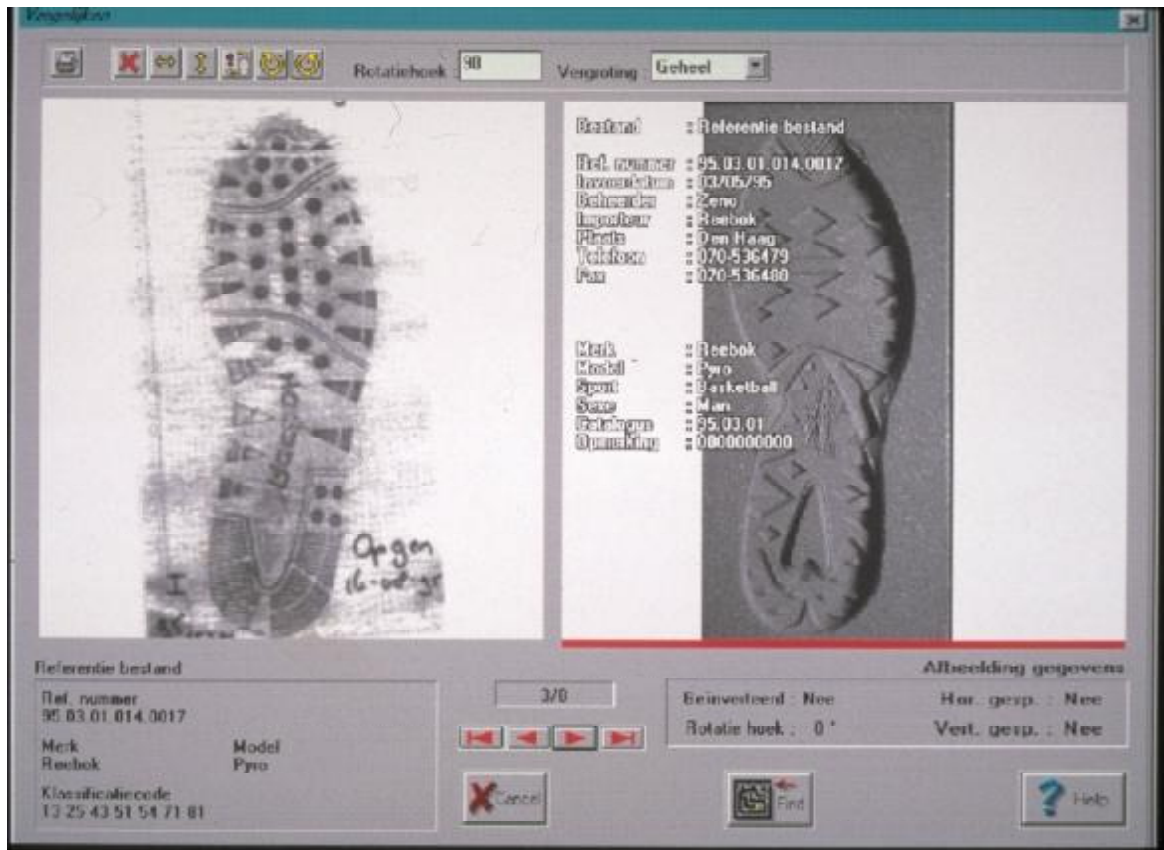
Figure 5-6 : Comparison Screen : on the left a test shoe mark of a suspect and on the right an impression from the database of commercially available shoes

Our approach consists of first segmenting the different profiles of the shoe marks. After the segmentation step, the profiles are labeled[88] and classified.

In order to recognize profiles in the shoe marks, the following paradigm is applied. First, the image is thresholded. This means that the grey levels are converted to a binary image with a certain threshold level.

Once the image has been thresholded, a wide range of binary imaging operations can be applied. As a first step, the connectedness in the binary image is analyzed.. We regard adjacent 1's as connected, whereas horizontally and vertically 0's are connected, but diagonally adjacent 0's are regarded as disconnected. In other words, the foreground is '8-connected' and the background is '4-connected' (Figure 5-8). This convention is followed in the subsequent discussion.

Figure 5-7 : Shoe mark in a foam box

Now that we have a definition of connectedness, we can distinguish shapes in binary images, and should be able to label them. Labeling is achieved by scanning the image sequentially, until an object has been encountered. Then, a note is made of the scanning positions and a propagation routine is initiated to label the whole object with a one. A separate image space is used for allocating the labels. Next, the scan is resumed, ignoring the points already labeled, until another shape is found, which is labeled with a two in the separate image space. This procedure is continued until the whole image has been scanned and all shapes have been labeled. The user can

P and 4−connected neighbors   P and 8−connected neighbors
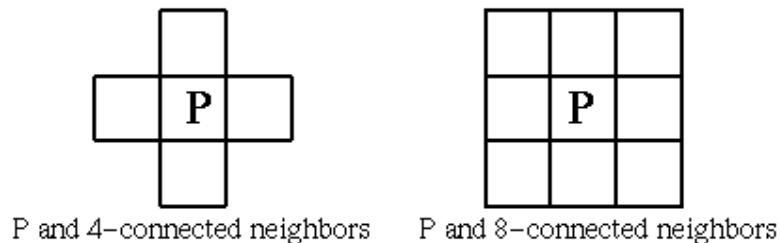
Figure 5-8 : Labeling process with 4 and 8 connected neighbors

Figure 5-9 : Example of segmenting and labeling a shoe mark
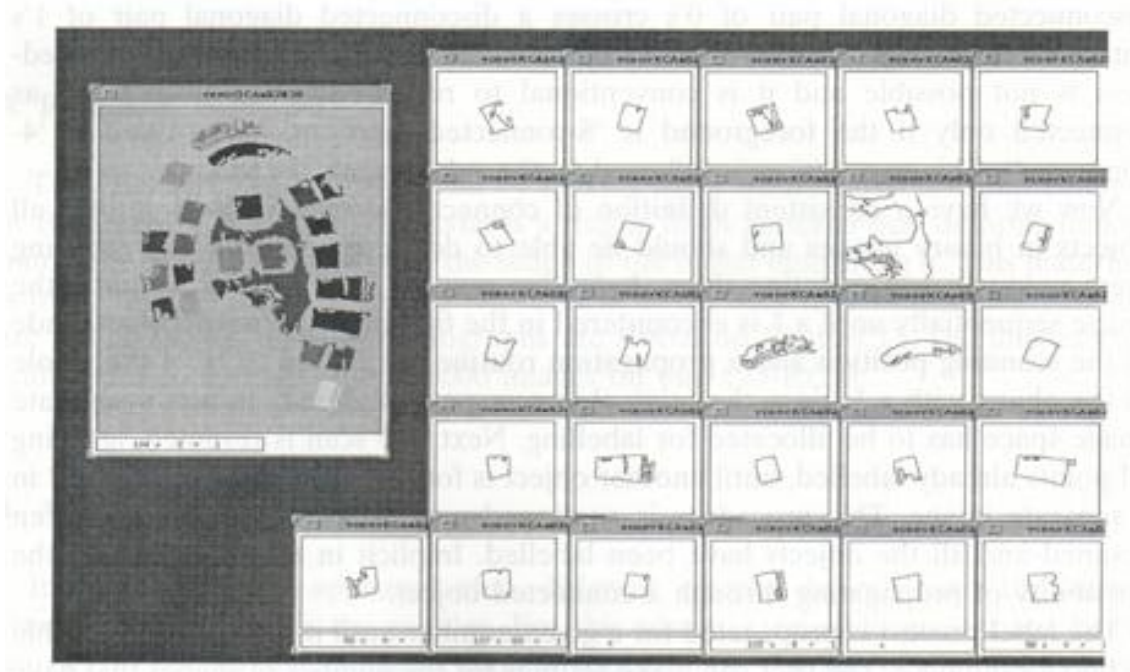
Figure 5-10 : **Segmenting and labeling of images from shoe marks.**
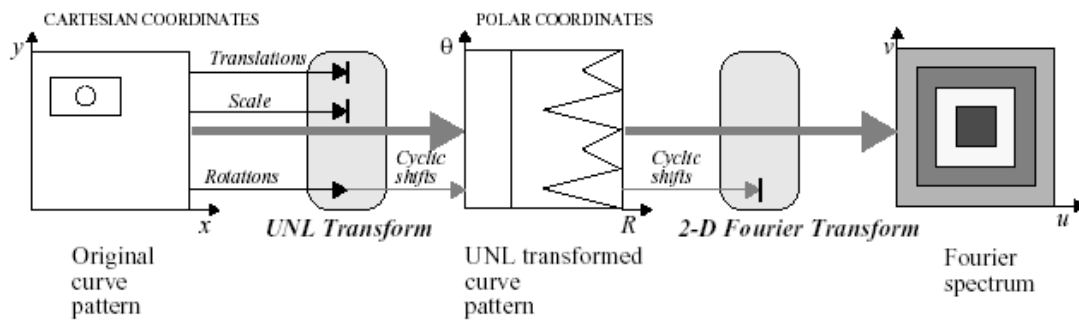
Figure 5-11 : Illustration of UNL Fourier Features

make settings for the number of objects to be recognized and the sensitivity of the algorithm by choosing a minimum region size.   An example of the labeling process as implemented in Khoros[89] is shown in

Figure 5-10, where we have used the labeling algorithm with settings number of objects = 24 and smallest region size is 2 %.

5.3 Feature Extraction

In order to extract the information of the labeled shapes, Fourier Features and Invariant Moments have been implemented.

5.3.1 UNL Fourier Features

The labeled shoe marks are analyzed with software from the UNL (Universidad Nova de Lisboa)[90]. UNL Fourier descriptors are an extension and improvement over standard Fourier descriptors[91] in the sense that they handle open curves, lines etc.

The UNL Fourier features are computed in two stages (Figure 5-11). In the first step, the input image (consisting of binary curve patterns) is transformed from a Cartesian coordinate system to a polar coordinate system by the UNL Transform. The second step is a Fourier transform.

For the UNL transform, the polygons are first estimated, then a transform to line functions is performed and finally the transformed line curves are instantiated in the polar coordinate system. This transform also performs a normalization in terms of translation and scale changes in the original pattern. In other words, it eliminates

translation and scale changes that might have occurred in a given instance of an image.

Rotations of the original pattern result in the cyclic shift of the UNL transformed patterns. This is eliminated in the second processing step by the 2D Fourier transform. The Fourier transform takes the image of the UNL Transformed curve patterns as input. The spectrum of the Fourier Transform is insensitive to any cyclic shifts in its input pattern, hence eliminating the rotation of the original pattern. The characteristics of the UNL Fourier Features, make the representation invariant to translation, scale changes, and rotation of an object.

The UNL transform of a whole object is defined as the union of the UNL transforms of all line segments of which the pattern is composed.

Let $\Omega(t)$ be a discrete object composed of n pixels $z_i = (x_i, y_i)$. Let $\hat{O} = (\hat{O}_x, \hat{O}_y)$ be the centroid of the object and let M be the maximum Euclidean distance form the centroid $\hat{O}$ to all pixels z_i.

The mapping $U(\Omega(t))$ - the line segments $z_{ij}(t)$ between the two neighboring pixels $z_i = (x_i, y_i)$.and $z_j = (x_j, y_j)$. that compose the object $\Omega(t)$, $U(z\text{-}ij(t))$ from the Cartesian to the polar coordinate system, defined by the following formula is the UNL transform of the discrete object :

$$U: ((0,1) \rightarrow R^2) \rightarrow ((0,1) \rightarrow R^2) \qquad \forall i = 1...n \qquad t \in [0,1]$$

$$U(z_{ij}(t)) = \varsigma_{ij}(t) = (R_{ij}(t), \theta_{ij}(t)) = \left(\frac{\| z_i + t(z_j - z_i) - \hat{O} \|}{\hat{M}}, \text{atan}\left(\frac{y_i + t(y_j - y_i) - \hat{O}_y}{x_i + t(x_j - x_i) - \hat{O}_x} \right) \right)$$

(4)

After the line segments z_{ij} have been transformed to curves ς_{ij} analytically, they must be instantiated. That means that a discrete curve pattern must be generated in the discrete polar coordinate system. This is achieved by quantizing the continuous parameter t into k discrete steps. The only condition for the generation process in the polar coordinate system, is that no gaps may occur when the parameter t is gradually increased from 0 to 1 in k steps. Hence k must be sufficient large. The size of k is determined by the resolution of the image in the polar coordinate system.

For the similarity measure, the Euclidean distance between the UNL Fourier Features in the database is computed.

5.3.2 Invariant Moments

In invariant moments, the recognition of different patterns should be independent of size, position, and orientation.

The two-dimensional (p,q) order moment of the density-distribution function $\rho(x,y)$ is defined as:

$$m_{pq} = \int_{-\infty}^{\infty}\int_{-\infty}^{\infty} x^p y^q \, r(x,y)\,dxdy;$$

$$p,q = 0,1,2,..... \qquad\qquad\qquad (5)$$

The first moment μ_{00} is denoted by m. Setting $\bar{x} = m_{10}/m$, $\bar{y} = m_{10}/m$, central moments μ_{pq} are defined by

$$m_{pq} = \int_{-\infty}^{\infty}\int_{-\infty}^{\infty} (x-\bar{x})^p (y-\bar{y})\,dxdy \qquad\qquad (6)$$

p,q = 0,1,2,…..

For a digital image, the integrals are replaced by summations :

$$m_{pq} = \sum_x \sum_y (x-\bar{x})^p (y-\bar{y})^q \, r(x,y) \qquad\qquad (7)$$

The normalized central moments, denoted by h_{pq} are defined as $h_{pq} = m_{pq}/(m_{00})^g$

where $g = 0.5(p+q)+1$

From the second and third order moments, a set of seven invariant moments can be derived by Hu's method[92]:

$$m1 = h_{20} + h_{02}$$

$$m2 = (h_{20} - h_{02})^2 + 4h_{11}^2$$

$$m3 = (h_{20} - h_{02})^2 + (3h_{21} - h_{03})^2$$

$$m4 = (h_{30} + h_{12})^2 + (3h_{21} + h_{03})^2$$

$$m5 = (h_{30} - 3h_{12})\ (h_{30} + h_{12})\big[(h_{30} + h_{12})^2 - 3(h_{21} + h_{03})^2\big] + (3h_{21} - h_{03})(h_{21} + h_{03})\big[3(h_{30} + h_{12})^2 - (h_{21} + h_{03})^2\big]$$

$$m6 = (h_{20} - h_{02})\big[(h_{30} + h_{12})^2 - (h_{21+}h_{03})^2\big] + 4h_{11}(h_{30} + h_{12})(h_{21} + h_{03})$$

$$m7 = (-h_{30} + 3h_{12})\ (h_{30} + h_{12})\left[(h_{30} + h_{12})^2 - 3(h_{21} + h_{03})^2\right] + (3h_{21} - h_{30})(h_{21} + h_{03})\left[3(h_{30} + h_{12})^2 - (h_{21} + h_{03})^2\right]$$

The invariant moments representation is invariant under affine variations of the image content (shift, scaling, rotation).

5.4 Classification

To classify more Fourier Features, two methods have been used : a neural network and Sammon Mapping.

5.4.1 Neural Network

A single-hidden-layer feed forward network trained with back propagation[93] is used as neural network. Experimental results have shown[94] that this type of network can classify with high accuracy noiseless as well as noisy images. Therefore, we chose a single-hidden-layer network. The program used is SNNS from the University of Stuttgart[95].

5.4.2 Sammon Mapping

Sammon mapping[96] is a method for visualizing higher (>3) dimensional data. Sammon's mapping is an iterative method based on a gradient search. The aim of the algorithm is to represent points in an n-dimensional space, in a lower dimensional space, usually in two-dimensions. The algorithm finds the location in the target space so that as much as possible of the original structure of the measurement vectors in the n-dimensional space is conserved (see Figure 5-12). The numerical calculation is time consuming, which can be a problem with a massive data set. On the other hand, it is able to represent the relative distances of vectors in a measurement space and is thus useful in determining the shape of clusters and the relative distances between them.

5.5 Experiments

In initial experiments with foam boxes, which are three-dimensional impressions, problems occurred with the labeling and recognition due to the variation in lighting conditions. For this reason we made black shoe marks on carbon foil which were digitized with a 600 dpi-scanner for further testing. In these shoe marks, the different shapes are clearly visible. The testing of shape classification was performed on ten different shoe marks, and the total number of shapes that were classified was 189.

5.5.1   UNL Features in combination with a Sammon Map

In Figure 5-13 the Sammon-map is shown with the two best Fourier features. In this Sammon map, clusters are visible of shapes. However, in this map there are also shapes that overlap. More features are required for this method. In Figure 5-14 is shown that many different shapes can be distinguished from each other by using 32 features. As could be expected, the difference between horizontal and vertical lines is not easy to distinguish.

N-dimensional data space
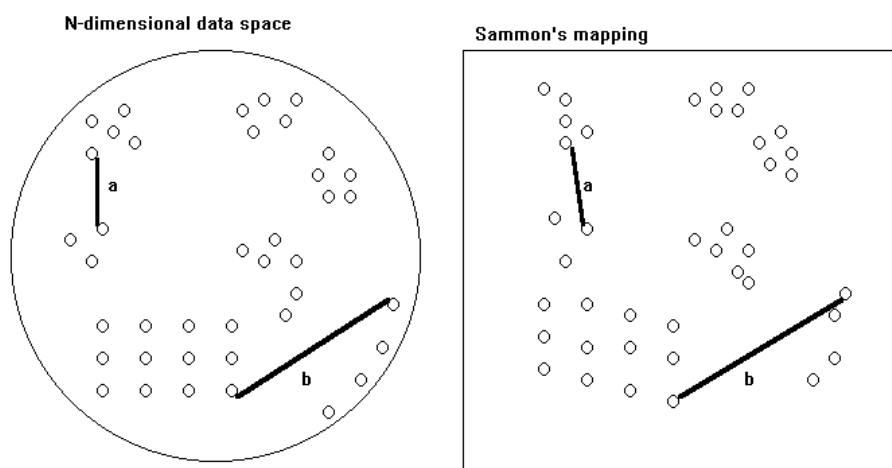
Sammon's mapping

1) Initialize the Sammon's mapping with random coordinates (2-d)
2) Calculate the relative pairwise error of each data point pair between spaces
3) Calculate a gradient which shows the direction to minimize the error
4) Move the data points in Sammon's mapping according to the gradient
5) Repeat steps 2 - 4 until error is below given limit

MAJOR DRAWBACK: very calculation intensive
                      => large data collections take a long time to calculate

Figure 5-12: Basic principle of Sammon's mapping
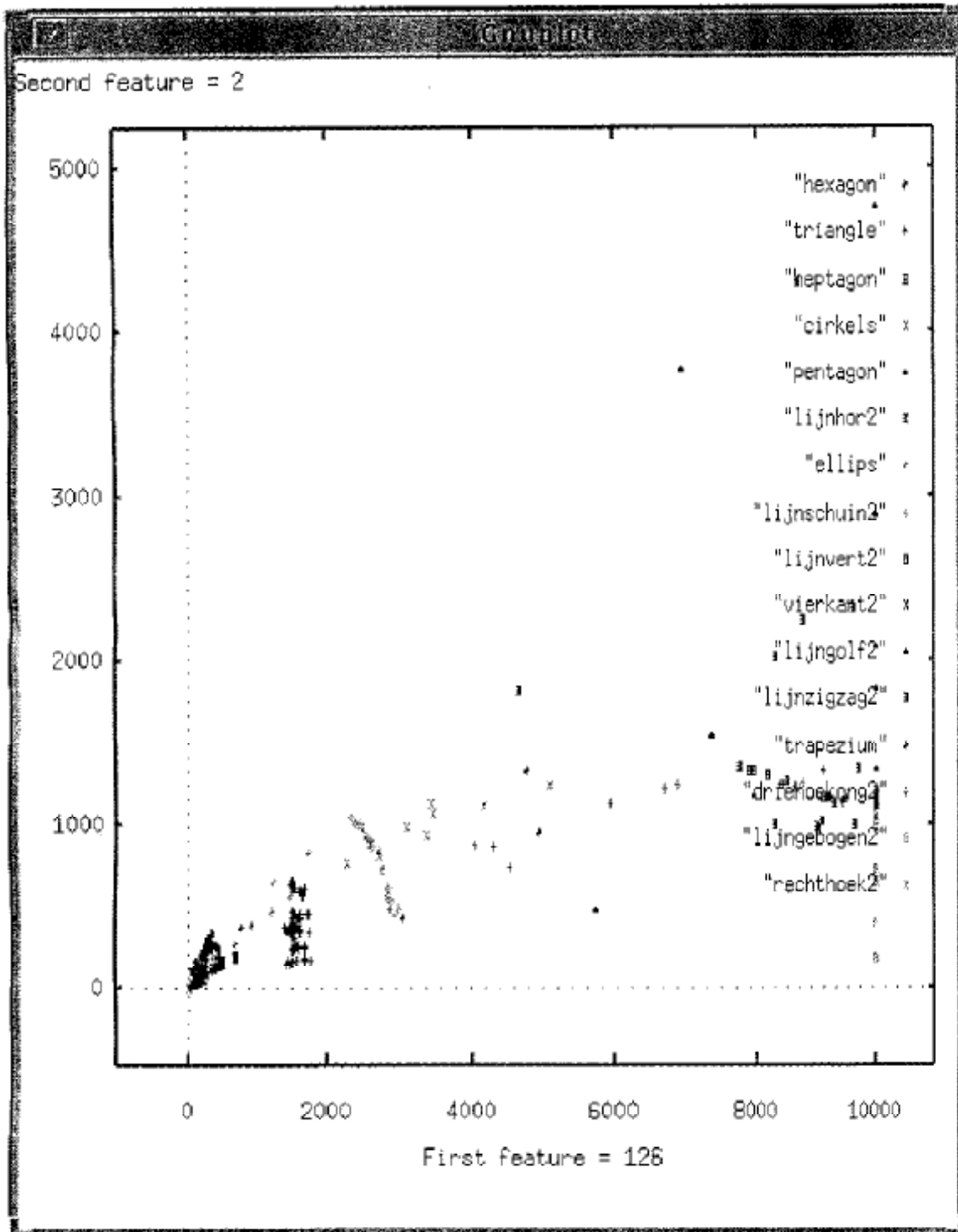
Figure 5-13 : Sammon-map of the two best UNL Fourier features for several shapes visible in ten different shoe marks.
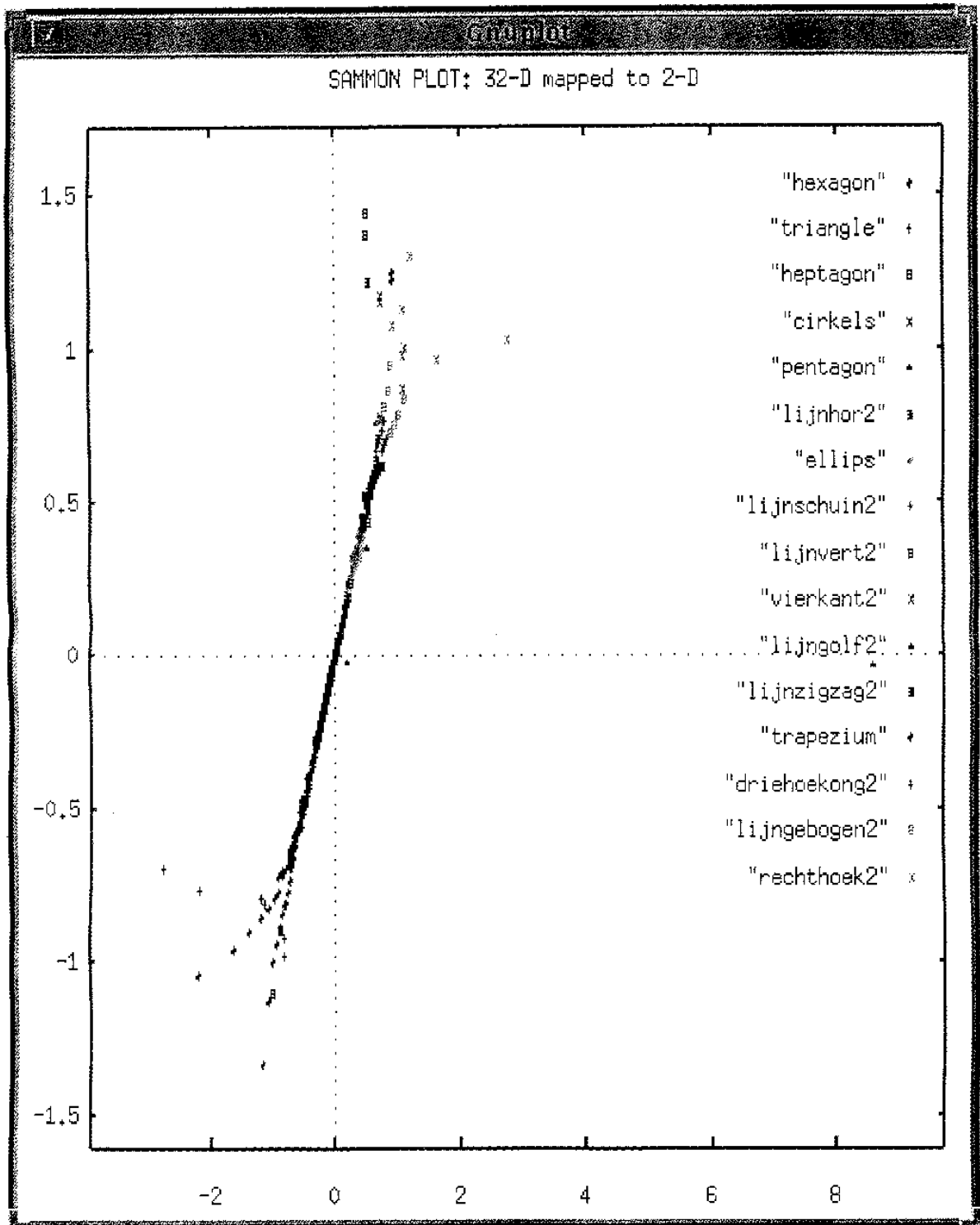
Figure 5-14: Sammon-plot of the 32 best UNL Fourier features for several shapes visible in ten different shoe marks.

5.5.2 UNL Features in combination with a Neural Network

We trained the neural network with 10 shoe mark examples that were clearly visible. When classifying one new shoe mark with this network, it appeared that the simple shapes (triangles, rectangles, circles) could be classified with this network and the UNL Fourier Features. With this approach we could not distinguish between lines and rectangles very well. (In Figure 5-15 a schematic view of the shoe mark system is shown.)

Table 8 : Invariant moments of lines and rectangular shapes in shoe profiles

Invariant moments	M1	M2	M3
Square	0.1665	0	0
Rectangle (1 x 1.05)	0.1667788	4.275	0
Rectangle (1 x 10)	0.8145	6.80625	0
Line	>0.8415	>6.80625	0
Triangle (symmetric)	0.1924656	0	4.565308e-3
Triangle (asymmetric)	0.1595188	0	0
Quarter of a circle	1.77873e-1	2.845261e-3	8.84429e-4
Half of a circle	0.2040900	1.335299e-2	1.190370e-3
Circle	0.1591552	0	0

5.5.3 Invariant moments

Since the approach with the Fourier Features, did not handle lines and rectangles in a proper way (we defined a line as an area that is smaller than height : width = 10: 1), the use of invariant moments[97] is implemented.

For a good quality shoe mark with lines and rectangular shapes, we have determined invariant moments M1, M2, and M3. The results are shown in Table 8. With this method, it is possible to distinguish properly between lines and rectangles.

5.6   Conclusions and future research

In this research, a database for shoe mark comparison has been developed that has been used by the Dutch police. From the research of automated classifying of shoe mark shapes with UNL Fourier Features and invariant moments, we conclude that simple shapes (circles, lines, triangles) can be classified automatically.

Automatic classification of the shoe-sole-patterns in a foam box is difficult, since these have three-dimensional information that is depending on the lighting. Making two images illuminated from both sides of the foam box might solve this problem. Another solution is making a 3D-acquisition of the image. At the time of this research suitable 3D-scanners were not within our reach.

The shoe marks that are found at the scene of crime generally do not have a good quality, since they are often partial and contain much noise, depending on the surface where they are formed on. Therefore, they will be difficult to classify automatically. Since shoes from suspects and shoes from shops are available, good quality test prints can be obtained under optimal conditions.

The best approach of classification is to let the user classify the shoe mark by showing examples of shoe marks on the screen. If the position of the separate profiles is taken into account, this will result in higher rankings. The use of automatic classification, with the method described, is usable for suggesting classification codes to the user. User interaction is required. More research on shape recognition of shoe profiles is required in order to implement this in widely used shoe mark databases.

This research has been focused on shape recognition. At the time of writing computing power was limited, because of which simple methods have been implemented that work fast. The spatial relationships between the different shapes of the shoe profile were not taken into account. In new research[98] these have been accounted for by means of fractals and multi-scale methods. It is expected that other

shape recognition methods as implemented in MPEG-7 will improve the results that are obtained in this research. However, from our experiences with the system, we conclude that improvement of the image acquisition should have the highest priority. At the time of writing, computing power and memory was limited; thus more sophisticated implementations were tested. The spatial relationships between the different shapes of the shoe profile were not implemented. This implementation will improve the results. The shoe mark classification developed for this project is used by the police in The Netherlands.

Shoe mark systems are frequently used in the United Kingdom, Switzerland and Japan. The English software package SICAR[99] is one of the commercially available products for shoe mark that has been available on the market since 1997. In SICAR, automatic classification has not been implemented yet.

Such database retrieval systems were often developed by government forensic laboratories for their own use. In The Netherlands, we have seen some results with these systems. Automatic classification and comparison are possible for good-quality shoe marks. In practice, the problem with shoe marks is that they are often of poor quality, and for that reason automatic classification is not feasible. Shoe marks are valuable in forensic science, although they are time-consuming for collection and comparison. In regions with many violent crimes, we see that this kind of evidence is less common. For a homicide, shoe marks in blood are important parts of evidence that are sometimes skipped due to time limitations. For this reason the use of shoe mark, databases should be promoted, since more crimes can be solved.

Statistics with shoe mark databases and shoes that are on sale are possible; it is very difficult, however, to draw strong conclusions from these databases if the information of the distribution channels is not known. If a certain sole pattern seems to be unique and not seen before, it could be that the shoe is not in the database yet. In addition, in some cases shoe profiles are copied by other manufacturers, and this could result in wrong conclusions. If higher-resolution images are used, it is possible to store the identifying characteristics. If large databases of these characteristics exist, it is theoretically possible to draw conclusions from the shapes of damages and wear.

```
┌─────────────────────────┐
│                         │
│        Shoeprint        │
│                         │
└───────────┬─────────────┘
            │
            ▼
┌─────────────────────────┐
│     Pre-processing :    │
│                         │
│     Fourier features    │
│     Invariant moment     │
│                         │
└───────────┬─────────────┘
            │
            ▼
┌─────────────────────────┐                        ┌──────────┐
│ Extraction low level    │────────────────────────│  Shape   │
│ features                │                        │          │
└───────────┬─────────────┘                        └──────────┘
            │
            ▼
┌─────────────────────────┐
│ Extracting high level   │
│ features                │
│ Not implemented :       │
│ position                │
└───────────┬─────────────┘
            │
            ▼
┌─────────────────────────┐
│                         │
│   Textual descriptors   │
│                         │
└───────────┬─────────────┘
            │
            ▼
┌──────────────────────────────┐
│           Indexing           │
│ learning neural network or   │──────┐
│ Sammon map                   │      │
└───────────┬──────────────────┘      ▼
            │                    ╭──────────╮
            │                    │          │
            │                    │ Storage  │
            ▼                    ╰────┬─────╯
┌──────────────────────────────┐     │
│       Retrieval :            │◄─────┘
│   on textual descriptors     │
│ and/or similarity measures of│
│          features            │
│ using trained net or Sammon  │
│            map               │
└───────────┬──────────────────┘
            │
            ▼
┌─────────────────────────┐
│                         │
│      Visualization      │
│                         │
└─────────────────────────┘
```
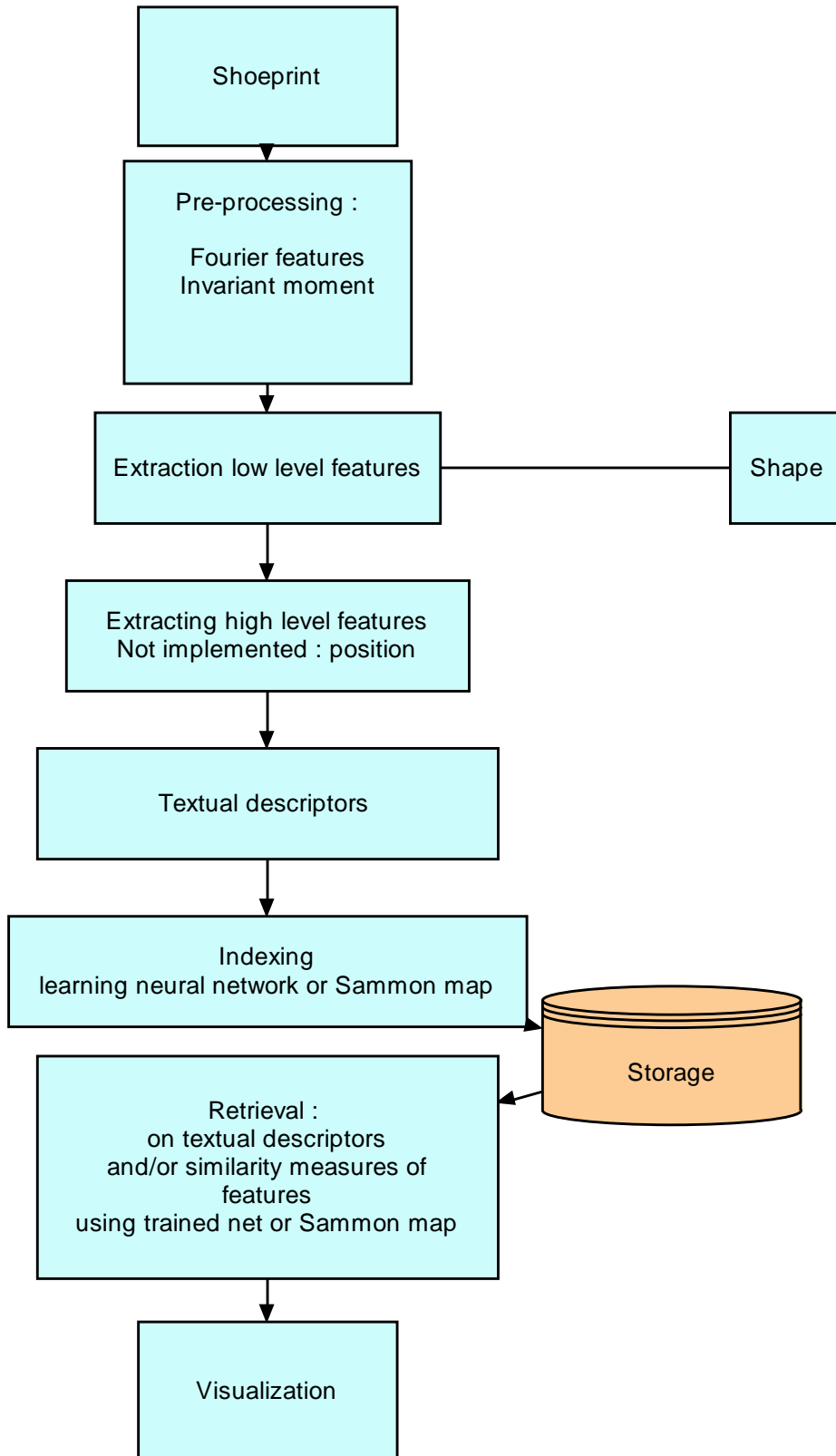
Figure 5-15 : Flow chart of shoe mark system

6 Databases of logos of drug tablets

Abstract

In this chapter, an evaluation is presented of methods for shape based image retrieval of logos of drug tablets.

On a database of 432 tablets that contain illicit products, we have compared log polar matching with the MPEG-7 shape comparison methods, which are the contour-shape, bounding box and region-based shape methods. For the comparison of algorithms, a test set of three drug tablets were used. Twenty-five Images of each pills were acquired by rotating them in steps of fifteen degrees. With this test set, a comparison of rotation insensitivity of the shape based retrieval methods, is possible.

From our experiments it appeared that log polar matching resulted in top positions of the relevant matches for the shape of the logo. For improving the results of log polar matching, we have developed a method for splitting the logo from the shape of the drug tablet. With the separate logo images, the results with log polar matching, improved, since all relevant images now were in top positions. A disadvantage of log polar matching is that it takes much computing power.

With the MPEG-7 shape comparison methods the matching results also improved after segmenting the logo from the background of the tablet. After the segmentation, the contour-shape based method gave similar results as the log polar correlation, at much less computational cost. The other MPEG-7 shape comparison methods performed less compared to log polar and contour shape.

6.1 Introduction

At the drugs department of the Netherlands Forensic Institute (NFI) a large number of tablets with illicit products, mostly containing MDMA (3,4-Methylenedixy-N-Methylamphetamine, also commonly known as Ecstasy, XTC etc) and amphetamine,

Figure 6-1 : Example of imprint on a drug tablet

are submitted for forensic analysis. Information on the chemical composition and the physical characteristics (e.g., diameter, shape, height and weight) of clandestine tablets as well as images of the tablets are available in a database. The illicit manufacturers often make use of punches resulting in tablets that bear an imprint consisting of all sorts of registered trademarks and fantasy figures (logos). In Figure 6-1, an example of a logo (imprint) on a drug tablet is shown.

Databases of chemical composition and images of logos are used for finding the manufacturers and for acquiring information on distribution of these illicit drugs. If the stamp is found at a manufacturer, it is possible to conduct a tool mark examination between the stamp and the marks on the tablet. From this examination it is sometimes possible to determine if a specific drugs tablet has been produced with a specific stamp.

In this research an evaluation will be made of methods that are applicable for content-based image retrieval of the logos on the drugs tablets. The need for correlation algorithms of logos arises if databases of drug tablets contain many items.

The images of the tablets are acquired with a standard camera with a side light source. This approach may result in differences in the images of the logos due to light variations caused by differences in angle of incidence of the light source. Another factor that has to be considered is that a tablet itself can be damaged, and the logo is not completely visible anymore. Since the three-dimensional logo is captured with a regular camera, the resulting shadow image has to be compared. Furthermore, the

tablets can be slightly shifted or rotated. Accordingly, the method for content-based retrieval of the images in the database of logos of drugs tablets should be insensitive to rotation, translation, and light conditions.

In this chapter, a comparison of content-based retrieval methods that are applicable to shape recognition of logos on drugs tablets is given, together with practical tests, and conclusions based on this research.

6.2 Content Based Image Retrieval (CBIR))

Many research groups[100] are working on image retrieval based on contents. Current research is focused on accessing images and video in educational, entertainment, and publishing applications. Large-scale image databases include news collections and collections such as patent and trademark image databases. The research in the field of content-based image retrieval is focusing on several broad areas: image indexing and classification, image user interfaces and methods for image parsing.

The logos on drug tablets may indicate brand names or just be fantasy figures. At our Institute, a text string of what the examiner recognizes in the logo is entered as text in the database. The disadvantage of this approach is that different examiners will classify a logo with a different text string. The problem of different interpretations of images by different examiners is known in the literature[101]. Since some logos are similar to text, OCR (Optical Character Recognition)-methods[102] can also work for these databases. However, OCR works on a two-dimensional object, whereas the drug tablets are three-dimensional objects acquired as a shadow image.

An overview article of implementations of Content Based Image Retrieval can be found on the Internet[103]. In Content Based Image Retrieval, shape, color, texture and motion are the main features on which the images are distinguished.

Since logos are shapes, we focus on shape features in this paper. Two main types of shape features are commonly used:

- Global features (e.g., aspect ratio, circularity and moment invariants) [104]

- Local features (e.g., gradients)[105]

Other methods for shape matching include elastic deformation of templates,[106] and comparison of directional histograms of edges extracted from the image.[107]

In the case of a drug tablet there is a three-dimensional logo where only one 2D-view is available. If there would be a standardized way of digitizing the tablet each time in the same way, this would not be a problem, since the 2D-view is reproducible. This might be the case with known logos of trade marks or symbols where the examiner knows how to position the drug tablet. One study[108] has been carried out for 3D objects that are acquired as a 2D shadow image, which is used in this paper.

6.3   Existing CBIR Systems

To demonstrate the feasibility of new techniques, several experimental systems have been developed by research institutes and by commercial manufacturers.

6.3.1   Commercial Systems

An Available CBIR systems is QBIC of IBM. The system extracts and stores color, shape and texture features from each image in a database, and uses R^*-tree indexes to improve the search speed.[109] This database is available on the web. When searching for an image, the system matches features from the query with those of stored images and displays similar images on the screen as thumbnails. An evaluation copy is available from the web at http://wwwqic.almaden.ibm.com. Other well-known systems are Virage[110] [111] and Excalibur[112].

The system Imatch is a system at the low-end part of the market that can be downloaded from the Internet at http://www.mwlabs.de/.

A disadvantage for evaluation of these commercial systems is that there is no source code available and the algorithms used are neither described in literature nor in patents.

6.3.2   Developments by Research Institutes

A CBIR initiative that has the source code available on the web is Photobook[106] (http://www-white.media.mit.edu/vismod/demos/photobook). This system is also known for its face comparison features.

The University of Singapore had a research project[113] on CBIR of trademarks where Fourier Descriptors and Moment Invariants measure features of logos. Since the logos in our database often contain trademarks, this research is similar to our approach. Another project that is related to trademark retrieval is PicToSeek.[114]

In the past, we have tested Fourier Descriptors and Invariant moments for the shape of profiles in shoe marks.[115]

The ISO (International Standardization Organization) MPEG (Moving Picture Experts Group)-have issued standards for video and audio compression, which are used in a wide variety of equipment and on the Internet. Whereas MPEG-1, MPEG-2, and MPEG-4 focused on coding[116] and compression, MPEG-7[117] [118] is emerging as a new standard for searching in video and audio streams. The source codes of the algorithms and the test environment are available. MPEG-7 does not define a single system for content description but a set of methods and tools for the different steps of multimedia description. It aims to standardize the set of descriptors, the set of description schemes, a language for description schemes, and methods to encode descriptions.

6.4   Shape Recognition methods

Since this study focuses on shape recognition, we now describe the shape recognition methods that are implemented in the MPEG-7 framework: object bounding box, region-based shape, and contour-based shape. The shape recognition methods in MPEG-7 determine features that are indexed in a database. In this study, the shape recognition methods of MPEG-7 are compared with log-polar matching[75].

6.4.1 Object bounding box

The object bounding box descriptor addresses the coarse shape description of visual objects. A bounding box of a visual object is the tightest rectangular box that fully encompasses that visual object. The descriptor can define bounding boxes for 2D and 3D objects.

The descriptor consists of three parts. The first part describes the size of the bounding box itself. The size is described in normalized coordinates, so that the description is resolution independent.

The second part is the density of samples in an object's bounding box and serves as a confidence measure for this descriptor. It can be used to compute the area of a 2D object or the volume of a 3D object.

The third part is optional and describes the spatial position of the visual object in 3D coordinate axes and its orientation.

The shape descriptions of objects consists of three parts (Figure 6-2):

- Segmentation (just a simple kind of segmentation with labeling pixels)

- Extraction of the bitmap of the object of interest

- Estimating the bounding box

The process of estimating the bounding box is broken down into:

- Estimating the orientation of the object (computing the principal axes of the object. The object is in binary format.)

The matching process in general works as follows :

1. Compute descriptors for bounding boxes (sizes) of all images in the database and of the image that is queried for

2. Compare the bounding box sizes for each image

3. Sort distances in ascending order

4. Present the top results in the sorting to the user
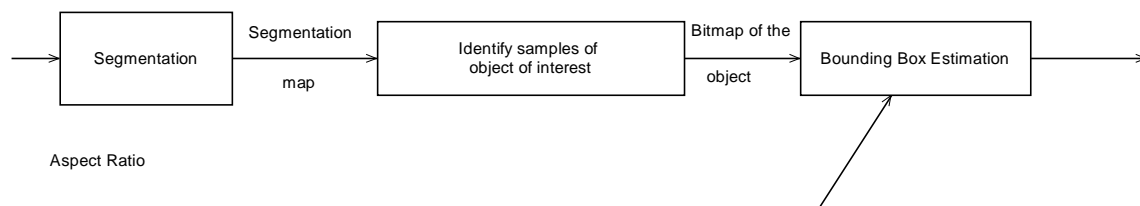
Figure 6-2 : Schematic overview of Bounding Box Estimation

6.4.2 Region-based Shape

The region-based shape descriptor expresses pixel distribution within a 2-D object region; it can describe complex objects consisting of multiple disconnected regions as well as simple objects with or without holes. It is meant to take into account imperfections of the segmentation process. The region-based descriptor can describe diverse shapes efficiently in a single descriptor and it is insensitive to minor deformation along the boundary of an object.

The descriptor belongs to the broad class of shape analysis techniques based on moments[119,120]. It uses a complex 2-D Angular Radial Transformation (ART)[121], defined on a unit disk in polar coordinates.

The process for determining the descriptor consists of:

- Extraction of vertices (segmentation: extraction of the bitmap of an object of interest, estimation of a closed contour and encoding of the polygon vertices)

- Determining whether or not a given point is inside or outside the figure represented by the vertices

From each shape, a set of ART (Angular Radial Transformation) coefficients F_{nm} is extracted, using the following formula:

$$F_{nm} = \langle V_{nm}(r,q), f(r,q) \rangle = \int_0^{2p} \int_0^1 V_{nm}(r,q), f(r,q) r dr dq \qquad (8)$$

where $f(\rho,\theta)$ is an image intensity function in polar coordinates and $V_{nm}(\rho,\theta)$ is the ART basis function of order n and m. The basis functions are separable along the angular and radial directions and are defined as follows:

$$V_{nm}(r,q) = \frac{1}{2p} \exp(jmq) R_n(r) \qquad (9)$$

with

$$R_n(r) = \begin{cases} 1 & n=0 \\ 2\cos(npr) & n \neq 0 \end{cases} \qquad (10)$$

The default region-based shape descriptor has 140 bits. It uses 35 coefficients quantized to four bits/coefficient.

Some important features of this descriptor are :

- It gives a compact and efficient way of describing properties of multiple disjoint regions simultaneously.

- Sometimes during the process of segmentation, an object may be split into disconnected sub-regions. Such an object can still be retrieved, if the

information which regions it was split into is retained and used during the descriptor extraction.

- The descriptor is robust to segmentation noise, e.g., salt and pepper noise.

Since the region shape descriptor makes use of all pixels constituting the shape within an image, it can describe any shape, i.e. not only a simple shape with a single connected region as in Figures 6-3 (a) and (b) but also a complex shape that consists of holes in the object or several disjoint regions as illustrated in Figures 6-3 (c), (d) and (e), respectively.

The region shape descriptor can not only describe diverse shapes efficiently in a single descriptor, but also is also robust to minor deformation along the boundary of the object. Figures 6-3(g), (h) and (i) are very similar shape images for a cup. The differences are at the handle. Shape (g) has a crack at the lower handle while the handle in (i) is filled. The region-based shape descriptor considers (g) and (h) similar but different from (i) because the handle is filled. Similarly, Figures 6-3(j) (k) and (l) show a part of a video sequence where two disks are separated. With the region-based descriptor, they are considered similar.
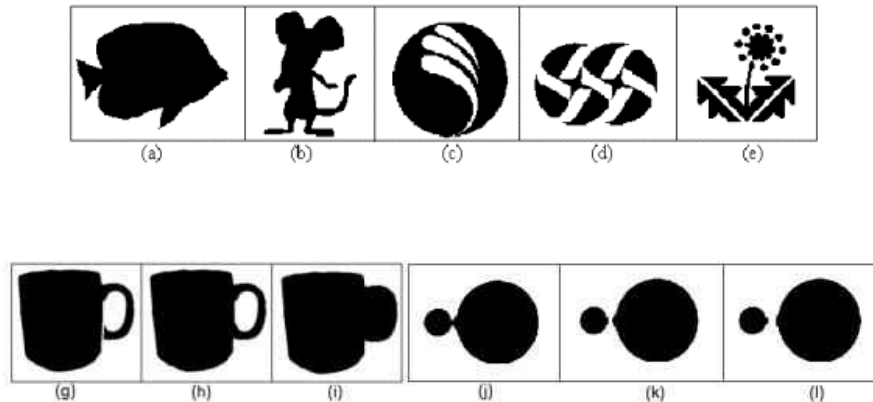
Figures 6-3 a-i: Examples of images for region-based shape
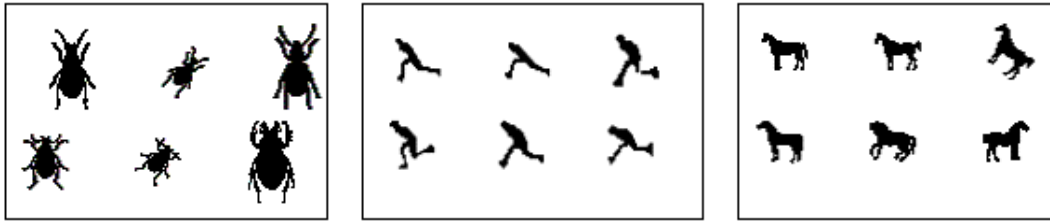
Figure 6-4 : Example of images of MPEG-7 database with CSS (a) shape generalization properties (perceptual similarity among different shapes), (b) robustness to non-rigid motion (man running), (c) robustness to partial occlusion (tails or legs of the horses)

6.4.3 Contour based Shape

Contour-based shape descriptors capture characteristic shape features of an object or region based on its contour. It uses the Curvature Scale-Space representation as described by Mokhtarian[122], which captures perceptually meaningful features of the shape.

The representation in Curvature Scale-Space (CSS) has the following properties:

- It captures the characteristic features of shape

- It reflects properties of the human visual system

- It is robust to partial occlusion of the shape

- It is robust to perspective transformations

- It is compact

Some of the above properties of this descriptor are illustrated in Figure 6-4, each frame containing very similar images according to CSS, based on the actual retrieval results from the MPEG-7 shape database.

The CSS image is a multi-scale organization of the curvature zero-crossing points of the contour as it evolves. Intuitively, curvature is a local measure of how fast a planar contour is turning. Contour evolution is achieved by first parametrizing using arclength. This involves sampling the contour at equal intervals and recording the 2-D coordinates of each sampled point. The result is a set of two coordinate functions (of

arclength) which are then convolved with a Gaussian filter. The next step is to compute curvature on each smoothed contour. As a result, curvature zero-crossing points can be recovered and mapped to the CSS image in which the horizontal axis represents the arclength parameter on the original contour, and the vertical axis represents the standard deviation of the Gaussian filter.

The descriptor is defined by:

- The number of peaks in the image

- The highest peak height

- Parameters of the remaining peaks with reference to the highest peak. They are ordered in decreasing order.

- $circularity = \dfrac{perimeter^2}{area}$ (11)

- $eccentricity = \sqrt{\dfrac{0.5(i_{20} + i_{02}) + 0.5\sqrt{i_{20}^2 + i_{02}^2 - 2i_{20}i_{02} + 4i_{11}^2}}{0.5(i_{20} + i_{02}) - 0.5\sqrt{i_{20}^2 + i_{02}^2 - 2i_{20}i_{02} + 4i_{11}^2}}}$ **(12)**

where $i_{02} = \sum (y - y_c)^2 ; i_{11} = \sum (x - x_c)(y - y_c) ; i_{20} = \sum (x - x_c)^2$

- and (x, y) is each point inside the contour shape and (x_c, y_c) is the center of mass of the shape.

§ Convex contour curvature vector. This element specifies the eccentricity and circularity of the convex contour. The convex contour is defined as the curve smoothed by means of filtering until it becomes convex. It is obtained by smoothing with the filter parameters corresponding to the highest peak.

The representation of the contour shape is compact, it counts less than 15 bytes. Contour Based Shape description relies on the definition of an object by a closed contour. If this is not available, it should be determined.

As an illustration of contour based description, consider the image given in Figure 6-5a which corresponds to a fish object. The figure shows intermediate steps that are taken to generate the CSS representation of the fish object. In Figure 6-5 (b), (d), (f), (h) and (j) the contour of the fish is shown with progressive levels of smoothing where

the zero-crossings have been represented as black dots and the CSS-images are shown next to them.

The matching of two CSS images consists of finding the optimal horizontal shift of the maxima in one of the CSS images that would result in the best possible overlap with the maxima of the other CSS image. The similarity measure is then defined as the sum of pair wise distances (in CSS) between corresponding pairs of maxima

6.4.4 Log Polar

In our research for correlation of impression marks on cartridge cases,[123] we have used log polar correlation.[124] This method is rotation, translation, and scaling invariant. The method is used for matching different images; however, it can also be used for searching in databases. The method is more time consuming than the methods that have been previously described in this chapter.
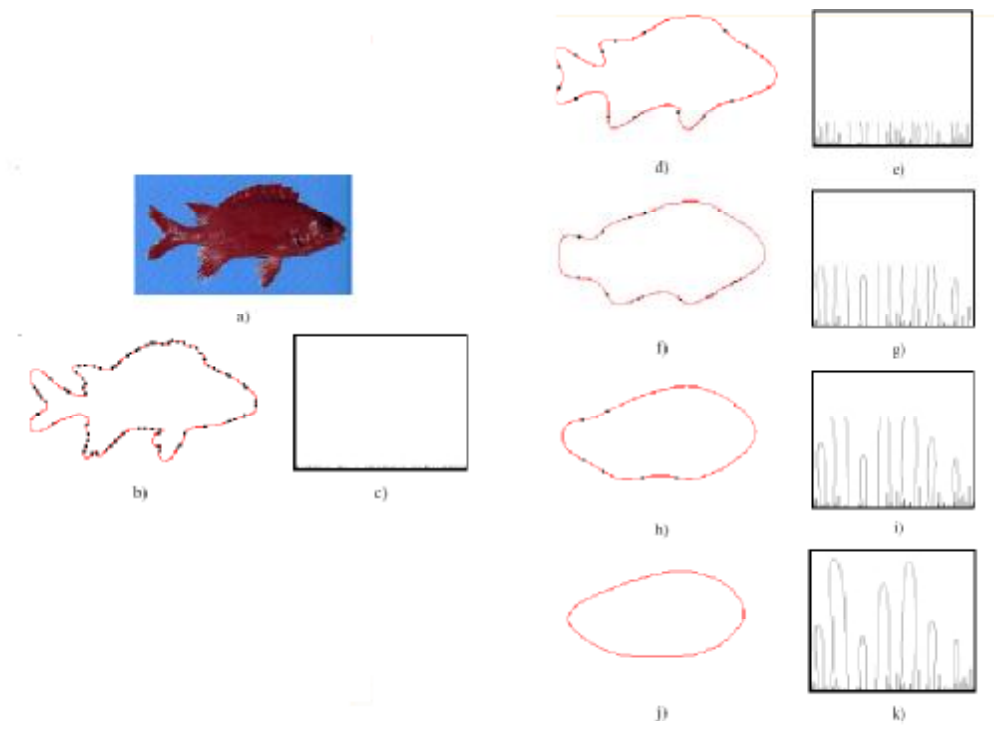
Figure 6-5: Example of fish object from http://www.ee.surrey.ac.uk/Research/VSSP /imagedb with corresponding progressive formation of the CSS representation.

By using invariant image descriptors in place of the original images, it is possible to avoid the problem that correlation results disappear in noise level. One such descriptor is the log-polar transform of the Fourier magnitude, which removes the effect of translation and uniform scaling into shifts in orthogonal directions[125].

In order to demonstrate the properties of this image descriptor, consider the comparison between two images f(x,y) and g(x,y), which are related by a four-parameter geometric transformation:

g(x,y) = f(α(x cos β + y sin β) - Δx, α(-x sinβ + y cosβ) - Δy)   **(13)**

The magnitudes of the Fourier transforms of f and g are invariant to translation, but retain the effect of scaling and rotation:

$$G(u,v)| = \frac{1}{a^2}\left|F\left(\frac{u\cos b + v\sin b}{a}, \frac{-u\sin b + v\cos b}{a}\right)\right|$$ (14)

where G(u, v) and F (u, v) are the Fourier Transforms of g (x, y) and f (x, y) respectively.

Mapping of the Fourier magnitudes into polar coordinates (r,θ) achieves the decoupling of the rotation and scale factors; rotation maps to a cyclic shift on the θ-axis, and scaling maps to a scaling of the r-axis:

$$|F_P(r,q)| = \frac{1}{a^2}\left|F\left(\frac{r}{a}, q+b\right)\right|$$

          (15)

with $r = \sqrt{u^2 + v^2}$ and $q = \tan^{-1} v/u$; F_P stands for polar Fourier Transform.

A logarithmic transformation of the r-axis further transforms scaling into a shift:

$$\left|F_{LP}(r,q)\right| = \frac{1}{a^2}\left|F_P(r - \ln(a), q+b)\right|$$ **(16)**

where F_{LP} stands for polar Fourier Transform and ρ=ln(r). The polar mapping followed by the logarithmic transformation of the r-axis is called the log-polar (LP) transform. In Figure 6-6 this is visualized.

The optimal rotation angle and scale factor can be determined by calculating the cross-correlation function of the log-polar transformed Fourier magnitudes of the two images. It is important to note that the cross-correlation needs to be circular along the θ-axis, and linear along the ρ-axis:
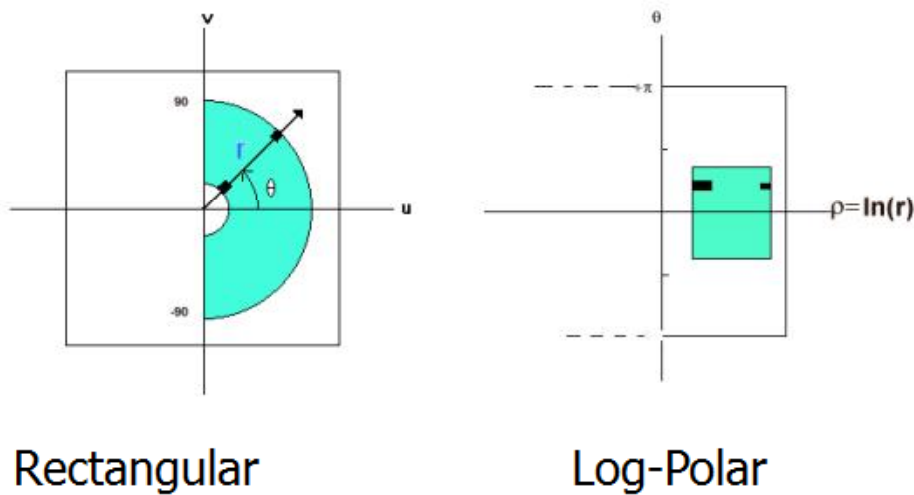
Figure 6-6: Conversion from Rectangular to Log-Polar

$$XC(R,T) = \sum_{r=r_{min}}^{r_{max}} \sum_{q=0}^{2p} F_{LP}(r+R, q+T) F_{LP}(r,q) \qquad \textbf{(17)}$$

where XC(R, T) is the two-dimensional cross-correlation function, with parameters R (difference in logarithm of scale factors) and T (difference in rotation angles).

One way to approach the spatially variant resolution of the log-polar domain is to have the resolution in the log-polar domain equal to the resolution in the rectangular domain. The log-polar domain resolution elements are:

$$\Delta q = \frac{\Delta l}{r}; \Delta r = \frac{\Delta r}{r}$$

where

$\Delta\theta$: resolution elements in angular direction

Δρ : resolution elements in logarithm of radius-direction

Δl : arc length between neighboring points in the rectangular domain

Δr: resolution element in the radius direction

r : radius coordinate

6.5   Test Database

At our institute, an image database of 432 drug tablets is available. The database exists of drug tablets that have been investigated from 1992 until December 2000. The database is available on line in QBIC implementation at http://forensic.to/drugstablets.

Our test set contains three drug tablets. . These tablets are acquired in 25 different angles of rotation (in steps of approximately 15 degrees) to determine whether the algorithms are indeed rotation invariant. We acquired had 25 images for each tablet, so in total we have 432 + 75 images in the database. In Figure 6-7, the three different tablets that we have selected are shown.

Recall of images in the database

If we look for the best search reduction, we should only find the relevant images in the top positions of our search, so we should filter[126] γ:

$$g = \frac{Number\_of\_irrelevant\_images\_in\_the\_database}{Total\_number\_of\_images\_in\_the\_database} \qquad \textbf{(18)}$$

For the experiments, we used ranking based on similarity measure. For measurement of the performance of the matching algorithm, we compare the test set with the complete database. If we compare a drugs tablet with the complete database, we present the number of relevant images that are in the top positions of the ranking. For a measure of efficiency of the matching algorithm, also the

Figure 6-7: Test images used for the comparison of algorithms (from left to right: "Bacardi" / "Mitsubishi" / "Playboy")

percentage of the database that has to be browsed through, until the user finds all relevant images, is reported. A flowchart of methods used in the visual information system of drug tablets is shown in Figure 6-8.

6.6   Experiments

6.6.1   Plain images

We have compared the results obtained with Object Bounding Box, Contour Shape, and Region Shape. The results are shown in Table 9. The first number in this table is the number of hits in the top positions (25 means all of the relevant images are in the first positions, since we have included 25 images of the same drugs tablet in different positions in the database). The second number shows the percentage of the database that has to be browsed through until all images are retrieved, which gives a measure of efficiency.

The log polar method works best on shape. However, this method takes much computing power (for searching the complete database it took several days on a Pentium II 333 Mhz –computer, compared to several seconds with the other methods after indexing).

Table 9: Comparison of Log Polar with MPEG-7 algorithms (Object Bounding Box. Contour Shape and Region Shape) with the test set of drugs tablets. The first number in each cell is the number of relevant matches in the first position(s), and the second number is the percentage of the database that has to be browsed, before all relevant images are found.

	Log Polar	Object Bounding Box	ContourShape	RegionShape
"Bacardi"	25; 5%	23 ; 8 %	1 ; 22 %	4 ; 10 %
"Mitsubishi"	23; 7%	2 ; 22 %	1 ; 22 %	3 ; 22 %
"Playboy"	20 ; 12 %	3 ; 17 %	1 ; 22 %	1 ; 22 %

6.6.2 Preprocessed Images

To improve the results for the matching process (in the previous approach the complete image was compared), it is necessary to extract the shape of the logo out of the image. We segment the logo itself with a standard procedure. The procedure is as follows:

- First apply histogram normalization to the image, then threshold it to a binary image

- *For finding the shape of the tablet*: label (as shown in chapter 5.2) the image with a Minimum Region Size of 27 percent (this value is determined from analyzing several tablets)

- *For finding the edges of the tablet:* threshold; the background of the pills is black, so the threshold is possibly at a gray level of 50.

- *For filtering the edges of the tablet:* make the selection 5 percent smaller

- Then multiply the thresholded and resized image with the image (Figure 6-9, right)

- The final result is the logo (Figure 6-9, left)
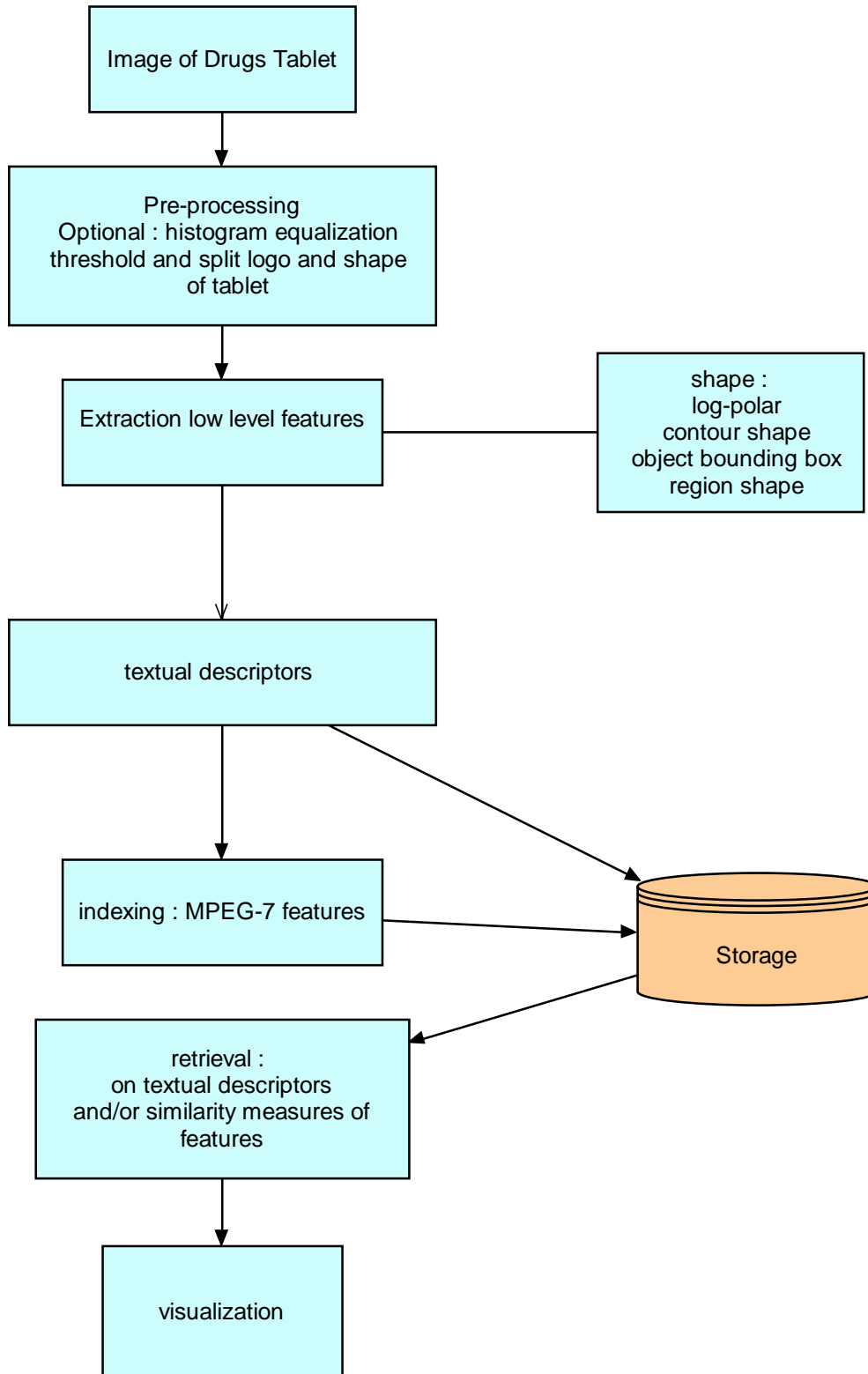
Figure 6-8: Flowchart of methods used in visual retrieval system for drugs tablets

Table 10: Results with Log Polar compared to MPEG-7 algorithms after pre-processing with the test set

	Log Polar	Object Bounding Box	ContourShape	RegionShape
"Bacardi"	25 ; 5 %	1 ; 33 %	25 ; 5 %	4 ; 22 %
"Mitsubishi"	25 ; 5%	1 ; 68 %	24 ; 5 %	3 ; 22 %
"Playboy"	25 ; 5 %	1 ; 75 %	25 ; 5 %	1 ; 22 %

In Table 10, the results of this procedure are shown. The log polar method gives optimal results, since all relevant images of our test set are in top position. The time to complete the matching of all pills from the test set with the pills from the database was several days compared to several seconds with the Contour Shape method after indexing with the same Pentium II-333 Mhz processor. The time for indexing these images with the Contour Shape method was 24 minutes.

6.7   Conclusions and Discussion

We have shown that the use of contour-based shape description methods that are available in the MPEG-7 framework results in optimal efficiency of retrieval of logos of drugs tablets from a database. This method uses the Curvature Scale-Space representation, which captures perceptually meaningful features of the shape. The log-polar shape description gave slightly better results for our test set at the cost of a significantly larger computing time. In future implementations, Curvature Scale Space can be used in combination with Log-Polar to make a pre-selection of images.

The results of this research are limited to the three different test cases and the database of tablets that have been used. It is expected that logos of tablets that have been damaged (which happens if the tablets not properly stored) will not be retrieved with similar accuracy. For searching damaged drug tablets, the textual description of the logo that is entered in the database should be used for retrieval.

In future research 3D-images that are acquired by coded light equipment will be tested with different image search algorithms, since it is expected that depth information of the logos will improve the retrieval appreciably.

Figure 6-9: Splitting of shape of tablet and logo with the algorithm described

If a stamp contains identifying characteristics, it is possible that those characteristics are also visible in the tablet. Before a database is built it is necessary to examine, in real practice cases, whether such identifying characteristics are visible.

7 Summary and Discussion

In forensic science, the number of image databases is growing rapidly. For this reason, it is necessary to have a proper procedure for searching in these images databases based on content. The use of image databases results in more solved crimes; furthermore, statistical information can be obtained for forensic identification.

Summary

This thesis investigates the applicability of image-matching algorithms in forensic image database retrieval.

The literature on *Content-Based Image Retrieval,* from which an overview is given in **Chapter 2**, encompasses a large range of topics. First, visual content (color, texture, structure, motion, and shape) has to be analyzed in order to find features that can be used to separate relevant information. Similarity measures between the images in the database will sort the results with the most relevant on top, if the algorithm is working properly for the image. Chapter 2 included examples of biometric image databases in practice (fingerprints, faces, handwriting, and gait).

Chapter 3 describes a new approach to the matching of striation marks of tools. The angle of the tool with the surface, the material of the surface, and the way the tool is moved on the surface influence the shape of the striation mark. To extract a representative signature of this striation mark, an adaptive zoom-algorithm has been developed. The similarity measure is based on the standard deviation of the gray-value differences. The comparison of signatures should also deal with small changes in striation marks due to wear of the tool. The adaptive zoom-algorithm is also used for comparison. The development is based on the way a tool mark examiner conducts the comparison. The algorithm has been tested with striation marks made with six different screwdrivers. The matching striation marks were retrieved by using the algorithm. The Coded Light Approach resulted in slightly better correlation factors than with conventional side light.

In **Chapter 4**, image-matching algorithms to retrieve cartridge cases from databases have been compared. In this study, three methods for matching of breech face marks have been compared: standard deviation of the difference, log polar, and KLT. These methods have been tested with the following pre-processing methods: histogram equalization and filtering with one of the first four scales of the à trous wavelet transform.

In the experiments we mixed 49 known matching cartridge cases with 4900 images of breech face marks in a database. The standard deviation of the difference of histogram-equalized images of the breech faces resulted in first matching ranks in the database if they are acquired under strict standards for lighting and positioning. A brute force approach by shifting and rotating the cartridge case was not feasible, since too much computing power was required.

Log Polar matching of the third scale from the à trous wavelet transform worked well. With this method, all images were retrieved in the first position of the ranking. KLT in combination with the third scale of a trous worked for 11 breech face marks, as the relevant images were retrieved in the first position. The KLT-method is computationally efficient, and could be used as pre-selection, since all relevant images were retrieved in the first five percent of the database. In the next step, the log polar method could could be applied to the pre-selection to retrieve the matching shapes.

In **Chapter 5** the development of a system for image acquisition and comparison and a database of footwear shoe profiles (named REBEZO) is presented. The database consists of three files : shoes of suspects, shoe marks from scenes of crime and shoes from shops. An algorithm has been developed for the automatic classification of shapes in the shoe profiles. The algorithm first segments a shoe profile in distinguishable shapes. For these shapes Fourier features and invariant moments are calculated. The Fourier features are selected and classified with a neural network that is composed of a single-hidden layer feed forward network trained with back propagation. The neural network works for simple shapes (triangles, circles), but falls short with more complex shapes. Invariant moments can be used to differentiate a

line from a rectangle. More research is required before automatic classification of shoe marks may become of practical use.

The research in **Chapter 6** is focused on shape recognition of drug tablets (e.g., XTC). For large databases of drug tablets (>1000 items), content-based retrieval is a viable solution.

In a database of 432 tablets with illicit products, we have compared log polar matching with the MPEG-7 shape comparison methods, (contour-shape, bounding box and region-based shape methods). For the comparison of algorithms, a test set of three drug tablets were used. Twenty-five images of each pill were acquired by rotating them in steps of fifteen degrees. With this test set, it was possible to compare the rotation insensitivity of the shape based retrieval methods.

From our experiments it appeared that log polar matching resulted in top positions of the relevant matches for the shape of the logo. For improving the results of log polar matching, we have developed a method for separating the logo from the shape of the drug tablet. With the separate logo images, the results with log polar matching, improved, since all relevant images now were in top positions. A disadvantage of log polar matching is that it takes much computing power.

With the MPEG-7 shape comparison methods the matching results also improved after segmenting the logo from the background of the tablet. After the segmentation, the contour-shape based method gave similar results as the log polar correlation, at much less computational cost. The other MPEG-7 shape comparison methods performed less compared to log polar and contour shape.

General Discussion

From the experiments described in this thesis with the databases of toolmarks, cartridge cases, shoe marks and drugs tablets, it appeared that a reproducible image acquisition method should be used. Further, a pre-processing step is necessary for filtering the relevant regions of the image for the comparison. From the study in this thesis, is concluded that there is no single system to treat all image databases. For each database a different approach is necessary, depending on the marks that are used for the comparison.

In order to control the use of these databases, methods are needed that predict the performance on larger databases. Representative test sets should be available for evaluating the performance of matching algorithms in the forensic databases. The performance of matching on a specific types of marks depends also on future developments in products that cause these marks. For instance, if firearms are used where the breech face marks are hardly visible or if the breech face marks are not characteristic anymore, this will reduce the results of using the cartridge case database.

Forensic scientists often give a conclusion based on experience, not on statistics. The forensic databases could provide a reliability measure on the uniqueness of certain identifying characteristics., which results in usefulness in the interpretation of the evidence. For the shoe mark and drug tablet systems the identifying characteristics are often small irregularities. They are not visible in the low resolution images that have been used in our research. For the shoe mark and drug tablet systems, higher resolution images are necessary to obtain the characteristics. The cartridge case system and the tool mark system have these identifying characteristics available. More research on statistical measures from forensic image databases is desirable.

The results of using the databases can not only result in data for court, but also for operational activities. By using the new investigative power due to fast treatment of image database, it is possible to derive information on the operational activities. Examples are new waves of drugs on the market and extensions of the traffic of those drugs, or the use of a specific kind of firearm in a group of criminals.

In order to optimize information retrieval from the various databases, a data searching strategy should be developed that combines the information in the multiple databases. This is a way to alleviate the problem that often only partial profiles are found at the scene of the crime. In some cases, e.g. weak evidence from a shoe mark could be combined with weak evidence from a fingerprint which results in stronger evidence.

8 Samenvatting

In forensisch onderzoek neemt het aantal beschikbare beeld databases toe. Om hierin op een efficiente wijze te kunnen zoeken, is het van belang om inhoudsgestuurde zoek-algoritmes te gebruiken en te ontwikkelen. Het is de verwachting dat het gebruik van beeld-databases zorgt voor een hoger oplossing-percentage van misdrijven. Verder kan hieruit belangrijke statistische informatie worden gehaald voor forensische identificatie.

Dit proefschrift beschrijft de toepasbaarheid van beeld-vergelijkings algoritmes in forensische beelddatabases. Aangezien in de praktijk een vergelijkings-algoritme niet altijd uitsluitend de relevante beelden laat zien, wordt een lijst van beelden getoond, waarbij de meest gelijkende beelden (volgens het beeld-vergelijkings-algoritme) bovenaan staan. In de praktijk is het van belang dat de relevante beelden in de eerste posities van de lijst staan, zodat de gebruiker niet de gehele lijst hoeft te bekijken.

De literatuur over inhoudsgestuurde beeldvergelijking, waarvan een overzicht is gegeven in Hoofdstuk 2, omvat een brede hoeveelheid onderwerpen. Allereerst, moet visuele inhoud (kleur, textuur, structuur, beweging en vorm) worden geanalyseerd om beeld-eigenschappen te vinden die relevant zijn. Metingen aan de overeenkomsten van beelden in de database resulteren in een lijst van beelden, waarbij de meest relevante bovenaan in de lijst staan, indien de meting juist wordt uitgevoerd. Hoofdstuk twee beschrijft ook voorbeelden van biometrische beeld databases, zoals vingerafdrukken, gezichten, handschrift en de manier waarop iemand loopt.

Hoofdstuk 3 beschrijft een nieuwe methode voor het vergelijken van krassporen bij werktuigsporen. De hoek van het werktuig met het oppervlak waarin het krasspoor wordt gevorm, het materiaal van het oppervlak en de manier waarop het werktuig wordt voortbewogen beinvloeden de vorm van een krasspoor. Om een representatieve signatuur te verkijgen van het krasspoor, is een adaptief zoom-algoritme ontwikkeld. De meting aan de overeenkomsten is gebaseerd op de standaard deviatie van het verschil in grijswaarde. Het algoritme moet ook rekening houden met kleine veranderingen in het krasspoor door slijtage van het werktuig.

Voor de vergelijking van de signaturen wordt ook gebruik gemaakt van het adaptief zoom-algoritme. De ontwikkeling van dit algoritme is mede gebaseerd op de manier waarop een werktuigsporendeskundige het onderzoek uitvoert. Het algoritme is getest op zes verschillende schroevedraaiers van hetzelfde merk. De overeenkomstige krassporen werden teruggevonden met behulp van dit algoritme. Door gebruik te maken van een 3D-meting van het krasspoor met behulp van gecodeerd licht werden betere correlatie factoren gevonden dan met grijswaarden.

In Hoofdstuk 4, worden beeldvergelijkingsmethoden vergeleken voor patroonhulzen uit vuurwapens. In deze studie zijn drie methoden voor inhoudsgestuurde beeldvergelijking, vergeleken met elkaar. Dit zijn de standaard deviatie van het verschil, log polair en de KLT (Kanade Lucassen, Tomassi)-methode. Deze vergelijkingsmethodes zijn getest met de volgende voorbewerkingsmethodes : histogram equalizatie en het filteren met behulp van één van de vier schalen van de à trous wavelet transformatie.

In experimenten zijn 49 hulzen gebruikt uit 19 verschillende vuurwapens. De overeenkomstige paren zijn hierbij bekend. Deze 49 hulzen zijn gecombineerd met een database van 4900 hulzen. De standaard deviatie van het verschil van de histogram-geequalizeerde beelden van indrukken van de patroonkamer in het slaghoedje werden teruggevonden in de eerste positie. Hierbij werd gebruik gemaakt van stricte standaarden van beeld-acquisitie waarbij licht en positie zo reprocudeerbaar mogelijk zijn. Een brute force methode die rotatie en een translatie compenseert was niet bruikbaar, aangezien hierbij teveel rekentijd nodig was.

Vergelijking met behulp van de log polaire methode van de derde schaal van een a trous wavelet transformatie resulteerde in een optimaal zoekresultaat, waarbij alle relevante beelden werden gevonden in de bovenste positie van de lijst. Met behulp van de KLT-methode werden elf van de negentien hulzen gevonden in de bovenste posities van de lijst. De KLT-methode is rekentechnisch efficient en kan worden gebruikt als voorselectie, aangezien alle relevante beelden in de eerste vijf procent van de lijst werden teruggevonden. Om dit in de praktijk te gebruiken, kan hierna de log polaire methode worden gebruikt.

In Hoofdstuk 5 wordt de ontwikkeling van een systeem (genaamd REBEZO) voor de acquisitie en vergelijking van schoensporen beschreven. De database bestaat uit drie

bestanden : schoenen van verdachten, schoensporen van de plaats delict en schoenen die in de handel verkrijgbaar zijn. Voorts is een algoritme voor de automatische klassificatie van vormen van de schoenprofielen ontwikkeld. Het algoritme segmenteert eerst een schoenspoor in de onderscheidbare vormen van het schoenprofiel. Van deze vormen worden Fourier Features en invariante momenten berekend. De Fourier Features zijn geselecteerd en geclassificeerd met behulp van een single layer feed forward neuraal netwerk met back-propagation. Het neurale netwerk gaf goede resultaten voor de classificatie bij eenvoudige vormen, zoals circels en driehoeken, maar bij meer complexe vormen werkte het niet. Invariante momenten zijn gebruikt om een lijn van een rechthoek te onderscheiden. Meer onderzoek is noodzakelijk voordat automatische classificatie in de praktijk kan worden toegepast.

Het onderzoek in Hoofdstuk 6 richt zich op vormherkenning van logo's op drugspillen (zoals XTC). Voor grote bestanden (meer dan 1000 verschillende logo's) van drugspillen zijn inhoudsgestuurde methodes voor het zoeken bruikbaar. Bij kleinere hoeveelheden kan ook op een handmatige wijze worden gezocht door een logo te klassificeren.

In een database van 432 illegaal gemaakte drugspillen, hebben we log polaire vergelijking vergeleken met vorm-vergelijkingsmethodes die afkomstig zijn uit MPEG-7. Deze vorm-vergelijkingsmethodes zijn : contour-shape, bounding box and region-based shape. Voor de vergelijking van de algoritmes, zijn drie drugspillen gebruikt. Van elk van de pillen zijn 25 opnames gemaakt in stappen van vijftien graden in rotatie. Met behulp van deze test-set van beelden is het mogelijk om de rotatie-gevoeligheid van de vorm vergelijkingsmethodes uit te meten. Een voorbewerkingstap is toegepast waarbij het logo uit het beeld van pil wordt gefilterd.

Uit onze experimenten, bleek dat log polair vergelijken resulteerde in de bovenste posities van de lijst van relevante beelden voor de logo's. Een nadeel van de log polaire methode is dat het rekenintensief is.

De MPEG-7 contour-shape methode resulteerde in dezelfde resultaten als de log polaire methode, waarbij minder rekentijd benodigd was. Met behulp van de overige geteste MPEG-7 algoritmes werden mindere resultaten bereikt.

Discussie

Uit de experimenten bij dit proefschrift, blijkt dat het van belang is om een beelden van goede kwaliteit te hebben die op een reproduceerbare wijze worden opgenomen. Voor een optimale werking van de algoritmes is het noodzakelijk om een voorbewerkingstap te gebruiken om de relevante informatie uit het beeld te halen. De voorbewerkingstap en de vergelijkingsstap zijn beiden afhankelijk van het spoor dat vergeleken moet worden.

Het is wenselijk om een statistisch model te ontwikkelen, zodat voorspeld kan worden hoe een bepaalde beeld-vergelijkingsmethode zal werken op grotere bestanden. Hiertoe dienen representatieve verzamelingen te worden opgezet om de werking van de algoritmes te vergelijken.

Beeld-bestanden zijn niet alleen van belang voor forensische informatie voor de rechtbank, maar zijn ook van belang voor de opsporing. Door de snelle verwerking van beelden, blijkt het in de praktijk mogelijk om sneller een misdrijf op te lossen. Verder kan ook belangrijke informatie worden verkregen uit de beeld-databases, bijvoorbeeld nieuwe trend in de drugs-markt en trends op het gebied van bepaalde type wapens bij criminele organisaties.

Door het combineren van de verschillende soorten beeld-bestanden kan extra bewijsmateriaal worden verkregen, die voordien niet bekend was. Twee relatief zwakke aanwijzingen van verschillend bewijsmateriaal (bijvoorbeeld een onduidelijk schoenspoor en een onduidelijk vingerspoor), kunnen samen resulteren in een sterker bewijs.

Curriculum Vitae

The author was born in Oosterhout, the Netherlands, on September 26, 1967. At the age of two he moved with his family to the Hague. After finishing high school (St. Aloysiuscollege, The Hague), he went to the college of technology (TH Rijswijk), where he received a Bachelor of Science degree. His graduation project concerned the development of a gamma-detector with ^{3}He in Silicon at the University of Delft.

In 1998 he worked at Océ Nederland BV on research concerning image processing in digital (color) photocopiers. In 1990 he switched to the Patent and Information office of this company, where he investigated infringements of patents and researched new developments on color copiers and image processing.

In 1991, he moved to the Netherlands Forensic Institute in Rijswijk, as forensic scientist on shoeprints and toolmarks. In the subsequent years, he did several hundreds of tool mark and shoeprint examinations, and developed databases for shoeprints and toolmarks. In 1994, he was appointed as an expert witness on these fields. In 1995, he moved as a forensic scientist to the Firearms laboratory, where he did several cases on firearms, and also had to testify in court as an expert witness case in the "ballpoint case".

Since 1994, he has been developing a web site http://www.forensic.to to promote exchange of information on forensic science.

In 1995, he was also awarded by the Science and Technology Agency in Japan and worked for 3 months at the National Research Institute of Police Science on image restoration.

In 1997, he switched to the Digital Evidence Section, as a forensic scientist in image processing. On the field of image processing and photogrammetry he had to testify six times in court and conducted casework in approximately 60 cases of CCTV-images. In 1999 he was appointed as Research and Development Coordinator at the Digital Evidence section. In 2000, he was appointed as chairman of the SPIE working group Investigative Image Processing. Since 2001 he is also coordinating the Research and Development program for the High Tech Crime Units of the Dutch Police.

9   Publications

This list contains published and submitted articles to International Proceedings and Journals.

Journals

Geradts Z; Bijhold, J; Poortman, A, Hardy, H; "Databases of logos of Drugs Tablets", submitted for publication

Geradts Z; Bijhold J; "Content Based Information Retrieval in Forensic Image Databases"; Journal of Forensic Science, 2002, 47(2), pp40-47.

Geradts Z; Bijhold J. Hermsen R, Murtagh F; "Image matching algorithms for breech face marks and firing pins in a database of spent cartridge cases of firearms", Forensic Science International, 2001, 119(1), pp 97-106.

Geradts, Z; Bijhold, J; "New developments in forensic image processing and pattern recognition", Science and Justice, 2001, Vol. 41, No. 3; pp.159-166.

Geradts Z; "Correlation techniques for cartridge cases", AFTE-Journal, 31(2), 1999, pp 120-134.

Geradts Z; Keijzer, J; "The Image database REBEZO for Shoe marks with developments on automatic classification of shoe outsole designs", Forensic Science International, 1996, 82(1), pp 21-31.

Geradts Z; "The production of replicas of bullets and cartridges", AFTE-Journal, 1996, 28(1), pp. 41-44.

Geradts Z; "TRAX for tool marks", AFTE-Journal, 1996, 28(3), pp183-190.

Geradts Z, Keijer J, Keereweer I; "A New Approach to Automatic Comparison of Striation Marks", Journal of Forensic Science; 1994; 39(4), pp 974-980.

Proceedings and Book Chapters

Geradts Z; Hardy H; Poortman A, Bijhold J; "Evaluation of contents-based image retrieval methods for a database of logos on drug tablets", Proceedings SPIE, 2001, 4232, pp 553-562.

Geradts Z; Bijhold J; Hermsen R; Murtagh F; "Image matching algorithms for breech face marks and firing pins in a database of spent cartridge cases of firearms", Proceedings SPIE, 2001, 4232, pp 545-552.

Geradts Z; Bijhold J; Kieft M; Kurosawa K; Kuroki K; Saitoh N; "Methods for identification of images acquired with digital cameras", Proceedings SPIE, 2001, 4232, pp 505-512.

Geradts Z.; Zaal D; Hardy H; Lelieveld J; Keereweer I; Bijhold J; "Pilot investigation of automatic comparison of striation marks with coded light", Proceedings SPIE, 2001, 4232, pp. 49-56.

Geradts Z; Bijhold J; "Forensic Video Investigation", Multimedia Video-based Surveillance Systems, Requirements, Issues and Solutions, Edited by Foresti FL; Mahonen, P, Regazzoni, CS; 2000, Kluwer Academic Publishers, Chapter 1

Murtagh F; Bouridan A; Nibouche M; Alexander A; Crookes D; Campbell J; Starck J; Geradts Z, "Multiresolution and Fractal Analysis Methods for Content-based Retrieval", Proceedings of the Irish Machine Vision and Image Processing conference 2000, pp 175-185.

Geradts Z; Bijhold J; "Pattern Recognition and Image Processing in Forensic Science, Proceedings of the Irish Machine Vision and Image processing conference 2000, pp 24-34.

Daubos T; Geradts Z; Starck J; Campbell J; Murtagh F; "Improving video image quality using automated wavelet-based image addition", Proceedings SPIE, 1999, 3813, pp 795-801.

Geradts Z; Bijhold J; "Forensic video investigation with real-time digitized uncompressed video image sequences", Proceedings SPIE, 1999, 3576, pp.154-164.

Geradts Z; Bijhold J; Hermsen R; "Pattern recognition in a database of cartridge cases", Proceedings SPIE, 1999, 3576, pp 104-115.

Bijhold J; Geradts Z; "Forensic photo/videogrammetry: Monte Carlo simulation of pixel and measurement errors"; Proceedings SPIE, 1999, 3576, pp. 239-246.

Daubos T; Geradts Z; Starck J; Campbell J; Murtagh F; "Automated Wavelet-base image addition: Applications to surveillance video"; proceedings of the Irish Machine Vision and Image Processing Conference 1999, pp. 16-23.

Geradts Z; Dofferhoff G; Visser R; "Using high-speed video in ballistic experiments with crossbows", Proceedings SPIE, 1997, 2942, pp 64-70.

Geradts Z; Keijzer J; Keereweer I; "Automatic comparison of striation marks and automatic classification of shoe marks"; Proceedings SPIE, 1995, 2567, pp 151-164.

10 References

1. Wegstein JH; Rafferty JF; "The LX39 latent fingerprint matcher", NBS Special Publication, 1978, 500(36), pp.15-30.

2. Kupferschmid TD; Calicchio T; Budowle B; "Maine caucasian population DNA database using twelve short tandem repeat.", Journal of Forensic Sciences, 1999, 44(2), pp. 392-395

3. Werrett DJ; "The national DNA database", Forensic Science International,1997, 88(1) , pp. 33 42.

4. Sibert RW; "DRUGFIRE revolutionizing forensic firearms identification and providing the foundation for a national firearms identification network", USA Crime Lab Digest,1994, 21(4), pp. 63 68.

5. Phillips PJ; "An introduction to evaluating biometric systems", Computer, 2000, 33(2), pp. 56-63.

6. Evett IW; Williams RL; "A review of the sixteen points fingerprint standard in England and Wales", Fingerprint Whorld, 1995, 21, pp.125 143.

7. Del Bimbo, A; "Visual Information Retrieval", Morgan Kaufmann Publishers, San Fransisco,1999.

8. Abbasi S; Mokhtarian F; "Shape Similarity Retrieval under affine transform: application to multi-view object representation and recognition", Proceedings of the International Conference on Computer Vision, 1998, pp. 306-312.

9. Chang, SK; Hsu, A; "Image information systems: Where do we go from here?", IEEE Transactions on Knowledge and Information Engineering, 1994, 4(5), pp.644-658.

10. Agrain P; Zhang H; Petkovic D; "Content-based representation and retrieval of visual media: a state of the art review", Multimedia Tools and Applications, 1997, 3(3), pp. 179-202.

11. Swain, MJ; Ballard, DH; "Colour Indexing",International Journal of Computer Vision, 7(1), pp. 11-32, 1991.

12. Haralick R; Shapiro L; "Glossary of computer vision terms", Pattern Recognition, 1991, 24(1), pp. 69-93.

13. Haralick R; "Statistical and structural approaches to texture", Proceedings of IEEE, 1979, 67(5), pp. 786-804.

14. Tuceryan N; Jain AK; "Handbook of pattern recognition and computer vision", World Scientific Publishing Company, 1993, pp. 235-276.

15. Koenderink JJ; "The structure of images", Biological Cybernetics, 50, 1984, pp. 363-370.

16. Witkin A; "Scale space filtering", Proceedings of 7th International Conference on Artificial Intelligence, 1983, pp. 1010-1021.

17. Simoncelli E; "Distributed representations of image velocity", Vision and Modeling Technical Report, 1992, 202, MIT Media Laboratory.

18. Pluim JPW, Maintz A, Viergever MA; "Mutual information matching in multiresolution contexts", Image and Vision Computing, 19(1-2), 2001, pp 45-52.

19. Aksoy S; Haralick RM; "Probabilistic vs. geometric similarity measures for image retrieval", Proceedings of Computer Vision and Pattern Recognition (CPRV'00), 2000, pp. 112-128

20. Borgefors G, "Hierarchical chamfer matching: a parametric edge matching algorithm", IEEE Transactions on Pattern Analysis and Machine Intelligence, 1988, 10(6), pp. 849 - 865.

21. Youille AL; Honda K; Peterson C; "Particle tracking by deformable templates", Proceedings International Joint Conference On Neural Networks, 1991, pp. 7-11.

22. Yossi R; Tomasi C; "Perceptual metrics for Image Database Navigation"., Kluwer Academic Publishers 2001.

23. Samet, H; "The design and analysis of spatial data structures". Addison Wesley, 1989.

24. Bentley JL, "K-d trees for semidynamic point sets," in Sixth Annual ACM Symposium on Computational Geometry, vol. 91. San Francisco, 1990, pp. 187-197.

25. Guttman A; "R-trees: A dynamic index structure for spatial searching," Proceedings of ACM SIGMOD International Conference on Management of Data, 1984, pp. 47-57.

26. White D, Jain R; "Similarity indexing with the SS-tree", In Proceedings 12th IEEE International Conference on Data Engineering, 1996, pp. 516-523.

27. Chang SK; "Towards a theory of active indexes", Journal of Visual Languages and Computing, 1995, 5, pp. 101-118.

28. Witten I; Moffat A; Bell T; "Managing gigabytes: compressing and indexing documents and images, Morgan Kaufmann Series in Multimedia Information and Systems, 1999.

29. Van Bemmel JH; Willems JL; "Handboek medische informatica", Bohn, Scheltema & Holkema, 1989, p. 230.

30. http://www.nist.gov/srd/list_all.htm

31. Miller B; "Vital signs of identity", IEEE Spectrum, 1994. 31(2), pp. 22-30.

32. Henry, E.R (1900), "Classification and uses of finger prints, Routledge, London.

33. Halici, U, Jain L.C., Erol, A; "Introduction in finger print recognition", from Inteligent Biometric Techniques in Fingerprint and Face Recognition", CRC Press International Series on Computational Intelligence, 1999, pp. 1-34.

34. Atick, J.; Griffin, PM.; Redlich, A. N.; "FaceIt: face recognition from static and live video for law enforcement", Proceedings SPIE, 1997, 2932, pp. 176-187.

35. Rowley, H.A.; Baluja, S., Kanade, T.; "Human face detection in visual scenes', in D.S. Toretzky, M.C. Mozer, M.E. Hasselmo (Eds), Advances in Neural Information Processing, 1996, 8, pp. 875-881.

36. Howell AJ; "Introduction to face recognition", CRC Press International Series on Computational Intelligence, 1999, pp. 219-283.

37. Samal A; Iyengar PA; "Automatic recognition and analysis of human faces and facial expressions: a survey". Pattern Recognition, 1992, 15, pp 65-77.

38. Penev P; Sirovich L; "The Global dimensionality of face space", Proceedings of Fourth IEEE International Conference on Automatic Face and Gesture Recognition 2000, pp. 264-270.

39. Van den Heuvel H; "Positioning of persons or skulls for photo comparisons using three-point Analyses and one shot 3D photographs", Proceedings SPIE, 1998, 3576, pp 203-215.

40. Maat GJR; "The positioning and magnification of faces and skulls for photographic superimposition", Forensic Science International, 1989, 41, pp 225-235.

41. Bierman, L; "FaceScan ineffective ACLA says", January 4th 2002, Palm Beach Post, page 1.

42. Schomaker L; Vuurpijl L; "Forensic writer identification: A benchmark data set and a comparison of two systems", Report from the University of Nijmegen, 2000.

43. Phillip M; "Efficiency control studies of the FISH system under real world conditions"; Proceedings of the third European Conference of Police handwriting Experts, October 5-7, 1992, Rome, Italy.

44. Kroon L; "Computer aided analysis of handwriting by the NIFO-TNO approach", presented at the 4th European Handwriting Conference for Police & Government Handwriting Experts, October 12th – 14th, 1994, London, pp. 40-53.

45. Foster J; "New area based Measures for gait Recognition", Audio-And Video-Based Biometric Person Authentication: Proceeding of the Third International Conference, Avbpa 2001 Halmstad, Sweden, June 6-8, 2001, pp. 312-317.

46. Geradts Z; Merlijn M; Bijhold J; "Use of gait parameters of persons in video surveillance systems.", submitted to Proceedings SPIE Investigative and Trial Image Processing, 2002.

47. Product Silmark of BVDA Netherlands -
http://www.bvda.nl/EN/sect4/en_4_1a.html

48. Foley J; van Dam A, Feiner S; Hughes J; " Computer graphics: principles and practice, 2nd ed. in C", The Systems Programming Series, Addison-Wesley, 1996.

49. Sato K, Inokuchi S "Three dimensional surface measurement by space encoding range imaging", Journal of Robotic Systems, 1985, 2, pp. 27-32.

50. Frankowski G; "Method and device for 3D measurement", Patent WO98/12501, 1998.

51. Van Beest M; Zaal D ; Hardy H ; "The forensic application of the MikroCad 3D imaging system", Information Bulletin Shoe mark and Tool marks, 2000, 6(1), pp. 65-72.

52. Geradts Z; Keijzer J; Keereweer; "A new approach to automatic comparison of striation marks", Journal of Forensic Sciences, 1994, 39(4), pp. 16-24.

53. Deinet W, Katterwe H, "Studies of models of striated marks generated by a random process", Journal of Forensic Identification,1995, 45(1), pp. 30-38.

54. Uchiyama T; "The probability of corresponding striae in tool marks", AFTE-Journal, 1993, 24(3), pp. 273-290.

55. Luchowski L; Philipp M, "Data types and operations for striated tool mark identification.", Archiwum Informatyki (Archives of Theoretical and Applied Computer Science), 1998, pp. 321-340.

56. http://www.isaspro.com/ (in German)

57. Baldur R; Barret R, "Computer automated bullet analysis apparatus – uses microscope to examine and record surface measurements on computer to enable bullet type identification", patent WO9220988, may 1991.

58. Luchowski L, Geradts Z; "Identification of comparison criteria by similarity-only teacher input", Archiwum Informatyki Teoretycznej i Stosowanej (in Polish), 2000, pp. 102-130.

59. Jones BC; "Intelligent image capture of cartridge cases for firearms examiners", Proceedings SPIE,1997, 2942, pp 94-104.

60. Baldur R; "Method for monitoring and adjusting the position of an object under optical observation for imaging", US Patent 5,633,717, 1996.

61. Baldur R; "Method and apparatus for obtaining a signature from a fired bullet", US patent 5,659,489, 1997.

62. Baldur R ; "Fired cartridge examination method and imaging apparatus". US patent 5,654,801, 1995.

63. Baldur R; "Computer automated bullet analysis apparatus", US patent 5,390,108, 1991.

64. Smith CL, "Fireball: A forensic ballistics imaging system", Proceedings of the IEEE International Carnahan Conference on Security Technology, 1997, pp 64-70.

65. De-Kinder J, Bonfanti M, "Automated comparisons of bullet striations based on 3D topography", Forensic Science International, 1999, 101, pp 85-93.

66. Puente Leon F; "Automatische Identifikation von Schußwaffen", Fortschritt-Berichte VDI, Reihe 8(787) Düsseldorf, VDI-Verlag, ISBN 3-18-378708-3, 1999.

67. Smith CL; "Optical imaging techniques for ballistic specimens to identify firearms", Proceedings of IEEE International Carnahan Conference on Security Technology, 1995, pp 275-289.

68. Faloutsos C; Barber R; "Efficient and effective querying by image content", Journal of Intelligent Information Systems, 5, pp 231-262, 1995.

69. Lew MS; "Content based image retrieval : optimal keys, texture, projections and templates", Series on Software Engineering and Knowledge and Engineering, 1999, 8, pp 39-47.

70. Gonzalez, RC; Woord, RE; "Digital image processing", Addition-Wesley Publishing, 1993, p. 173.

71. Starck JL; Murtagh F; A. Bijaoui; "Image processing and data analysis", the Multiscale Approach, University Press, 1998, Cambridge, ISBN 0 521 59914 8.

72. Holschneider M; "A real-time algorithm for signal analysis with the help of the wavelet transform", in J.M. Combes e.a., editors. Wavelets: Time Frequency Methods and Phase Scale, Springer Verlag, Berlin,1989, pp 286-297.

73. Geradts Z; Keijzer J; Keereweer I; "A new approach to automatic comparison of striation marks", Journal of Forensic Sciences, 1994, 39, pp 974 –982.

74. Anuta PE, Spatial registration of multispectral and multitemporal digital imagery using fast Fourier transform Techniques, IEEE Transaction on Geosciences and remote sensing, 8, 1974, pp 353-368.

75. Casasent D; Psaltis D; "Position, rotation and scale invariant optical image matching", Applied Optics 15, 1976, pp 1795-1796.

76. Shi J ;Tomasi C; "Good features to track", Proceedings IEEE Conference Computer Vision and Pattern Recognition in Seattle, 1994, pp 593- 600.

77. Bres S; Jolion JM; "Detection of interest points for image indexation", Proceedings of third international conference VISUAL'99, Amsterdam, , Lecture notes in computer science, 1614, Springer-Verlag, 1999, pp 427-434.

78. Birchfield S, "Derivation of Kanade-Lucas-Tomasi tracking equation"", Stanford, May 1996, http://vision.stanford.edu/~birch/klt/derivation.ps.

79. Karins JP; Mills SA; Dydyk RB; "Optical processor for fingerprint identification", Proceedings of the SPIE - The International Society for Optical Engineering Conference, Proceedings SPIE, 2940 1997, pp. 108-115.

80. Perez-Poch A; Velasco J, "Cheap and reconfigurable PC-board for real-time optical Applications using liquid crystal displays", Proceedings of SPIE, 1997, 2774, 757-65.

81. Bodziak WJ; "Footwear impression evidence", Elsevier, New York, 1990.

82. Ashley, W; "Shoe sole pattern file", State Forensic Science Laboratory, Victoria, Australia, International association of forensic studies; thematic symposia: footwear and type tread impressions", Adelaide, 1990 and European meeting for shoe mark/tool mark examiners, May 8-11, 1995, National Bureau of Investigation, Finland.

83. Davis, RJ; "An intelligence approach to footwear marks and tool marks", Journal of Forensic Science Society, 21, 1981, pp 183-193.

84. Ebding T, "Spurennachweis und Spurenrecherche : Das Spuren-Recherche-System ISAS Pro", Kriminalistik, 11, 1994, pp. 732-734.

85. Mikkonen S; Astikainen T; "Databased classification system for shoe sole Patterns - identification of partial footwear impression found at a scene of crime", Journal of Forensic Science, 39(5), 1994, pp 1227-1236.

86. Smithers Biomedical Systems, Kent, Ohio, Unites States of America

87. Konstantinides K; Rasure JR; "The Khoros software development environment for image and signal processing", IEEE Transactions on Image Processing, 1994.3(3), pp 243-52.

88. Davies E; "Machine Vision : Theory, algorithms, practicalities", Academic Press, 1990.

89. http://www.khoral.com

90. Rauber TW; Barata MM; Steiger-Garção AS, "A toolbox for analysis and visualization of sensor data in supervision", Universidade Nova de Lisboa - Intelligent Robotics Group, 2825 Monte de Caparica - Portugal - postscript document at internet ftp-address fct.unl.pt, 1994.

91. Jian AK; "Fundamentals of digital image processing", Prentice Hall, 1989, Chapter 9 on Image Analysis and Computer Vision.

92. Hu M; "Visual pattern recognitions by moment invariants", IRE Transactions on Information Theory, 1962, 8, pp. 179-185.

93. Rumelhart DE; Hinton GE; Williams RJ; "Learning internal presentations by error propagation", In : D.E. Rumelhart and J.L. McClelland, Eds, Parallel Distributed Processing; Exploration in the Microstructure of Cognition, 1, MIT-Press, Cambridge, MA, 1986.

94. e.g., Khotanzad A; Lu JH; "Classification of invariant image representations using a neural network", IEEE Transactions on Acoustics and Speech Signal Processing, 1990, 38, pp. 1028-1038.

95. Kingston J; "Neural networks in forensic science", Journal of Forensic Science, 1992, 37(1), pp. 252-264.

96. Sammon Jr JW; "A non-linear mapping for data structure analysis", IEEE Trans. on Computers, C-18(5), 1969, pp. 401-409.

97. Reddi S; "Radial and angular moment invariants for image identification", IEEE Transactions on Pattern Recognition and Machine Intelligence, 1981, 31(2), pp. 240-242

98. Murtagh F; Alexander A; Bouridane A; Crookes D; Campbell JC; Starck JL; Bonnarel F; Geradts Z; "Fractal and multiscale contents based image retrieval", Proceedings IMVIP 2000, Belfast, pp. 127-150.

99. http://www.fosterfreeman.co.uk/sicar.html

100. Jorgenssen C, "Access to pictorial material: a review of current research," Computers and the humanities, 1999, 33(4), pp. 293-318.

101. Ogle VE, Stonebraker M, "Chabot: retrieval from a relational database of images" IEEE Computer, 28(9), 40-48.

102. Witten I, Moffat A, Bell T, "Managing gigabytes compressing and indexing documents and Images", Second edition, Academic Press, 1999, chapter 9.

103. http://www.jtap.ac.uk/reports/htm/jtap-039.html

104. Niblack W, Zhu X, Hafner J, Breuel T, Ponceleon D, Petkovic D, Flickner M, Upfal M; Nin S; Sull S; Byron B; "Updates to the QBIC System", Storage and Retrieval for Image and Video Databases, 1997, VI(3312), pp. 150-161.

105. Mehrotra R; Gary JE; "Similar-shape retrieval in shape data management," IEEE Computer, 1995, 28(9), pp. 57-62.

106. Pentland A, "Photobook: tools for contents-based manipulation of image databases", International Journal of Computer Vision, 1996, 18 (3), pp. 233-254.

107. Jain AK, Vailaya A, "Image retrieval using color and shape," Pattern Recognition, 1997, 29 (8), pp. 1233-1244.

108. Chen JL; Stockman CC, "Indexing to 3D model aspects using 2D contour features," Proceedings of IEEE Conference on Computer Vision and Pattern Recognition, 1996, pp. 913-920.

109. Faloutsos C; "Efficient and effective querying by image content," Journal of Intelligent Information Systems, 1997, 3, pp. 231-39.

110. Bach J; Fuller C, Gupta A; Hampapur A; Horowitz B; Humphrey R; Jain R; Shu C; "Virage image search engine: an open framework for image management," SPIE-proceedings, 1996, 2670, pp. 76-87.

111. Popescu M, Gader P; "Image content retrieval from image databases using feature integration by Choquet integral.", Proceedings SPIE, 1996, 3656, pp. 552-560.

112. Feder J, "Towards image contents-based retrieval for the World Wide Web," Advanced Imaging 11, pp. 26-29.

113. Wu JP; Lam CP; Mehrtre BM; Gao YJ; Desai A; "Contents-based retrieval for trademark registration", Multimedia Tools and Applications, 1996, 3, pp. 245-267.

114. Gevers T, Smeulders A, "PicToSeek: A color image invariant retrieval system, image databases and multi-media search," Series on Software Engineering and Knowledge Engineering, 1997, 8, pp. 25-37.

115. Geradts Z.; Keijzer J; "The image-database REBEZO for shoe marks with developments on automatic classification of shoe outsole designs," Forensic Science International, 1996, 82, pp. 21-31.

116. Hanjalic A; Langelaar G; van Roosmalen P; Biemond J; Lagendijk R; "Image and video databases: restoration, watermarking and retrieval," Advances in Image Communication, 2000, 8.

117. Lay J; Guan L; "Searching of an MPEG-7 optimum search engine, storage and retrieval for media databases 2000", Proceedings SPIE, 1999, 3972, pp. 573-580.

118. Martinez JM, "MPEG-7 Overview (Version 3.0)", international organization for standardization ISO/IEC JTC1/SC29/WG11 N3445, Coding of Moving Pictures and Audio, 2000.

119. Ten CC; Chin TR; "On image analysis by the methods of moments", IEEE Transactions on Pattern Analysis and Machine Intelligence, 1988, 10, pp. 496-513.

120. Koenderink JJ; Van Doorn AJ; "Surface shape and curvature scales", Image Vision Computing, 1992, 10(8), pp. 41-49.

121 Kim WY; Kim YS; "A new region-based shape descriptor"", 1999, ISO/IEC MPEG99/M5472.

122. Mokhtarian F; Abbasi S; Kittler J; "Efficient and robust retrieval by shape content though curvature scale space," Series on Software Engineering and Knowledge Engineering, 1997, 8, pp. 51-58.

123. Geradts Z; Bijhold J; Hermsen R; "Use of correlation algorithms in a database of spent cartridge cases of firearms," Proceedings of ASCI'99 conference, 1999, pp. 301-314.

124. Anuta PE, " Spatial registration of multispectral and multitemporal digital imagery using fast Fourier transform techniques," IEEE Trans Geo Elect, 1970, 8, 353-368.

125. Casasent D; Psaltis D; "Position, rotation and scale invariant optical correlation", Applied Optics, 1976, 15, 1795-1799.

126. Salton G; McGill M, Introduction to modern information retrieval, McGraw-Hill, 1983.